UNIVERSITY OF TROMSØ UIT

-The Arctic University of Norway

FACULTY OF SCIENCE AND TECHNOLOGY
DEPARTMENT OF GEOLOGY

Tectonic environment, geochemistry and petrology of the Tromsøysound iron ore

Eirik Pettersen

GEO-3900 Master's Thesis in Geology

November 2013

Abstract: The geochemistry, mineralogy and associated basic rocks of the Tromsøysound iron ore field was studied for this thesis. The iron ore field lays in the Tromsø Nappe an ultra-high-pressure terrain in Troms, Northern-Norway, and has undergone some partial melting and metasomatism. The ore mineral is magnetite. The tectonic environment is investigated but inconclusive.

Index

1 Introduction 7
1.1 Purpose 7
1.2 Iron Ore 7
2 Regional geology 9
2.1 The Caledonides 9
2.2 The Tromsø Nappe 11
3 Pervious Works 15
3.1 1900 to 1920 15
3.1.1 Occurance 16
3.1.2 Qualities of the ore 19
3.1.3 Quantity 23
3.2 Activity in the 1940s 24
3.2.1 Report by Jens Bugge 25
3.2.2 Eriksens report 26
3.4 Dispute 27
3.5 Later works 29
4. Methodology 31
4.1 Sample collection and preparation 31
4.2 Microscopy and EMPA 31
4.3 XRF analysis 32
5. Field relationships 33
6. Petrography 43
6.1 Description of thin sections 43
Solligangen Profile 51
6.2 Description of minerals 58
7. Whole rock geochemistry 65
7.1 Mineralized samples 65
Strongly magnetic 65
Weakly magnetic 67

7.2 Samples with basic composition *70*
8. Discussion *77*
8.1 Categorization of rocks *77*
8.2 Geothermometry *79*
8.3 Magnetite mineralizations *81*
Metallogenesis *82*
9. Conclusion *85*
References *87*
APPENDIX A Whole rock geochemistry *91*
APPENDIX B Electron Micro Probe Analyzes *96*
APPENDIX C Sample locations map *108*
Appendix D R. Storens map from (Hasselbom et al., 1909) *110*

1 Introduction

1.1 Purpose

In a belt along the Caledonian nappes in Troms and Nordland; from Tromsø in the north to Bogen in the south there is a string of iron ore deposits. In connection with NGU's focus on mineral resources in northern Norway, NGU will be carrying out detailed studies to estimate if there is commercial potential in these deposits.

This master thesis focuses on the iron ores of the Tromsøsund iron ore field, which is the northernmost of this string of iron ore deposits. The study primarily focuses on detailed descriptions of the ore types, but also the wall rock. Metabasaltic wall rock will be analyzed for tectonic environment. All of this will be done by studies of thin sections and geochemical analysis of the rocks.

1.2 Iron Ore

Iron ore is as the name suggest ore that iron is derived from, this is done by melting the raw ore primarily Hematite (α-Fe_2O_3 70 % Fe), Maghemite (γ- Fe_2O_3 70 % Fe), Magnetite (Fe_3O_4 72.4% Fe) or Siderite ($FeCO_3$ 48.2%) but also iron hydroxides. Cut off grades for iron ore are usually around 30 wt % Fe (Pohl, 2011), with the exception of magnetite that can be exploited at 12-15 wt% Fe magnetic (Ohle, 1972), due to comparatively cheap magnetic separation. The raw ore is usually upgraded to 55-65 wt % Fe before shipping; ore that is already at a sufficient grade to ship directly is called direct shipping ore (DSO).

A number of factors other than iron concentration affect the value of iron ore; low Si and Al content as well as large grain size are favorable while Ti and V in sufficient quantities in magnetite is their primary ore and can be valuable by products specialist smelters but are traditional penalty element when producing iron and steel. Other common penalty elements are P, Mn, Cr, Ni, S, As, Cu, Zn and P (Pohl, 2011). Since limestone is used as flux for making iron Ca and Mg are viewed favorably.

2 Regional geology

The Tromsø Nappe where these mineralizations occur, are part of the Caledonian uppermost remaining trust sheet from an orogen between early Ordovician and early Devonian (Gee et al., 2008), termed the Uppermost Allochthon. Figure 1 illustrates the extent of the Caledonian orogeny.

2.1 The Caledonides

In late Ordovician to early Devonian the continents of Laurentia, Baltica and the Micro continent Avalonia collided forming the Caledonide orogeny. In northern Norway, Baltica and eastern Greenland adjoined with Baltica subducting under Laurentia in Silurian to early Devonian (Roberts, 2003). The remains of the orogeny extend for about 1800 km along the long axis and up to 300km in width (Gee and Sturt, 1985).

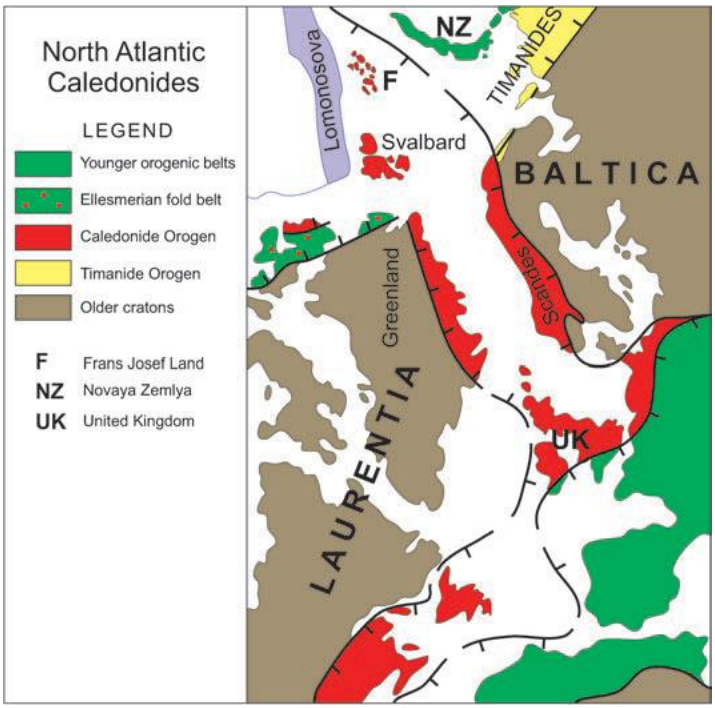

Figure 1 Outline of the North Atlantic Caledonides and relationship between Laurentia and Baltica (Gee et al., 2008)

In Scandinavia the collision of the continents telescoped parts of the margin of Baltica on to the Precambrian basement of Baltica followed by oceanic crust of the Iapetus Ocean and island arcs and finally parts of the Laurentian margin (Gee et al., 2008). These imbricated thrust sheets is usually divided in to four distinct thrust complexes, the Uppermost, Upper, Middle and Lower Allochthons (Andresen and Steltenpohl, 1994, Gee and Sturt, 1985). The middle and Lower Allochthons represent sediments deposited on the passive, rifted shelf and continental rise of Baltica after the opening of the Iapetus Ocean. The Upper Allochthon comprises a selection of ophiolites and island arcs. The Uppermost Allochthon is mostly inferred as being of Laurentian origin. This sequence of thrust sheets overlies Parautochthone and autochthone units in the eastern forelands (Roberts, 2003).

The closing of the Iapetus Ocean is marked by four tectonics events. The earliest the Finnmarkian event occurred in late Cambrian to early Ordovician as a cryptic arc was accreted on to Baltica. The event affected what is now the Middle Allochthon and the lower parts of the Upper Alllochthon in the northern parts of the Scandinavian Caledionides. The second phase involved the accretion of island arcs on both Laurentia and Baltica, the Taconian on the Laurentian side and Trondheimian event on the Baltican side. Figure 2 illustrates the inferred paleotectonic setting.

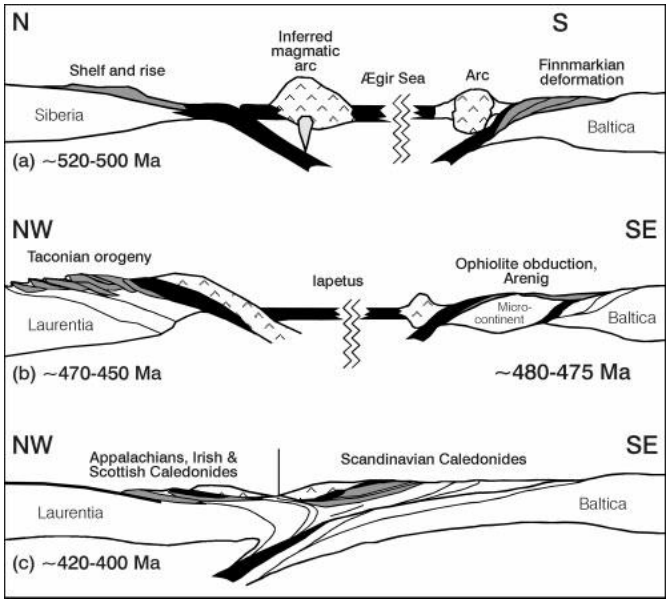

*Figure 2 Schematic cross-sections from (**a**) Late Cambrian to (**c**) Late Silurian/Early Devonian time, illustrating the suggested palaeotectonic settings for some principal orogenic events, culminating in the detachment of Taconian elements from Laurentia and their incorporation into the highest levels of Scandinavian Caledonide tectonostratigraphy. In (**b**), the inferred settings marginal to Laurentia (left) and Baltica (right) are shown, for different time periods (ROBERTS et al., 2002).*

The Taconian event occurred in mid to earliest late Ordovician and is found in the upper parts of the Upper Allochton and in the Uppermost Allochthon (Roberts, 2003). Finally the main event of the orogeny, the Scandian, occurred in late Silurian to early Devonian where Baltica was subducted under Laurentia and continent-continent collision occurred affecting all the tectonic units mentioned earlier (Roberts, 2003).

In the Troms area the paraautochthon and authochthon Dividal group overlies Precambrian basement rocks. Mostly the Helligskogen Nappe complex (BINNS, 1978), later called the Kalak Nappe complex (Andresen and Steltenpohl, 1994) of the Middle Allochthon overlies parautochthon Dividalsgroup but in places the Jerta Nappe of the Lower Allochthon is present (BINNS, 1978).

Over this again lays the lower units of the Upper Allochthon, which include the Vaddas, Kåfjord and Nordmanvik Nappes. These units are overlain by the Lyngen Ophiolite

and Balsfjord Nappe Complex which make up the upper parts of the Upper Allochthon (Andresen and Steltenpohl, 1994). Over this package lies what was called the Tromsø Nappe Complex which was later subdivided into the Nakkedal Nappe Complex and the Tromsø Nappe (Ravna et al., 2006). The Tromsø Nappe is separated from the underlying Skattøra Migmatite complex of the Nakkedals Nappe Complex by a thrust fault (Andresen, 1988).

In the Bogen area the stratabound-strataform Fe-Mn deposits are hosted in the fuglevan marble that has been dated to 660 Ma (Melezhik et al., 2003, Sandstad, 2012).

2.2 The Tromsø Nappe

The location of the Tromsø Nappe in the Scandinavian Caledonindes is shown in Figure 3. The Tromsø Nappe (figure 4) overlies the Nakkedal Nappe and is tectonically separated from it by a major thrust fault. The Tromsø Nappe consists of metasediments (schists, marbles, calc-silicates), with numerous bodies of mafic (eclogites and amphibolites) and ultramafic rocks (Ravna et al., 2006, Broks, 1985, Andresen, 1988). The ultramafic rocks contain up to 95% opaque minerals in some locations (Broks, 1985).

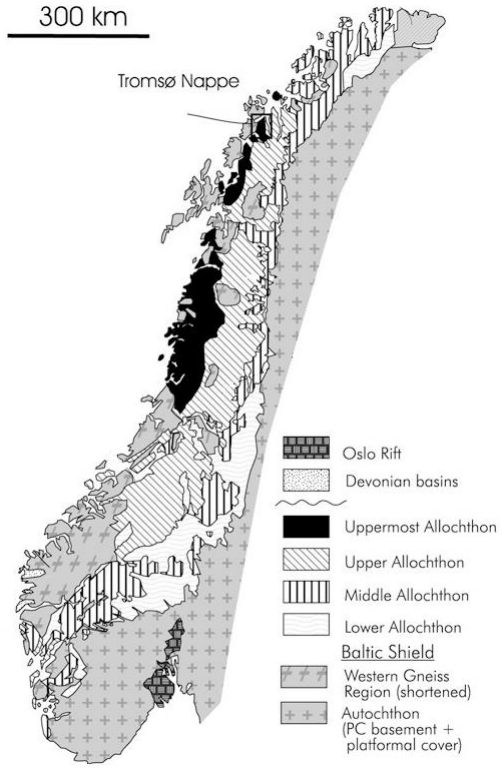

Figure 3 Tectono-stratigraphic map of the Scandinavian Caledonides modified from (Corfu et al., 2003)

The protolith age of the rocks in this nappe is poorly constrained. A minimum age for sedimentation is provided by a zircon date of 493 +5/-3 Ma from an ecoligitized felsic intrusion on Tromsdalstind (Ravna et al., 2006). A set of dates is set forth in (Øiesvold, 2007), that study was done on a road cut on the TromsøI Island and suggest deposition of sediments between 1000 and 500 Ma with provenance ages of 1500 to 1100 Ma.

The Tromsø Nappe can be considered a ultrahigh pressure terrain after the numerous eclogite, retrograde eclogite bodies that can be found in the Nappe (Broks, 1985, Ravna et al., 2006, Damberg, 2012, Corfu et al., 2003, KROGH et al., 1990) and micro-diamonds (JANÁK et al., 2013). Partial melting of eclogite is common (KROGH et al., 1990).

There has been documented three main deformation/metamorphic phases in the rocks of the Tromsø Nappe (KROGH et al., 1990). Krogh et al (1990) reported a first phase recording deep burial from 1.25 GPa and 638°C to 1.7-1.9 GPa. The second phase begins at 0.8 GPa and reaches peak temperature of 665 C and 1.0-1.1 GPa. This indicates uplift between phases 1 and 2. Post 3rd event mineral assemblages show pressures at 0.923+/-0.062 GPa and temperatures of 631+/-7 °C.

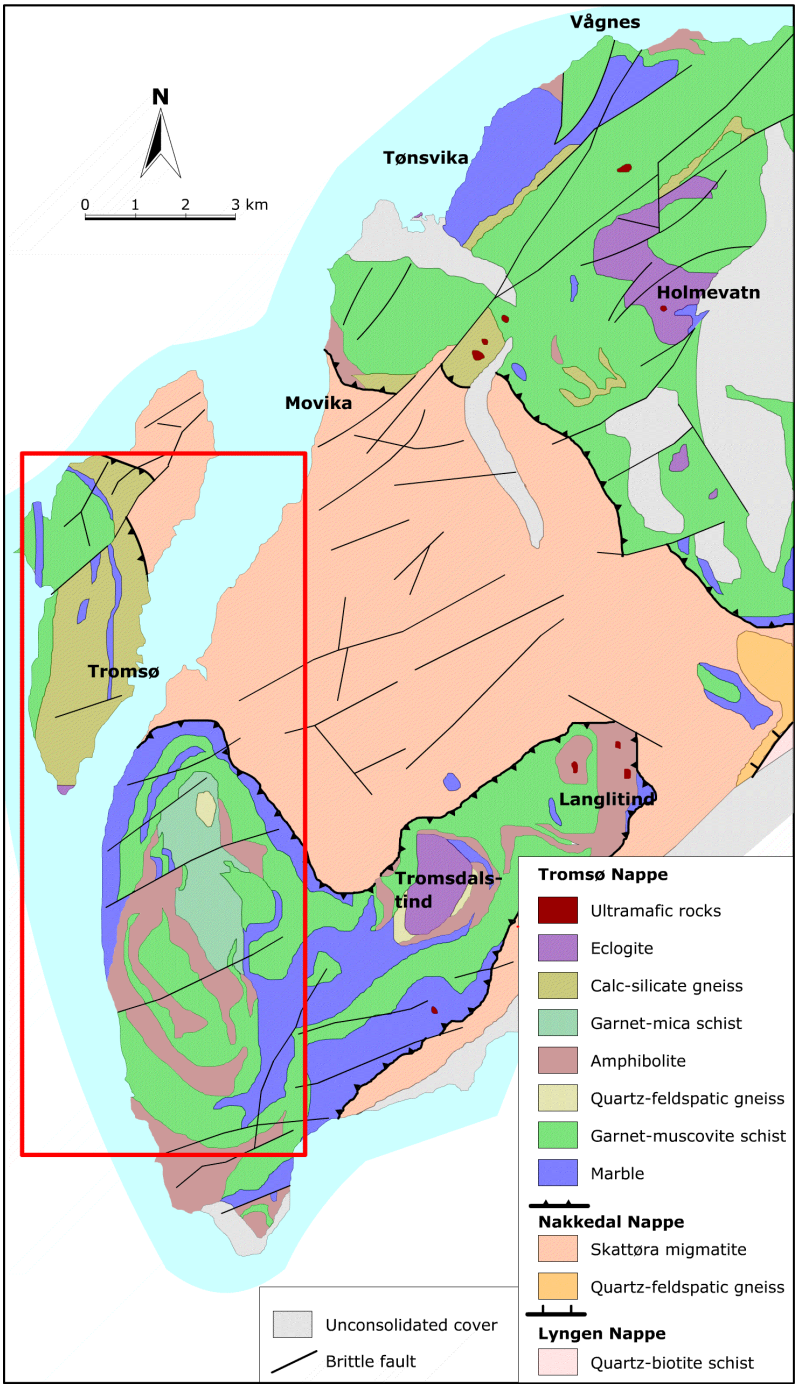

Figure 4 Tectono-stratigraphic map of the Tromsø area showing the Tromsø Nappe and approximate position of the iron bearing rocks (box).

More recent studies confirm the basic outline of deep subduction followed by uplift and a second episode of burial and imbrication on top of the Nakkedals Nappe, but diverge on PT-conditions. Corfu et al., 2003 places the age of the peak of the first high pressure episode at 452+/-1.7 Ma and uplift at 450+/-0.9 Ma, substantiating rapid uplift. (RAVNA and ROUX, 2006) estimate the PT conditions of the first phase to go from 1.4 GPa at 675°C up to 3.36 GPa and 735°C. Figure 5 shows the PT paths inferred by the earlier mentioned studies.

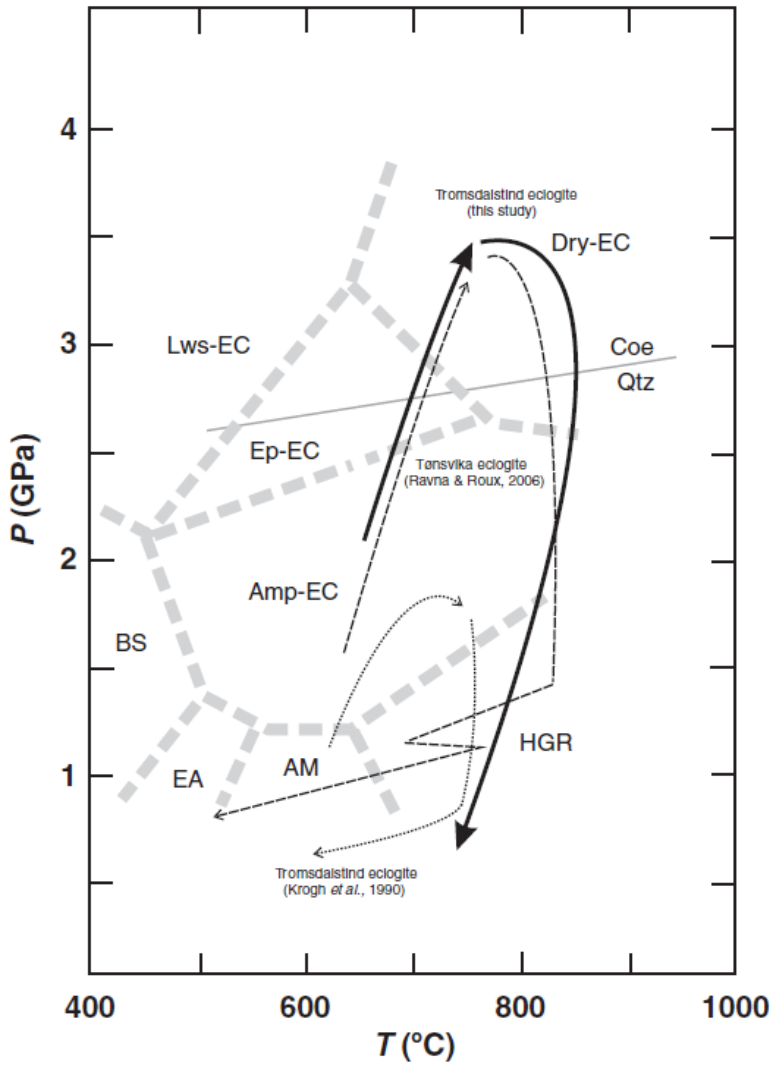

Figure 5 P-T Paths in the Tromsø Nappe from (JANAK et al., 2012).

3 Pervious Works

During the early 20th century there were made significant efforts to explore the magnetite rich rocks in the Tromsø area. The exploration activities got to a point where one was starting to plan a mine around 1909-1912 and several reports were commissioned (Hasselbom et al., 1909, Smith, 1909, Smith, 1910, Mathieu, 1911) for "A/S Nordenfjeldske Jern og staalverker" on their properties in the Tromsøsundet iron ore field. The plans called for a mine with an enrichment plant and a steelworks with electric arc furnaces and own power supply.

These efforts failed to establish an iron ore mine. The exploration of the deposits continued until 1918 but the available documentation ends by 1912. Some pieces of these works is found in some of the reports from the 1940s (Eriksen, 1943, Eriksen and Bugge, 1943), when interest in the fields were renewed. These reports from the 40s are criticized by the leader of the exploration activities before 1919 C. Lian and one of the earlier authors H.H. Smith (Lian and Smith, Mars 1944).

There was some interest in the field in 1948 but the 1944 report was apparently used to dismiss the field (Riiber and Smith, 1948).

Of more recent date is a 1967 a total intensity magnometry survey was flown over the main portions of the field (Håbrekke et al., 1967) and detailed mapping of parts of the area by T. M. Broks in 1985 (Broks, 1985).

3.1 1900 to 1920

During the early 20th century exploration activities in the field were carried out by "A/S Nordenfjeldske Jern og staalverker". A series of expert reports were made for raising capital in the international markets, "*Aktieneinladung mit rentabilitatsberecnungen fur A/S Nordenfjeldske Jern og Staalverker"* (Hasselbom et al., 1909) contains reports by Alfred Hasselbom, Th. Melvær, R. Stoeren and H.H. Smith edited and translated into German by H. Boholm. There is also an updated report by H.H. Smith (Smith, 1910) and a report by Mathieu (Mathieu, 1911).

The reports describe the location of the ore, the regional geography, climate and geology of the field. The reports then continue to descriptions of the locations of the individual ore deposits and characteristics of the ore and at the end calculate the tonnage.

All of these early reports describe the main deposits as being south of Tromsdalen and east of Tromsøsund and between the Balsfjord and Ramfjord on the eastern side of the Ramsfjord-peninsula, with a few deposits of minor interest west of the sound on the Tromsø

Island. The field extends for about 9 to 10 km from north to south and 3 to 4 km from east to west on the east side of the sound. The fields exposed ore area is given to be around 270 000 m^2 (Hasselbom et al., 1909). A map with profiles and some deposit numbers is attached to R. Storens report (Appendix D).

3.1.1 Occurance

R. Storen (Hasselbom et al., 1909) states that the ores are found in the Tromsø-mica-schist group which consists of regional metamorphosed schists, mostly quartz-, amphibolite-, epidote-, garnetbearing mica –schists and crystalline limestone (marble). In some of these mica and quartz schist, iron ore in the form of magnetite can be found both as a primary constitute and as an accessory. In the magnetite bearing schists there can sometimes be found iron poor schists. The layers continue with different pyroxene and mica gneisses and chalk schists.

R. Storen goes on to claim that these schists have been under "great pressure" and are folded, the main strike is NNE and the main dip is toward the west. Garnet and epidote indicate high pressure and is mostly found on top of the ridge and on the east side where the pressure has been the highest. According to R. Storen, at a place at the top of the cleft the pressure has not been directed entirely parallel to the layering causing displacements thus rendering the deposits discontinues. The magnetite bearing schists is associated with marble on both upper and lower sides of the deposits.

A. Hasselbom in (Hasselbom et al., 1909) states that work was carried out in Kalvedalen, Møllendalsaksla, Sollidalen north and south of the river, Fløyfjellet both north and south of this, Nordberg with more to expose these "iron bearing formations". Further he states that some of the ore bearing strata appeared to be parallel, while others appear to be on the same stratigraphic level.

Figure 6 shows the names of most of the deposits that are mentioned in the text.

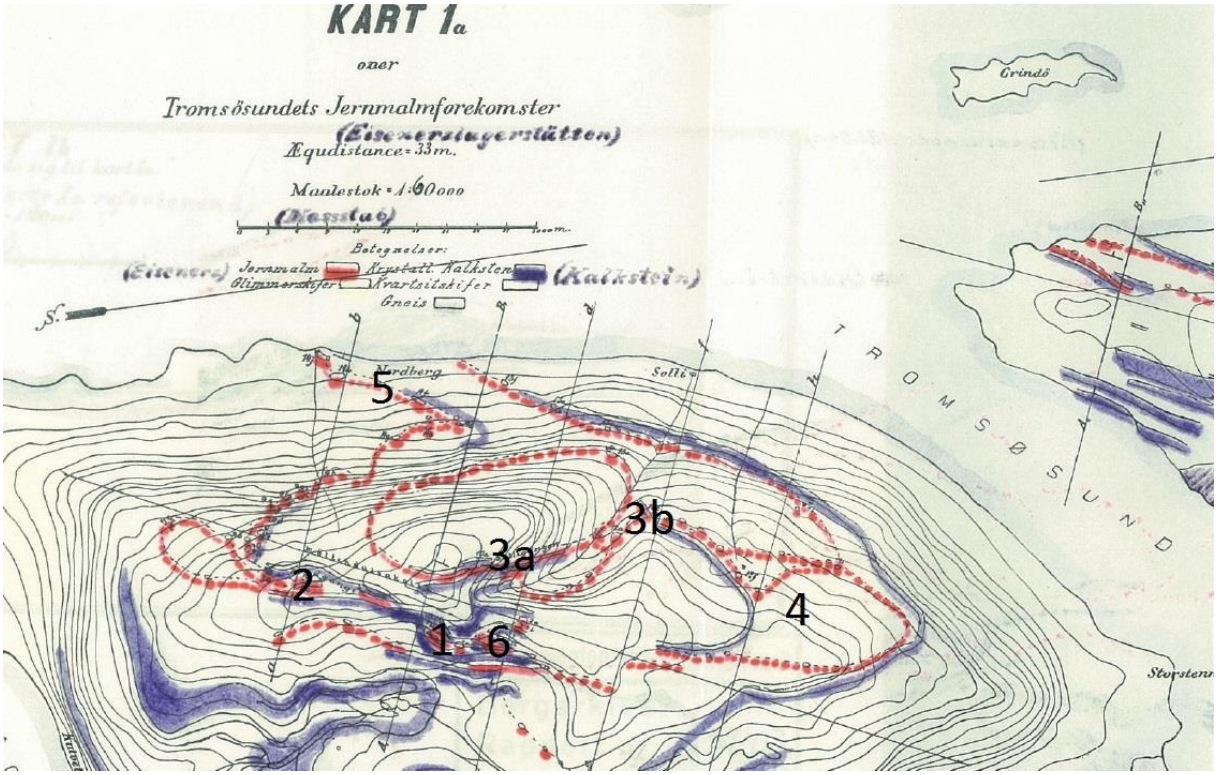

Figure 6. R. Storens map with location of the main deposits in the text. 1. Kalvebekli-deposit. 2. Møllendalsaksla/Sollidalsaksla`s deposit. 3a Solligangen/Sollidalen south of the river. 3b. Sollidalen north of the river. 4 Fløyfjeld/Bøntuva. 5. Nordberg. 6 The Solliskar deposit.

Kalvedalen

A. Hasselbom (Hasselbom et al., 1909) lists the extent of the ore deposits; the ores of the Kalvedalen (Djupdalen) are found between 550 and 700 m.a.s.l. and are exposed in a length of about 1000 m with average thickness of 25 meter. In most of this area the ore zone is not exposed, thus the thickness mentioned is a minimum thickness. In the footwall there is micashicst and limestone, in the hanging wall there is quartz rich micashist and some limestone.

Mathieu (Mathieu, 1911) reports that these deposits consist of 4 iron ore deposits and a graphite deposit. Maximum thickness of a deposit here is 70 m and the average for the main deposit is 54 m. The hill side that can easily be pit minded is from 525 m.a.s.l. to 725 m.a.s.l.

Møllendalsakslen/Bredgangen

A. Hasselbom in (Hasselbom et al., 1909) states that the ore on Møllendalsaksla (Sollidalsaksla) occur from 650 to 760 m.a.s.l. The ore is exposed in a length

of 900 meter. Average thickness is approximately 30 meter as a minimum; the wall rocks here are mica schist and gneiss.

Mathieu (Mathieu, 1911) has the following to say about the Møllendalsasklen deposits; in the southern plateau at a height of 700 m.a.s.l. there is a colossal deposit that has been explored by large exploration trenches. The ore is visible in a length of 950 m N-S with a dip of 45o to the west. The total thickness of the three parallel deposits varies from 40 to 105 m, total thickness in the thickest are 150 m consisting of 30 m ore, 5 m schist, 50 m ore, 25 m schist and 30 m ore. The deposits here are separated by schists. He expects the deposits to extend for 1300-1350 m although the observed length is only 950 m. The ores of the plateau can be divided into three types, a fine grained and a coarse grained magnetite ores. The third is not described.

Sollidalen

A. Hasselbom (Hasselbom et al., 1909) states that in the Sollidalen valley, the ore can be found both north and south of the river from 550 to 790 m.a.s.l. This ore is exposed in a length of 1450 meter and an average thickness of at least 25 m.

According to R. Storen in (Hasselbom et al., 1909) the Solligangen deposits on the southern side of the valley can be followed for 1580 m. The Solligangen deposit (10a) can be followed for 1450 m along the strike and 850 m in the dip direction.

Fløyfjellet (Bønntuva)

A. Hasselbom (Hasselbom et al., 1909) states that the ores of Fløyfjellet (Fløya, Bøntuva) can be found north and south of the summit at a height of 400 to 530 m.a.s.l. The ore is here exposed in a length of 1200 meters with an average thickness of 15 meter.

Deposits at Nordberg, the Tromsø Island and others

A. Hasselbom (Hasselbom et al., 1909) states that there are more deposits than what he describes in his report; these deposits such as at Nordberg and other places. With instrument (the type is not specified but most likely some kind of magnetic susceptibility measuring device) there has been proven an exposed ore area of 277 000 m2.

R. Storen (Hasselbom et al., 1909) says that the most promising deposits on the Tromsø Island is located at the farms Holt and Kveldstuen.

Mathieu has the following to report about the deposits west of Sollidalsaksla; there are deposits with 10-15 m thickness at the edge of the sound, however these deposits are not well explored. In addition there appears to be several 10 m thick exposures on the western flank of the mountain above Nordberg.

R. Storens map (Hasselbom et al., 1909) which can be found in Appendix D numbers the deposits but also shows the names of some of the deposits, the named deposits are indicated in Fig. 6. In his description he differentiate between two stratigraphic levels named after the deposits 10a Solligangen and 3b Bredgangen.

The deposits of the Møllendalsaksla/Sollidalsaksla were given the numbers 7a-c and 3a-b also deposits 9a-h are on the western slope of Sollidalsaksla above 300 m the Southernmost deposits at the fjord in R. Storens map.

The Nordberg deposits are designated with 14a-j.12a, c, f (Appendix D) are on the Western flank of Bøntuva-Fløyfjeld. 2a, b are on Bøntuva north of Soliskar. Deposits designated with 13 are on the slopes of Sollidalsaksla between Nordberg and the Solli River. 5a-c are the so called Kalvebekkli-deposits. Deposits 3a-b are the Solliskar-deposits just west of the Langgangen deposit 1a. On the western slope of Bønntuva-Fløyfjeld in northernmost part are the deposits designated with 11. The numbering of some of the deposits is not readable on this scanned version of the map.

3.1.2 Qualities of the ore

R. Storen lists samples he has collected from some of the deposits, table 1. He points out that there are several places where there might be direct shipping-grade ore of 40-60% Fe, in particular deposit 3b, 5a, 7a, 11a and 11.1. The bulk of the ore at deposit 3b have specific weight of 3.9 and an iron content of 38-39%, 0.2-0.3% P 0.1-0.2% S. The same is the case for deposit 4 but with slightly higher phosphorus content. At deposits 5abc the iron content is slightly lower, 34% on average.

H.H. Smith further describes these higher iron content ores with more than the regular 30-40% Fe. These ores can be found in thicknesses from 0.8 to 2 m in parts of Kalvebakken and also on Fløyfjellet and some places in the Solligangen. How big part of the field that these ores constitute he cannot say, but he thinks they account for a large part and that they will be important for any eventual operation.

As they claim there is no sharp distinction between the ore and wall rock it is difficult to determine what should be counted as ore and what is not. There was at the time of

the report done a great deal of work on Fløyfjellet and he suggests that more work is done at Møllendalsaksla. He has not taken any samples.

R. Storen has also done enrichment tests and concludes that dark minerals don't affect the end product significantly. There is also numbers for a poor ore type with 30% Fe and the results are similar for the normal sample with 37% Fe, after using a finer milling.

The ore contains a wide variation of magnetite grain sizes from very fine grains to 1mm to 1cm large grains. The ore that contains quartz is usually easy to crush. In his report he gives details on crushing experiments.

R. Storen then claims the eastern deposits are milled one can assume 2.4 t raw ore, 35% Fe to 1 t fines at 66-68% Fe. The ratio might come down to 2.3:1. Most of the field is quartz bearing which gives comparably high retention of iron during magnetic separation; other parts are pyroxene and almandine garnet bearing which also are magnetic.

According to H.H. Smith in the reports BA4177, BA2912 and BA2255 (Hasselbom et al., 1909, Smith, 1909, Smith, 1910) the ore appears to be banded or layered and schistose, the stripes consists of quartz and fine grained magnetite in layers of different thickness, from mm sized to considerably larger.

Smith also differentiates between two types of textures of the ore. A crystalline grainy texture and a porphyric texture, the crystalline grainy textures comes ranges from fine grained to coarser grained. The porphyric textures he has only seen on the top of Møllendalsaksla and in a spot on top of Fløyfjellet. The porphyric type contains pea sized magnetite grains in a fine grained magnetite matrix.

Lager-stätte	%Fe.	% Fe. mtg.	mg.	Hb.	Gr.	Ep.	Qu.	Gl.	Erz	Struktur
	29,9		"	"	"	"				fk.
	32,8		"	"	"					"
	48,8		"	"						"
	46,8		"	"						"
	35,2		"	"						gstr.,mtg.
	49,6		"	"						" "
	52,5		"	"						g.
3b.	20,4	39	"	"				"		gstr.,mtg.
	19,3		"	"	"	"		"		"
	38,3		"	"	"	"				"
	50,4		"	"						kompakt.
	57,8		"	"		"				komp.,d.
	62,4		"	"		"				" g.
	19,2			"			"			gstr.,fk.
	21,9			"			"			"
	16,8		"	"			"			
	29,2		"	"			"			k.
3d.		23								
	30,8		"	"						fk.
	14,2		"	"						k.
	19,2		"	"	"	"				mf.
	29,6		"	"	"	"				ausgeprägt
5a.	37,9	34	"	"	"	"				körniger
	35,6		"	"	"	"				Erz.
	47,2		"	"						
	42,4		"				"			gstr.,g.
	52,8		"				"			komp.,g.
7a		38								
	30,1		"	"			"	"		gstr.,g.
	36,8		"	"			"	"		"
	33,4		"	"						Mischung
7c.										von
	32,2		"	"						g. und fk.
	19,5		"	"	"	"	"			mtg.
	30,8		"	"	"	"	"			g.
6.		27,5	"	"			"			
	29,2		"	"		"	"			fk.
	30,4		"	"			"			g.
	19,9		"				"			gstr. k.
	35,2		"	"			"			"
	29,6		"	"			"			"
10a.		30,6								
	30,4		"	"			"			"
	36,8		"				"			gstr.,gk.
	31,8		"				"			"

Table 1. Table "mineral content" from R.Storens report in (Hasselbom et al., 1909). Lagerstate - Deposit number, Fe % mtg – average Fe content it can be assumed the Fe % is given as total Fe by weight. Minerals; Mg. – magnetite, Hb. – Hornblende, Gr. – Garnet, Ep. - Epidote, Qu. –Quartz, Gl. – mica. Grainsize; fk. – finegrained, k. –grained, mtg. – medium coarse, g. – coarse, where fk<k<mtg<g in size but it is uncertain what the absolute values of the sizes are. Gstr. – banded, kompakt – massive.

Appended to H.H. Smith`s report (Hasselbom et al., 1909) are geochemical analyses of the rocks and enrichment trails. The geochemical analyses of 11 samples were done by Th. Melvær at Norwegian-American Copper mining and smelting Co.. The result of these 11 analyses can be summarized as: between 30.39% and 41.31% Fe, 0.179% to 0.496 P. average 35.45% Fe, 0.07% S, 0.334% P+As, 2.97% Al2O3+TiO2, 9.81 % CaO, 3.30 % MgO, 0,15 % Mn, 32.43 % SiO2 and 1.05 % CO2. The analyses were done in September 1908.

Also Enrichment trails were done at Metalurgiska Patentaktiebolaget, Stockholm, Sweden, September 1908 and Mars 1909. The results are presented in table 2.

		Crushed to 1/6 mm		*First fines crushed to 1/10 mm*	
	In	*Fines I*	*Waste I*	*Fines II*	*Waste II*
Fe	*44.20 %*	*70.2 %*	*12.3 %*	*71.3 %*	*14.2 %*
P	*0.308 %*	*0.02 %*	*-*	*0.01 %*	*-*
S	*0.96 %*	*-*	*-*	*0.06 %*	*-*
Amount	*100 %*	*55.2 %*	*44.8 %*	*98.8 %*	*1.8 %*
Iron retained		*87.8 %*		*99.6 %*	

Table 2 Enrichment trails results. Note in the summary of the report fines and waste have been mixed-up. From (Hasselbom et al., 1909).

The results are equivalent to iron retention of 87.2% of the original iron content of the raw ore. There are presented another 2 trails, which were done in Mars 1909 after the same method as in 1908 but with ½ mm instead of 1/6 mm and 1/6 mm instead of 1/10 mm. This resulted in 72.2% iron retained from a sample of 35% total Fe and 83.4% for a sample of 43% total Fe.

3.1.3 Quantity

Mathieu (Mathieu, 1911) estimates the ore quantities as 24 Mt at Solligangen (100 m along dip), 16 Mt at Kalvebækli (45 m along dip), 29.5 Mt at Solliskar (different lengths along dip for the different deposits, between 30 and 125 m) and 17 Mt at Bredgangen (100 m along dip) which gives 86.5 Mt with an average grade of 34%. He stresses that the numbers is just given to give an idea of the scope of the project and he also points out that these calculations were done at just 18.5 of 2160 ha, 1/116 of the area that's mineralized.

H.H. Smith's opinion of the ore amount; from the special maps (probably the same maps that were used for R. Storens maps) he estimates an area of at least 277 000 m^2 and he somehow gets to 15.75 M m^3 total, although he doesn't make it clear how he gets this number. 15.75 M m3 which corresponds to 56.7 Mt raw ore. For 75% recovery this corresponds to 42.525 Mt ore. He makes a point of these numbers being only an indication of what there might be in the field given proper investigation and continues on with claiming there should be hundreds of Mt of ore above sea level.

R. Storen does his calculations on basis of the topographic map, exposed parts, exploration ditches and profiles that have been made and claim one can easily make good estimates of the tonnage since the topography makes it easy.

When he calculates the ore amounts, he makes three groups of confidence. The first contains knowledge from currently exposed areas and the dip of the schists, the lowest and highest exposures, and the specific weight from a number of analyses. The second level is somewhat confident; these numbers are based on the first level and exploration ditches, non-continuous deposits and with the use of 30 m thickness for these. The third level is uncertain as he uses the numbers from the first two confidence intervals and assumes they continue as shown in the profiles. The table of R. Storens calculations is shown in table 3.

Deposit Number	Exposed area in projection (m^2)	Extent in case			Height difference* (m)	m^2 confident ore area	m^2 somewhat confident ore area	Lenght of extent in direction of the dip from profiles (m)	Spesific weight	Confident ore amount		Somwhat confi-dent ore amount		possible ore amount	
		Exposed lenght	Thickness							M m^3	Mt	M m^3	Mt	M m^3	Mt
			Max	Avg											
1abc	23230	1600		25	22	8700	40000	22	3.5	0.19	0.66	0.88	3	8	28
2ab	8550	300	40	25	20	8000	8000	550	3.7	0.16	0.59	0.16	6	4	15
3ab	23520	450	60	50	46	20000	23000	550	3.9	0.92	3.50	1.06	4	12	45
4abc	10160	360	45	40	52	15600	20000	250	3.9	0.81	3.16	1.04	4	5	18
5abc	24690	980	30	23	100	22600	25000	250	3.7	2.26	8.36	2.5	9	6	22
6	13300	320	35	30	10	9600	27000	100	3.4	0.1	0.34	0.27	0.9	2.6	9
7abc	47860	700	40	30	60	21000	22000	1000	3.7	1.26	4.66	1.32	4.9	18	67
8ab	16600	310	70	28	55	17000	17000	600	3.6	0.93	3.35	0.94	3.4	10	36
9a-h	5000	1200	40	30	350	7800	36000		3.7	0.23	0.85	12.6	46		
10a	56800	1580	60	30	270	47400	47400	850	3.5	12.8	44.0	12.8	44.8	41	143
11a-l	21690	1350		30	145	13800	40500	850	3.7	0.97	3.50	5.8	21.5	34	128
12a-f	5000	600		30	140	5100	18000	600	3.6	0.1	0.36	2.5	8.5	11	40
13a-f	5000	800		30	200	7500	24000	450	3.4	0.37	1.25	4.8	16.3	10	34
14a-j	16250	1500		30	130	21000	45000	230	3.5	0.42	1.47	5.8	20.2	11	35
Sum	277000	12km		30	90	2251000	3993000	400	3.5	21	76.00	55	193	176	618
					140										
* Height differance betwen highest and lowest point of the deposit															

Table 3. Translated table from R. Storens report (Hasselbom et al., 1909)

A. Hasselbom estimates the tonnage of the field. He assumes the area of ore to be 270 000 m^2 and the specific weight of the ore to be 4.8 g/cm^3 which he rounds down to 1 Mt/m in the direction of the dip this gives 250 Mt for 250 m in the direction of the fall. Further he claims that the tonnage estimate is low, since the deposits to the south of the sollidals-river (5-700 m.a.s.l.) are at the same stratigraphic level as the deposits at Nordberg (sea level) and several kilometers apart.

Concluding remarks from the 1909-1911 reports

According to Mathieu (Mathieu, 1911), the exceptional location between two close by fjords and the size of the deposit will make that these mines can be operated with profitability. The technics for magnetic ore separation were well known and tested by that time (1911). He also states that these deposits are more favorably located than the Syd-Varanger field where they were operating a 20 km long railway.

He then goes into a sales pitch, where the only thing that's of import is his statement that the production will be the subject of big capital.

R. Storen (Hasselbom et al., 1909) points out that the topography will be deciding the sites of port and enrichment facilities, the main mining method initially is suggested to be opencast at least at start up. Total ore tonnage that can be mined is estimated at 193 Mt (top two confidence intervals), this can partly be mined as opencast as the topographic conditions are favorable, he assumes a 12km and 30 m thick iron ore deposit with at least 30% Fe to a depth of 140 m. 140 m along the dip is most certainly much less than the real extent, which most likely is ½ km or more along the dip, giving a quantum of more than 600 Mt.

He ends his report by stating that systematic exploration of the field will take a long time even though the natural conditions make such an undertaking easy. And with the current knowledge of the field (1909) it is a given that the total amount of ore that can be extracted is not limited by the figures given above. It is not an exaggeration that the total amount of ore in the field exceeds 1000 Mt.

3.2 Activity in the 1940s

Reports by J. Bugge and A. Eriksen from 1943 (Eriksen and Bugge, 1943) describe their finding from field work carried out in 1942 and 1943. Their work appears to be primarily concerned with the deposits at Solliskar and Solligangen. Both drilling and

exploration trenching were carried out on these deposits after a vertical magnetic intensity study were done.

3.2.1 Report by Jens Bugge

J. Bugge (Eriksen and Bugge, 1943) undertook field recognition from 19 to 27 July 1941, in the area of the Tromsø ore field using 1:100 000 and 1:200 000 maps. He later got ahold of a report by R. Storen, probably the one contained in (Hasselbom et al., 1909). He agrees with its main features.

The ore containing area is chiefly made up of sediments of the Tromsø-mica schist group. The Tromsø mica schist group consists of strongly regionally metamorphosed mica and hornblende schists alternating limestones, sandstone schists and so on. The iron ores in the field are limited to two stratigraphic levels in this package. The ore must be viewed as being of the sedimentary Bogen-Dunderland type. Even though the ore horizons are of great extent, it is only in places that the ore is of a sufficient grade to be considered for mining. These are foremost the deposits of Solliskar, Kalvelibaken, Møllendalsaksla and Solligangen.

The sediments in the area are strongly folded with fold axis approximately N-S, verging toward east. Overturning of the folds can be seen in places, partly also overtrusting, in the same direction. Observations south of Lake 451 in Kalvebakdalen fold structures (parasitic folds) in marble layers show pressure to be from the west. Same kind of folding can be seen just above the Kalvebakli deposit. He then describes the profile he made (figure 7) and notes the western side of the fold is less deformed then the eastern.

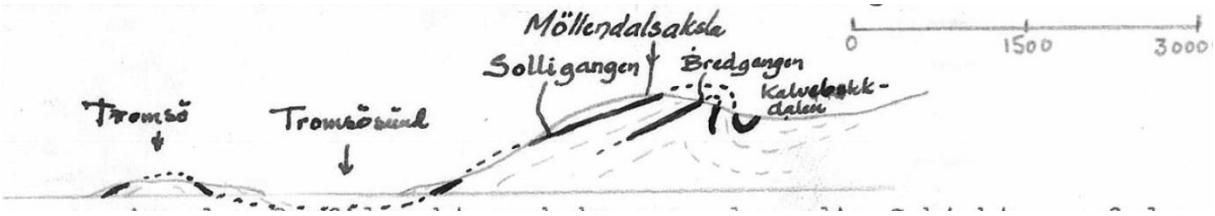

Figure 7. Schematic profile by J. Bugge, the profile extends from Tromsø NW and to Rødryggen SE.

On the west side of the fold the deposits can be followed for fairly long distances. Both above and below the ore bearing schist are mighty marble layers. On the eastern side of Sollidalsaksla, the deformation has been so strong that the ore bearing zones to some extent has been torn apart, resulting in the isolated deposits of Solliskar, Kalvbakli and Møllendalsaksla which originally probably belonged to the same stratigraphic level. Even

inside these deposits the ore can't be followed continuously. In Kalvebakli and Solliskar smaller lenses of ore can be found wholly surrounded by limestone.

One thing that detracts from the grade of the ore is the strong metamorphism that the area has gone through. The ore minerals have reacted with the wall rock and formed iron bearing garnets, hornblende, green pyroxene and epidote, which are common gangue minerals of this ore. Quartz, calcite and some apatite were also observed in thin sections. Magnetite is the only ore/opaque mineral that he reported.

That iron rich reaction minerals were formed can also be seen in chemical analysis and cores, giving large differences in total iron and magnetic iron.

J. Bugge summarizes that the extent of the iron ore bearing schist formations but the quality and thickness of the ore is significantly less than what former reports clamed. The eastern deposits show so much deformation that this will impact negatively on a mining operation.

3.2.2 Eriksens report

Detailed logs of the drilling and trenching are presented in their report (Eriksen and Bugge, 1943). Some of the boreholes appear to be re drilling of the 1917 drilling campaign. The drilling done in 1942 consisted of 228.47 m drilled with calyx type "scrap steel" (182.71m) and double core pipe diamond (45.76m) drills. The core percentages were between 80.2% and 100% (avg. 94.4%) for the calyx drill and 100% for the diamond drill. The core size of the diamond drill was 22 mm.

All the drilling done in 1942 was done on the Solliskar deposits. All core samples from the ore zone were crushed so they easily could be split in a coarse splitter, ¼ of the material was then further crushed for a further splitting into 5x80 grams samples for chemical analysis.

Eriksens evaluation of the Solliskar deposits

These deposits are made up of numerous ore "layers", varying from a few decimeters to 8 m thickness, separated by schists and limestone layers of similar sizes. The analyses of the ore zones with thickness from 4 to 20 m show raw ores with average total iron content of 21.2%, 15.9% HCl soluble iron and only 11.8% magnetic iron (the HCl soluble iron is the percentage of iron not of the total, while the magnetic iron is the amount of iron that is magnetic in the total) and 0.25% phosphorus. The ore is thus even poorer than the ones

found in Bogen and Sørreisa deposits and thus economically worthless. The microanalyses indicate the ore need to be crushed down below 150 mesh.

Solligangen

Magnetometry and field studies in 1942 established the northernmost 600 m of this deposit to be the most promising. During 1943, 5 diamond drilled cores (293.2m) were made and a few exploration trenches were studied. The ore samples were treated the same way as in 1942.

Evaluation of the Solligangen deposit

The core profiles and analyses show there being 1 to 3 main ore zones, all with a strike NNW and dip of 30 to 40 degree to the west. The thickness of the zones ranges between 11 and 1.5 m with total iron contents between 18 and 24%. The lower zone has an average thickness 9 m, which is the only that eventually could be mined, with 22.2% total iron, 16.9% HCl soluble iron, 14.0% magnetic iron and 0.39% sulfur.

This ore is so poor that it will be necessary to use 5.5 to 6 tons of raw ore for 1 ton product with 66% Fe. The Solligangen must therefore be considered as worthless as the Bogen and Sørreisa deposits.

Eriksen summarizes the findings in R. Storens report from 1909 (Hasselbom et al., 1909). Before he concludes he finds the thickness to be half of what the earlier report indicated in the examined parts and the ore poorer.

Eriksens Conclusion

Eriksen then concludes after having investigated the apparently richest parts from the magnetometric survey, that the ore in these parts only contains 12-14% magnetic iron. In addition he notes it might be problematic to keep even this grade under an eventual mine.

For the production of 1 ton of 66% product it will be necessary with 6 tons of raw ore. The deposits are irregular with lenticular shapes with interlaying unmineralized parts, similar to those in Bogen. The dip is not favorable for mining operations. The thickness is not great only 4 to 20 m. The tonnage could be big due to the extent, but being spread over a considerable area is something that is not favorable. Eriksen does not make any judgment on how large the amount of potential ore is from these surveys.

3.4 Dispute

A short exchange of letters between C. Lian who was in charge of all of the prospecting done on the field until 1917 and H.H. Smith is documented in BA3159 (Lian and

Smith, Mars 1944). The first letter is from Carl Lian who writes to H.H. Smith as he had previously been to the field and he wants to follow what is being written about it.

The iron ore field was given to A/S Syd-Varanger 12/5-1942. Upon this some exploration activity was undertaken. Lian's opinion was that they did rather superficial work. Due to this "shoddy" report the fields were dismissed.

Also Lian finds their judgment not to relate to reality. In 1915 there were dug two exploration drifts and and Lian points out that these drifts would be a natural starting point. However, these drifts are not even mentioned in the reports. He observed the pure magnetite layers to be very brittle and black. During drilling in Solliskar in 1917 he observed the rock cutting/drilling mud was black where they had loss of core. The mud wasn't taken care of by the drillers which he very much regrets. Lian complains about the inconsistencies and that Eriksen stopped drilling when they got into the ore (Figure 8).

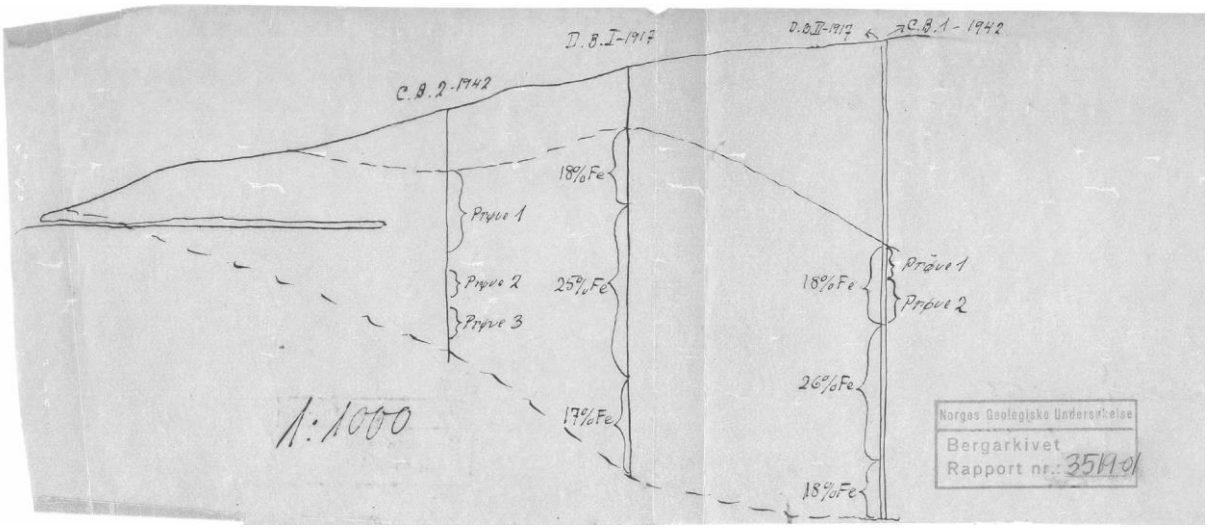

Figure 8. Sketch illustrating the 1917 (D.B.I-1917 middle and D.B.II-1917 right) and 1942 (C.B.1-1942 left and C.B.2-1942 far right) drill holes attached to C. Lians letter. Note the C.B.1 1942 stops when it gets into the ore.

What Lian finds most peculiar with the report of Eriksen is that the ore is so little magnetic; with it being very magnetic is one of the most distinctive features of the ore. He appears to be quite upset that Syd-Varanger only finds about half the ore to be magnetic. He refers to R. Storen's enrichment experiments on the ore in Sweden (in (Hasselbom et al., 1909)) as to the magnetic nature of the ore. There are also parts from 0.1 - 2 - 3 m containing rich ore with grades of 50% and more.

C. Lian thinks the way Syd-Varanger is condemning the fields outrageous**.**

H.H. Smith's reply starts by summarizing the report. Upon which he comments the report not being entirely in the realm of the real and doesn't paint a truthful picture of the field. He remarks that the conclusion is somewhat hasty as the field is deemed unsuitable for economic activity. Anyhow, A. Eriksen is leaving himself a possibility for retreat in his conclusion by pointing out that the scope of the exploration activities was very limited compared to the size of the field.

Then H.H. Smith states that further exploration work should be carried out by blasting, test mining and enrichment tests.

H.H. Smith notes the short time J. Bugge spent on the field and the lack of results for facilitating exploitation. He concurs with C. Lian's assessment of the omitting of the drifts and the drilling stopping when they get in to the ore. On the topic of the magnetic nature of the ore he disagrees with C. Lians interpretation of the data and explains how they should be read: the total content of 22.2% iron, with 16.9% HCl soluble iron and 14% magnetic iron of the total analysis corresponds to 63% magnetic iron. .

What the reason for omitting the rich ore parts during Eriksen's investigation he doesn't understand. He also states that the field has been treated sloppily.

3.5 Later works

A total intensity magnetic field survey was carried out during 1967 (Håbrekke et al., 1967). The survey was carried out by plane. Due to the steep nature of the terrain in the surveyed area there is noted that there is large variation in height above surface for the measurements. This magnetic survey didn't add much new information beyond what is already contained within R. Stoeren`s map from (Hasselbom et al., 1909) except for the few magnetic anomalies north of Tromsdalen in the Nakkedals Nappe.

In the early 1980s mapping was carried out by T.M. Broks in part of the area, most of the work was carried out between Tromsdalen and Sollidalen continuing onto the valley east of Sollidalsaksla/Møllendalsaksla towards Tromsdalstind. It appears when comparing the map in this study with the map from R. Stoerens map from 1909, that during this work the mineralized rocks were mapped as ultramafic, calc-silicate and amphibolite rocks.

4. Methodology

4.1 Sample collection and preparation

A number of samples were collected during the fall of 2012 and late summer 2013. Location of samples can be found in appendix petrology 2. The samples designated EP or DP were taken from various mineralized zones and their wall rocks. The samples that come from the profile in the Solligangen were designated SGP (figure 28). 31 samples were taken in a profile from the Solli "vein" (see Appendix C for sample localities), of these 15 were analyzed for major, minor and trace elements using XRF, another 2 samples were marbles and were not analyzed. One sample, EPG, was collected north of Sollidalen. The remaining samples were collected from the Solligangen deposit south of Sollidalen, the Kalvlibak deposit and the Møllendalsaksla/Bredgangen deposit on Sollidalsaksla.

All useable samples that were carried down in 2012 also the samples collected in 2013 were prepared for thin section, hand sample and XRF analysis by cutting away weathered parts and making suitable cuts for thin section and a sufficient part of the sample were crushed for XRF-analysis.

4.2 Microscopy and EMPA

A number of thin sections were made from the samples collected fall 2012. The samples for the thin sections were selected on basis of being mineralized, that is magnetic and the greatest possible range of textures and compositions. 15 of approximately 21 different mineralized textures were selected.

The polished thin sections were observed using Leica DM LM equipped with a Canon camera. Both reflected and transmitted light were used to determine mineral content. In addition EMP-analysis of 84 "spots" was conducted on a Cameca SX 100 electron microprobe analyzer at State Geological Institute of Dionýz Štúr, Bratislava, Slovak Republic (appendix Petrology1).

Mineral descriptions primarily from *Introduction to Mineralogy* (Nesse, 1999) transmitted light and *Tables for the Determination of Common Opaque Minerals* (Spry and Gedilinske, 1987) reflected light, in addition to EMPA-recalculations and backscatter pictures allowing for optical discrimination of Ti-Magnetite and magnetite.

Formulas for the minerals were calculated according to cation basis and $Fe^{2+/3+}$ were calculated by stoichiometry except for amphibole where the procedure from Recalculated after Appendix 2 of LEAKE et al. (1997). Clinopyroxene formulas were calculated for 4 cations and 6 oxygen; magnetites were calculated on the basis of 3 cations

and 4 oxygen, 8 cations and 12 oxygene were used for garnet, 8 cations and 12.5 oxygen were used for epidote and biotite was calculated at the basis of 8 cations and 11 oxygen. Garnet molecule fractions were calculated after the method of RICKWOOD (1968) but molecules where the cation amounts were less than 0.01 were not calculated. Pyroxenes endmembers were calculated using (Morimoto, 1989).

4.3 XRF analysis

44 samples were prepared for XRF-analysis by cutting into chips which were then put directly into a swing mill and crushed to a suitable grain size. Some samples were crushed in a jaw crusher before being put into the swing mill where they were ground to a suitable grain size.

Major and minor elements were analyzed on fused glass beads which were prepared by mixing sample and the flux agent Lithium-tetraborate (Li2B4O7) at a ratio of 1:7, 0.6000 g sample to 4.2000 g of Li2B4O7 in a small sample container/jar. The mix is the poured into a platinum crucible, which is placed above a turbo torch burner and the mold is then placed on top as a lid. The torch heats the crucible to about 1200 ºC. The liquid mixture is stirred after 3 min and should be ready to pour after another three. The liquid is poured onto the hot mold, the mold is then placed on a hot (approximately 300 ºC) ceramic plate to cool and the crucible dipped into a water bath for fast cooling before being placed in a hot citric acid bath for cleaning. Once the cooling glass bead start to give "cracking" sounds the mold is beaten on the ceramic plate till it loosens which can normally be seen. The bead is flipped on to a piece of non-chlorated paper when it is sufficiently cooled.

However high iron samples (Fe total >20 wt %) tend to darken so much that the bottom of the mold can't be seen and also tend to break before the glass bead lets go of the mold. To counter this last effect a dewatering agent, Lithium iodide (LiI), is added. The amount of LiI needed for the beads to slip was determinated experimentally to be about 100 mg for samples with more than 40 wt % Fe total. At times the high iron samples leave a gray-white coating with varying thickness on the Pt-crucible that is not readily dissolved in a timely fashion in citric acid, to avoid contamination of other samples the crucible was cleaned by melting 4.2 g of di-Lithium-tetraborate in it.

Trace elements were analyzed on pressed pellets consisting of 9.0 g of sample and nine 1g Mahlhlife wax pills which were mixed in a mortar. The mixture was then placed in a piston press and pressed into pills.

The XRF analyzes were done on a Bruker S8 Tiger at the University of Tromsø. Calibration ranges are given in Appendix A. Values lower than the calibration ranges should be good while values above are more error prone in particular for Iron which has a self-absorption effect that would cause the measured concentration to be lower than the real concentration.

5. Field relationships

Since the mineralization of iron oxides here is predominantly magnetite (as mentioned in chapter 3 and will be shown in chapter 6), the magnetic properties of the rocks can be used to estimate iron content to some degree. Differentiation of the samples into un-mineralized, low grade and high grade mineralization's was carried out by a relatively weak neodymium magnet. The magnet was put on the rock and if the magnet was easily removed, the sample was classified as weakly magnetic, if not it was classified as strongly magnetic. Proper magnetic susceptibility readings would make for easier replicated results and better prediction of iron content (Nagata, 1961, Eloranta, 1983).

The magnetite mineralization's occur disseminated in lenticular bodies as described in chapter 3. In a place on Solidalsaksla (EP024) the mineralization appears to be migmatitic and the wall rock appears to be eclogitic (Fig. 9a, c). Most of the mineralized rock is however gneiss. The mineralized rocks have poor cleavage, but are banded usually with less than 1 cm thick bands. However, in some places the bands can be of decimeter scale (Fig. 9b, 13b, c). Variation in composition, scale of banding, grain size and facies makes generalizing the character of the deposits somewhat difficult.

The gangue minerals in the mineralized zones are quartz, amphibole, clinopyroxene, garnet and epidote with minor carbonate and apatite. Marble is commonly found on either side of the mineralized bodies but also inside, as far as I can tell the marble doesn't directly come in contact with the mineralized zones as it is buffered by either calc-silicate rocks/skarn (Fig. 10a) or rocks of intermediate composition.

In Solliskar above the mineralization there is dendritic aplite veins (Fig. 11). The veins, in particularly the larger ones, have melonocratic halos. Just to the east there are calc-silicate rocks /skarn and marble and 600 m to WSW there are some larger aplitic dikes these do not show the same kind of melanocratic halos. This might imply a late stage of

dewatering/decarbonation reactions releasing fluids to drive metasomatism of the overlaying intermediate rocks.

In the Kalvebekkli deposit there are two drifts at 710 m.a.s.l. and 600 m.a.s.l. (Fig. 12). The mineralized rocks found in the dump of the upper of these appear to be of better grades than the exposed rocks (Fig. 13a). The mineralized rock can be followed between these two drifts and further up the hillside from the upper. At the lower drift there is a fold so that the strike of the mineralized rocks and adjacent marble changes from E-W to N-S.

At the Solligangen deposit which appears to be more than 1200 m long, a cross section was mapped after being sampled at an interval as close as possible to 1 sample/meter. Figure 15 shows the resulting profile with approximate position of the samples. The location of the samples can be seen in Appendix C. This was done in an old exploration trench (Fig. 10a, b, 10a). At the top of the trench sits a borehole dipping approximately South West (Fig. 14a) with a dip of 70^{o}, the apparent layering is dipping WSW at about 40 degrees. There is however a fold 20 m to the south that they may have been aiming for. A second borehole was located a bit further north dipping approximately East/44 (Fig. 14b). The thickness of the mineralized zone where the profile was mapped between is about 50 meters. The marble where a contact can be seen appears to form sharp contacts with a small ~1 m skarnified zone.

The deposits on Sollidalsaksla/Møllendalsaksla are often poorly exposed even where there are old trenches. The accompanying marble is a calcite marble.

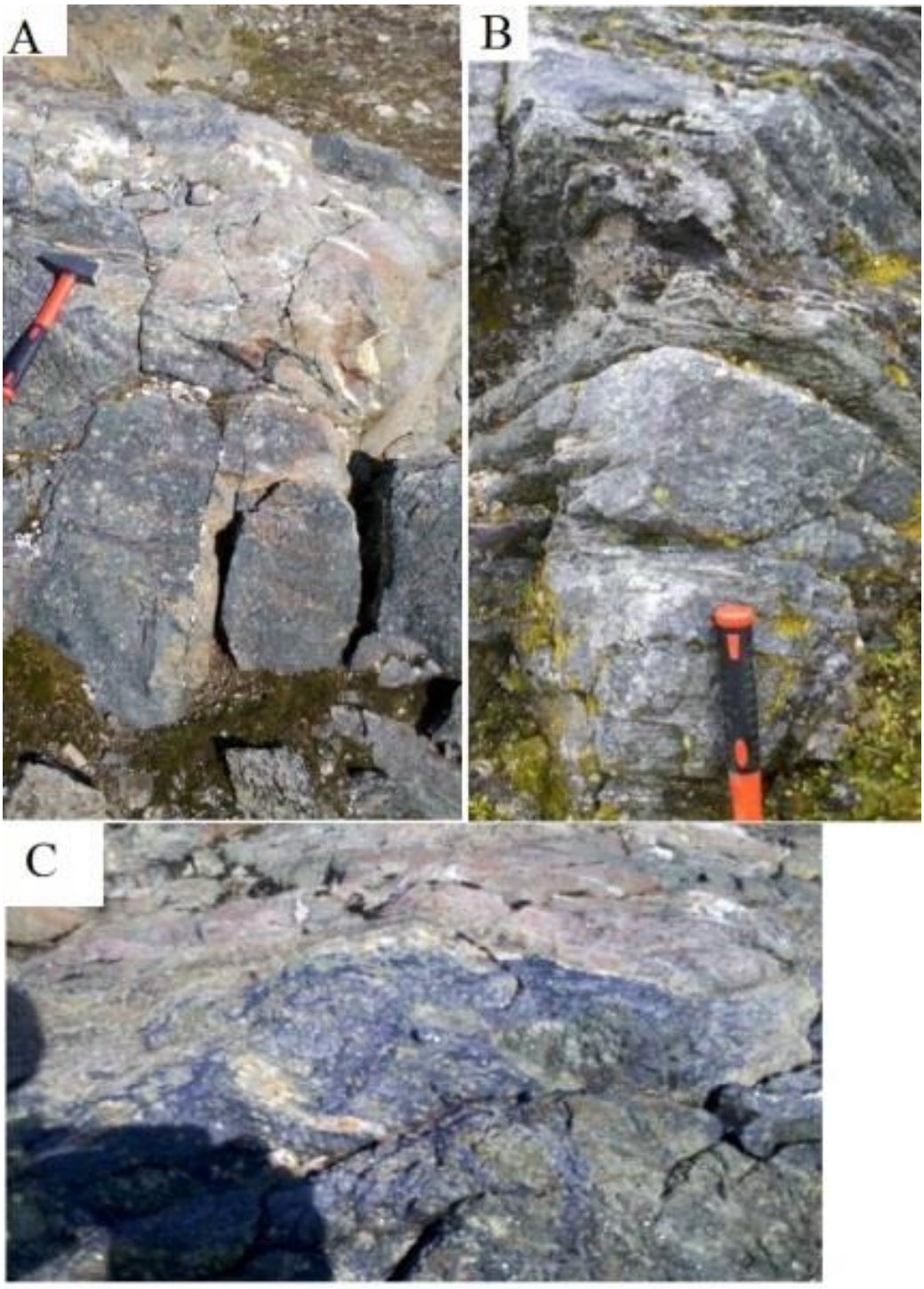

Figure 9 A&C) location EP024 mineralized rock- black-green, lower part, eclogitic (garnet, pyroxene, quartz) wall rock upper right part. B) Decimeter sized bands of mineralized gneiss, middle of the Solligangen profile.

Figure 10 A) Marble inside the mineralized zone Solligangen profile. The mineralized rock starts approximately 2 m above the marble. B) Middle part of the exploration trench from the Solligangen profile.

Figure 11 Dendritic aplite veins with melanocratic halos in fine grained intermediate to felsic rock above skarnoid rock above the Solliskar deposit.

Figure 12 Left; Lower drift at Kalvebekli with recent rock fall. Right; the upper drift dump, drift entrance just to the left of the white + (upper right).

Figure 13 A) Close up of rock from the dump at the upper drift in Kalvebekli apparently made up of mostly magnetite and a yellow-brown weathering mineral. B) "Strongly" magnetic gneiss, magnetite, quartz and green (amphibole, pyroxene or epidote) bands, Solligangen. C) Amphibole Quartz Garnet Magnetite Gneiss, Solligangen.

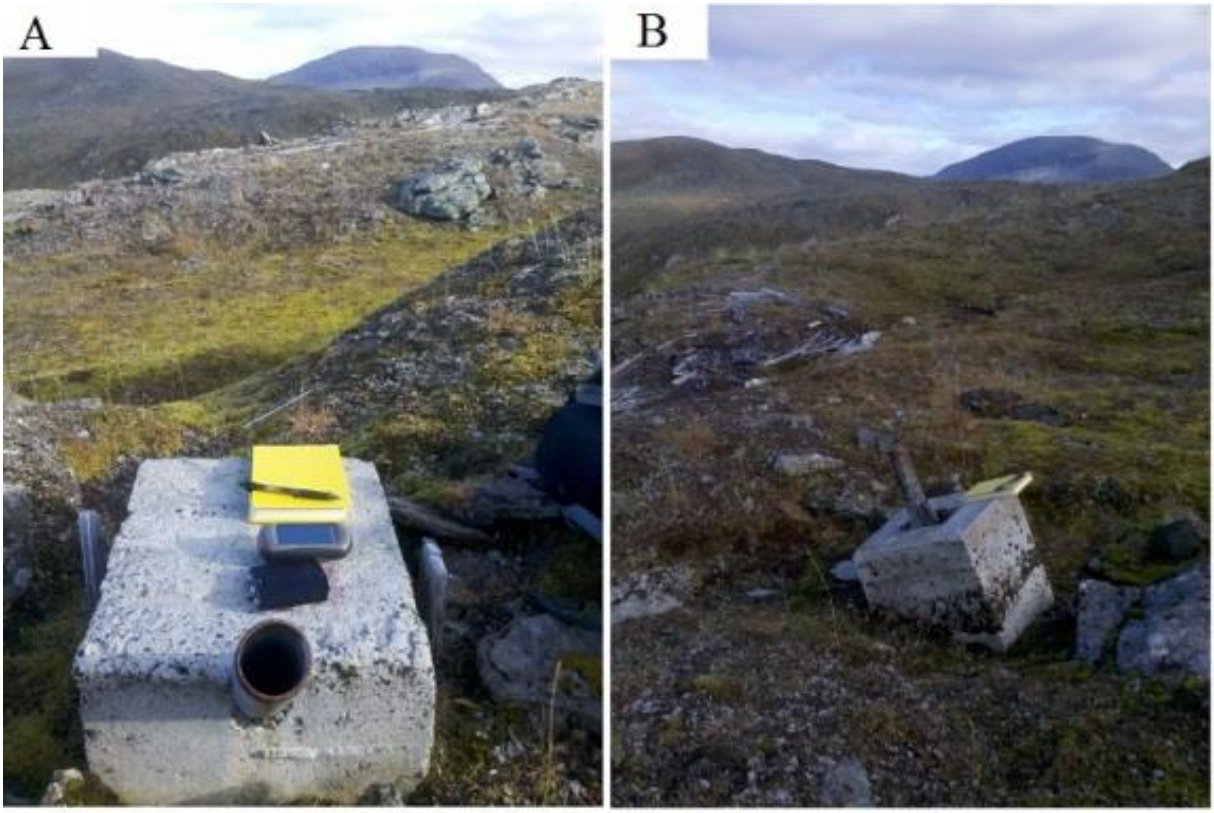

Figure 14 A) Borehole BHSG1 north of the profile in Solligangen, facing east, approximately perpendicular to the marble gneiss package. B) The second borehole above the mapped profile faces about northwest close to the same dip and dip direction of the marble and gneiss. Both pictures with Tromsdalstind in the back ground for reference.

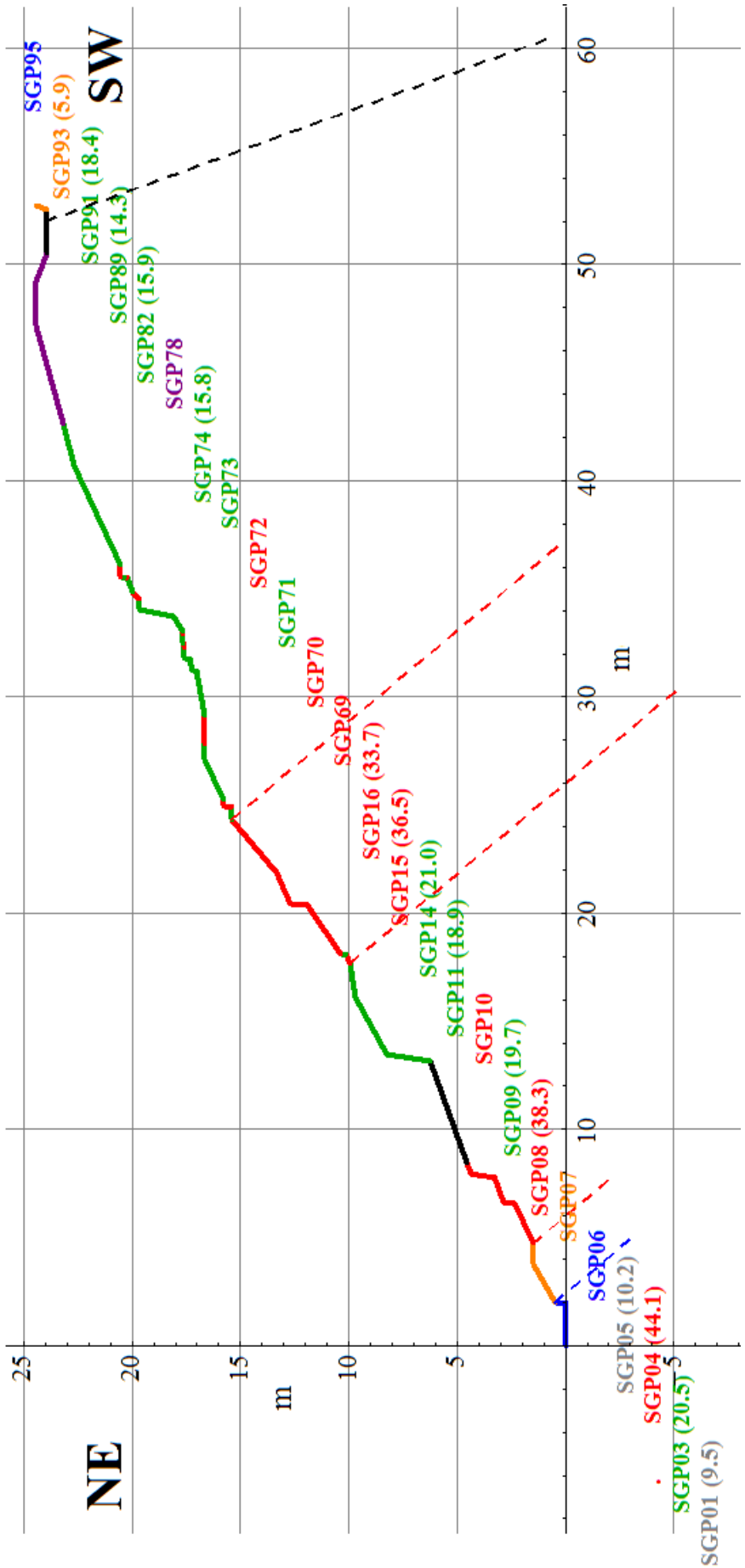
SW
NE
m
SGP95
SGP93 (5.9)
SGP91 (18.4)
SGP89 (14.3)
SGP82 (15.9)
SGP78
SGP74 (15.8)
SGP73
SGP72
SGP71
SGP70
SGP69
SGP16 (33.7)
SGP15 (36.5)
SGP14 (21.0)
SGP11 (18.9)
SGP10
SGP09 (19.7)
SGP08 (38.3)
SGP07
SGP06
SGP05 (10.2)
SGP04 (44.1)
SGP03 (20.5)
SGP01 (9.5)

Figure 15 Solligangen sampled and mapped profile; Profile colors: Red = strongly magnetic, Green = weakly magnetic, weathered rocks looks similar to the strongly magnetic rock, Purple = weakly magnetic, with more than 1 cm of withered surface distinctly red-brown colored, Blue = Marble, Black = no exposure, Upper Orange = augen gneiss, Lower Orange = unmineralized calc-silicated rock with quartz veins and layers rich in biotite and garnet.

Sample numbers show their relative position to the mapped profile; red = strongly magnetic, green = weakly magnetic, gray= non-Magnetic, purple = non-magnetic and strongly magnetic. Fe wt% in brackets. Lowest point in profile, ~660 m.a.s.l. at 34 W 421713 7721682.

6. Petrography

6.1 Description of thin sections

DP005

The thin section consists of 60% amphibole (0.25-0.75 mm), 25% magnetite (0.25-1.25mm), 15% quartz (0.25-0.5 mm), hematite and apatite <1% each.

Most of the magnetite occurs in 0.25 to 1.25 mm large crystals (Fig. 16 B, C) but is also found as lamella in amphibole, the lamellas appear both as a 1/250 mm and 1/20 mm wide lamellas. The small lamellae are typical 10-20 times longer than their width (Fig. 16 A). For the wide lamella they are from 2 to 10 times the width. Quartz or possibly feldspar also occurs as lamella and inclusion in amphibole. The rock is weakly banded. Zonation of amphibole is common.

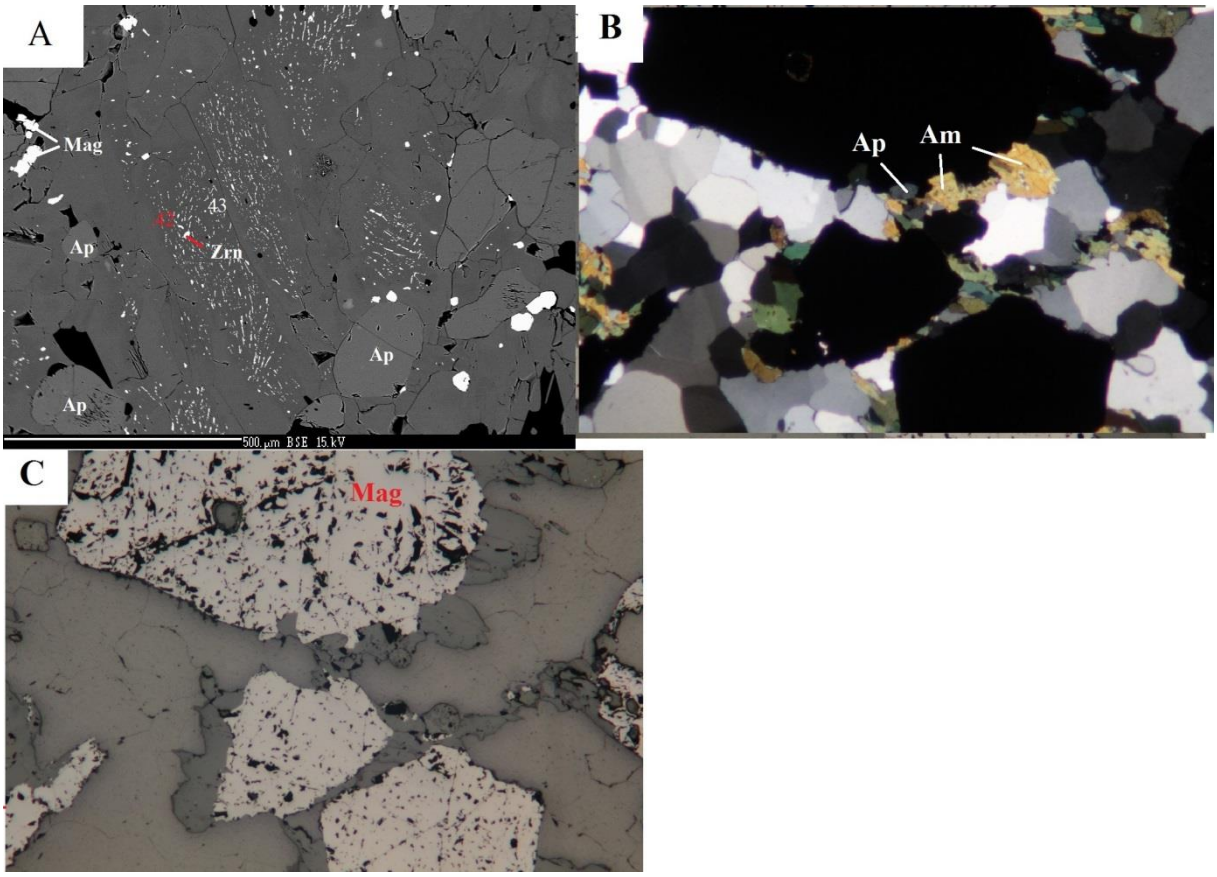

Figure 16 A) Magnetite exclusions in amphibole, BSE. B, C) Magnetite with quartz and amphibole, Field of view (FOV) = 3.6mm.

The hand specimen is weakly banded and consists of 50% black minerals primarily magnetite with 1-2mm in grain size, 35% green mineral (<1mm) and white fine grained minerals.

EMP-Analysis of 4 grains of amphibole shows 2 of ferro-edenitic compositions, 1 ferro-hornblende and 1 hastingite. Zoned amphibole was analyzed in two spots, which showed the lighter colored (PPL, darker in BSE) inner parts close to the magnetite lamella to be ferro-edenite, while the darker (PPL) outer zone is ferro-hornblende.

DP008

The thin section consists of 55% amphibole (0.25-0.5 mm), 15-20% quartz (<0.2 mm), 10% garnet (0.25-0.75 mm), 5-10% magnetite (<0.25 mm), 5% carbonate (0.1-0.5 mm) and less than 1% biotite.

Quartz and amphibole often occur as monomineralic bands. Garnet is also found in discontinuous bands and often has amphibole rims.

Figure 17 illustrates the most common textures of the thin section.

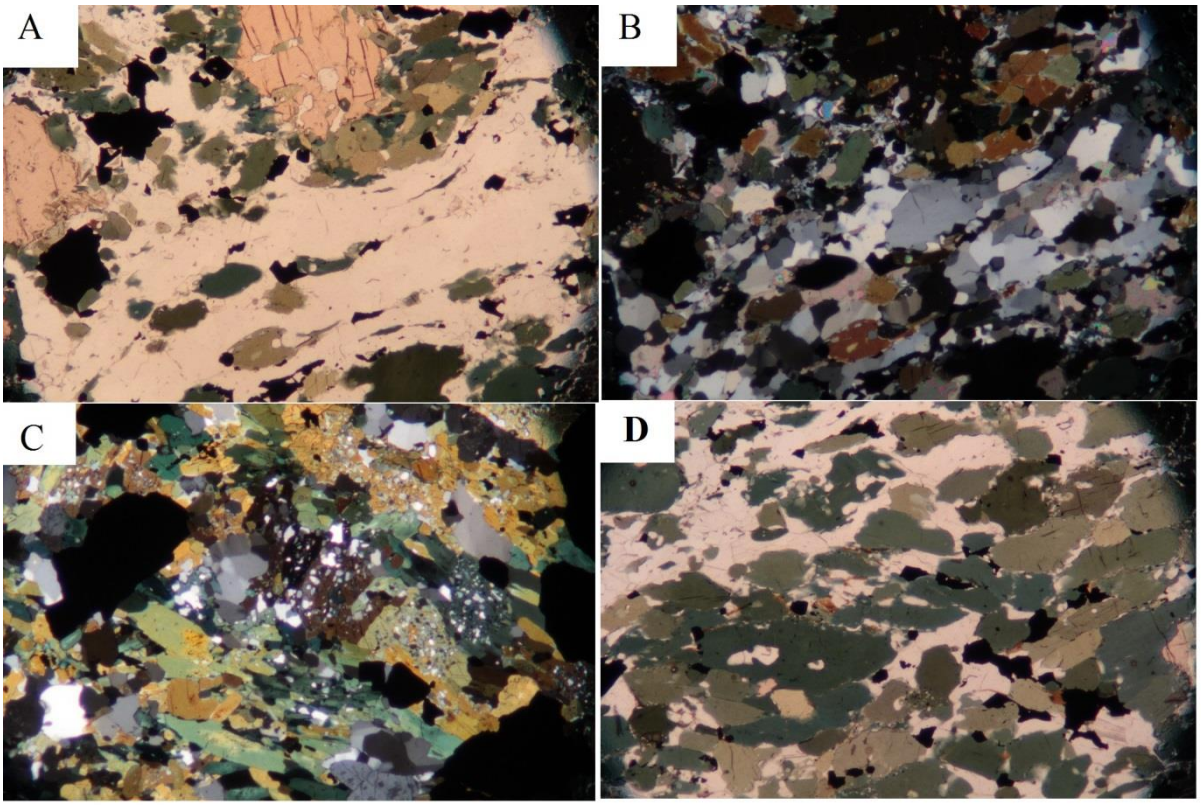

Figure 17 A and B) bands of quarts and amphibole, FOV = 3. 6mm. C) Symplectite of amphibole and quartz, XPL, FOV = 3.6mm. D) Amphibole, quartz bands, magnetite and carbonate bands, FOV = 3.6mm.

DP030

The thin section consists of approximately 30% amphibole, 5-10% clinopyroxene, 15% quartz, 30% opaque minerals (18% magnetite and 12% Ti-magnetite), 5% epidote, 3% apatite.

The rock is banded; quartz and magnetite form semi-continuous bands (Fig. 18 a, b). Ti-magnetite, magnetite, apatite, epidote and amphibole occurs in some places as aggregates (Fig. 18c).

EMP-analysis resulted in two amphibole compositions, 1 actinolite and 1 magnesio-hornblende.

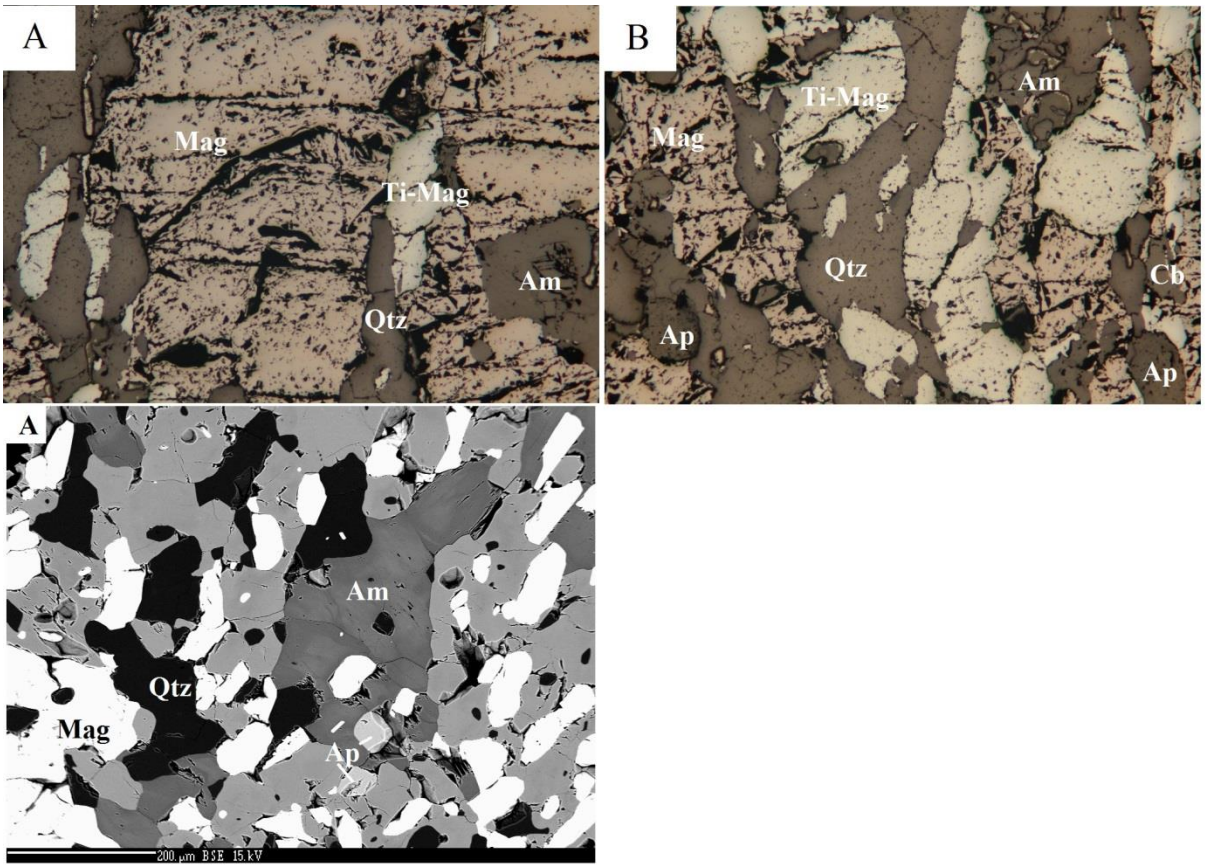

Figure 18 A) Magnetite, Ti-magnetite, quartz and amphibole, FOV = 3.6mm. B) Magnetite, Ti-magnetite and quartz bands with some amphibole, apatite and carbonate, FOV = 3.6mm. C) Zoned amphibole, in an aggregate together with epidote, magnetite and quartz, BSE.

DP031

The thin section consists of 40% garnet, 30% amphibole, 15% quartz, 10% carbonate, and 3% clinozoiste, 1% apatite and less than 1% allanite. Opaque minerals comprise another 5% of the total. The opaques are magnetite, Ti-magnetite and ilmenite. Ilmenite and Ti-magnetite show the usual exsolution pattern, ilmenite also shows symplectitic intergrowths with undetermined mineral(s) (Fig. 19 A and B). The thin section shows bands of quartz, garnet, carbonate and aggregates of plagioclase/quartz, amphibole, carbonate,

apatite and clinozoiste. Carbonate, amphibole, quartz and magnetite/Ti-magnetite form relative large grained aggregates in places. Garnet usually has an amphibole rand towards quartz and carbonate (Fig. 19 E and F). Garnet with clinopyroxene inclusion (Fig. 19 D) was used for Garnet-Clinopyroxene thermometry. The three amphibole analyzes right outside the garnet showed magnesio-hornblenditic compositions (#19,#20 in the upper part and pargasitic compositions (#21) in the lower. Allanite can be found in part of the sample intergrown with epidote (Fig. 19 C).

EMP-Analysis of 3 grains of amphibole resulted in 2 analyses of magnesio-hornblende and 1 analysis of pargasite.

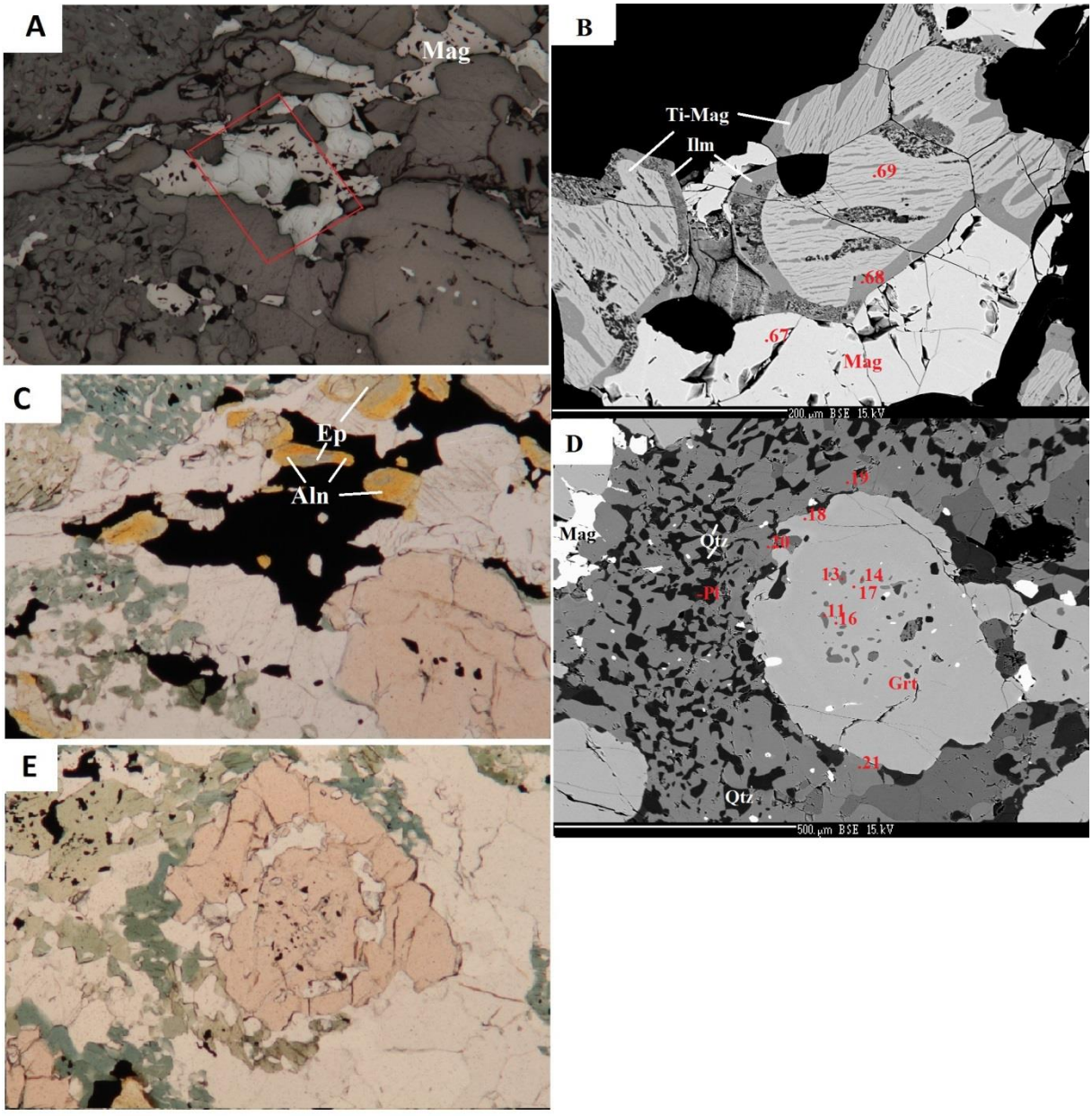

Figure 19 A) Reflected light, magnetite, Ti-magnetite exsolutions in ilmenite, red box is B, FOV 1.8mm. B) BSE, numbers 68 and 69 indicated location of analyses used for ilmenite-magnetite thermometer. C) Same as A with PPL, Epidote with unusual coloration, aggregates of Amphibole + quartz + Ti-magnetite +/- Plagioclase, Garnet with small reaction rim towards carbonate and Ti-Magnetite also with Ti-Magnetite inclusions. D) BSE, Garnet with clinopyroxene inclusions used for garnet-clinopyroxene thermometry. E) Garnet with growth zoning, Quartz, Carbonate and Magnetite inclusions in the interior, Quartz and Carbonate in a ring around the core and a nearly inclusion free outer ring, FOV 1.8mm.

DP035

The thin section consist of about 10% quartz, 20% amphiboles, 20% carbonates, 20% opaque minerals with about 10% of the opaque minerals being Ti- Magnetite while the remaining (90%) are Magnetite,15% epidote, 1-2% apatite, biotite, and much less than 1% zircon and ilmenite.

The quartz in this thin section forms narrow mono-mineralic bands. Larger amphibole crystals occasionally carry magnetite, quartz and epidote inclusions. Some of the epidote inclusions have allanite cores. Allanite also occurs in association with amphibole and carbonates. There are also aggregates of epidote, Ti-magnetite, quartz, amphibole, magnetite and ilmenite (Fig. 20).

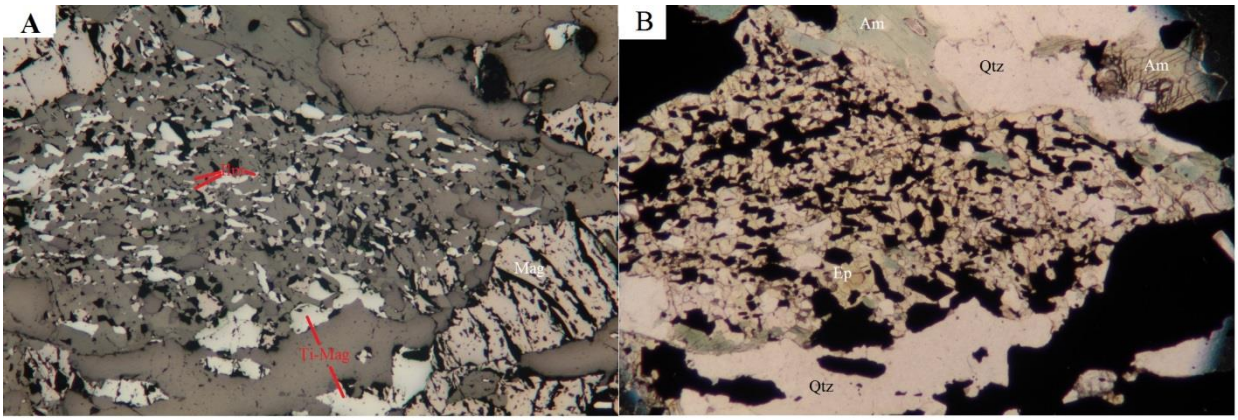

Figure 20 A, B) Epidote, Ti-magnetite, quartz, amphibole, magnetite and ilmenite aggregate, FOV = 3.6 mm.

EPG

The thin section is not optimal as the thin section only consists of one of the two rock types that were on the chip. The thin section consists of 40% quartz (0.2-0.5 mm) and about 30% of each of clinopyroxene (0.25-1.25 mm) and magnetite (0.2-0.75 mm). Magnetite

and quartz are subhedral to anhedral while pyroxene is euhedral to subhedral with occasional inclusions of magnetite. Recalculation of EMPA of clinopyroxene shows agerine-augite (Fig. 21). Magnetite in this thin section contains more Al than the magnetite in other places (0.03 - 0.037 apfu compared to less than 0.013 apfu).

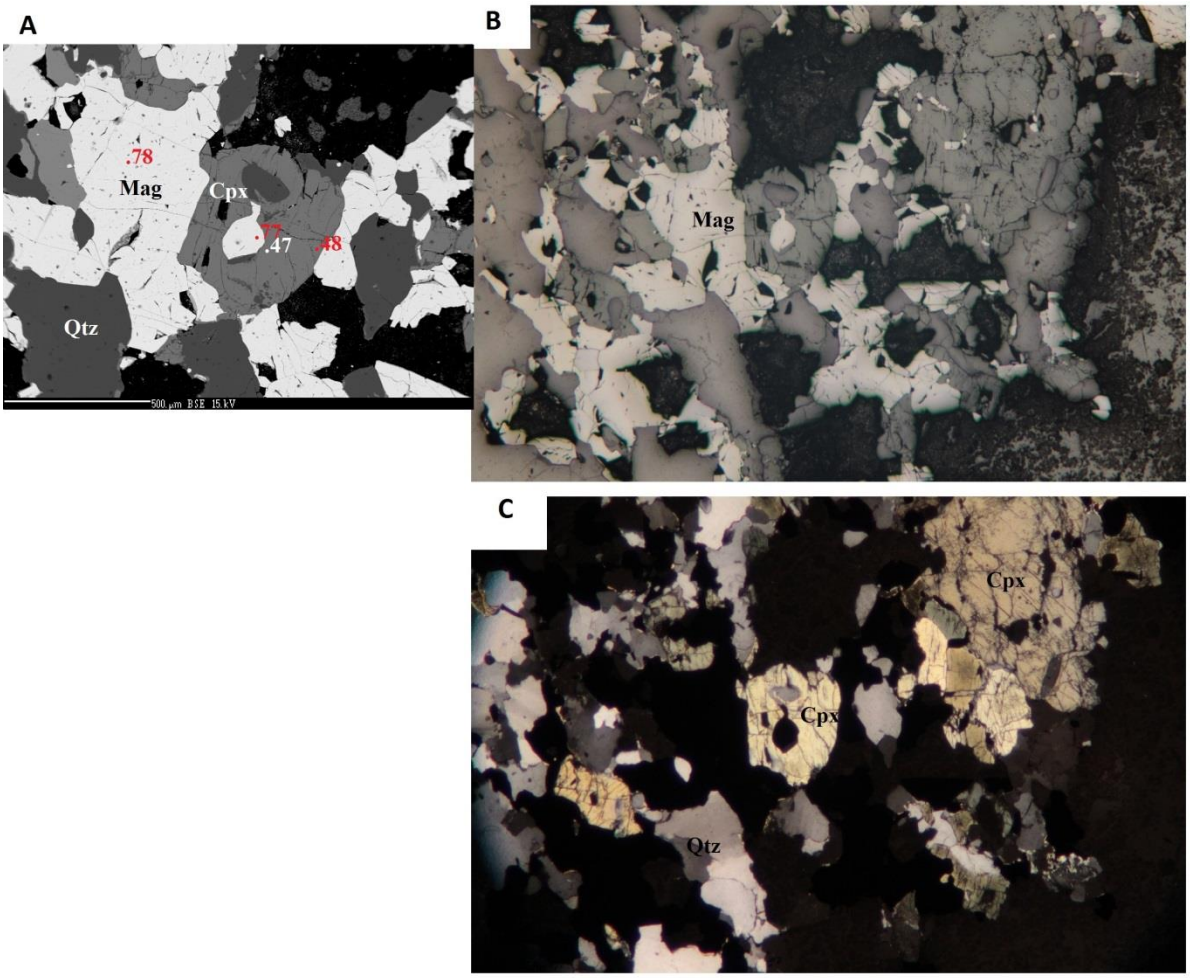

Figure 21 A) BSE image of clinopyroxene surrounded by magnetite and quartz, magnetite and quartz inclusions in agerin-augite. B, C) reflected light and XPL, magnetite clinopyroxene and quartz, FOV = 3.6 mm.

EP024B

The hand specimen is banded and consists of 65% magnetite (1-2mm), the other minerals are fine grained, 15% dark green mineral, 10% light green mineral and 10% white mineral.

The thin section contains 35% opaque minerals, 35% quartz (0.1-0.75 mm), 15% amphibole (0.1-0.3 mm), 5% epidote, <5% clinopyroxene and 2-3% apatite. The opaque minerals are dominated by 1-2 mm large magnetite crystals (Fig. 22 A and B) (magnetite comprises approximately 95%, Ti-magnetite another <5%) and hematite <<1%. Ti-magnetite occasionally has exclusion lamella of magnetite.

The thin section contains bands dominated by magnetite, quartz and aggregates (Figure 22 C, D, E and F) epidote + amphibole + quartz + opaque (90% magnetite, 10% Ti-magnetite). Inclusions are common in the larger magnetite masses (Figure 22 A, B and G).

Zoned amphibole was analyzed with EMP (Fig. 22 H), the inner core being made up of edenite (#37) and the rim of magnesio-hornblende (#38). The two EMP-analyzes of clinopyroxene recalculated show aegerin-augite (#35, #36).

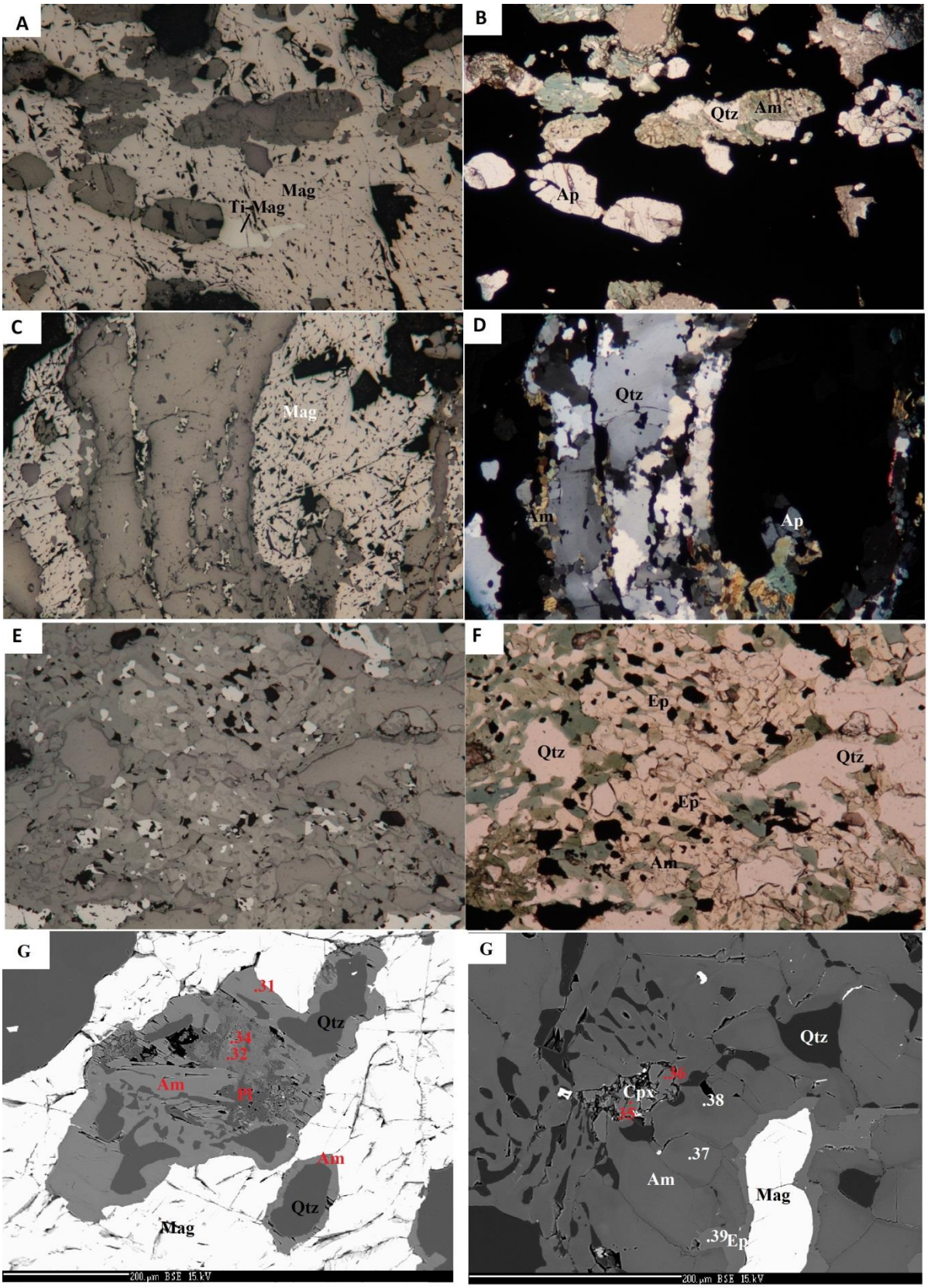

Figure 22 A) reflected light, FOV 3.6 mm, Apatite, amphibole + carbonate + quartz +apatite "inclusions" in Magnetite B) Same as A but PPL, epidot rim on Magnetite can be seen in the upper part C) Quartz bands separated by small magnetite bands between

two large magnetite bands, an amphibole band can be seen to the left of the quartz bands. Reflected light, FOV 3.6 mm. D) XPL same as C, epidote rim on the magnetite to the right can be seen towards quartz. E, F) center epidote + magnetite + amphibol + apatite aggregates with epidote dominating upper Left amphibole + quartz + magnetite aggregate, FOV = 1.8 mm.G) Shows inclusion in magnetite, BSE. The small inclusion in the lower left consists of quartz with amphibole rind along the contact to magnetite. In the large inclusion one finds magnesio-hornblende (#31, analysis 1 EP024B) rims the entire inclusions. 3 is Plagioclase, 4 clinopyroxene and 2 biotite. H) Agerin-augite with adjacent quartz + amphibole symplecite. Zoned Amphibole, Magnesio-Hornblnde darker shade at outer parts of the grains and edenite at the core of the amphibole grain. Epidote rim on magnetite.

EP053A

The thin section contains 35% clinopyroxene (0.5 mm), 30% garnet (0.2-2 mm), 15% magnetite (0.2-0.4 mm), 5-10% amphibole, 5% carbonate and non determinated epidote group mineral.

Bands of pyroxene, garnet and magnetite dominate the thin section.

A recalculated EMP-analyzis of amphibole shows magnesio-hornblende.

Solligangen Profile

SGP03

The thin section contains about 5% opaque minerals (Magnetite, Ti-Magnetite, Ilmenite and Hematite), 45% quartz, 30% garnet, 20% amphibole, 2% biotite, 1%> epidote. The hematite usually can be seen to overgrow magnetite, which retains an euhedral shape, larger grains of ilmenite show exclusion of Ti-Magnetite (Fig. 23 D). Garnet usually has a rim of amphibole (sometimes biotite) and has got inclusions of quartz and occasionally opaque minerals (Fig. 23 B, C). Subhedral to anhedral grains dominate the sample. Calcite shows exclusion of siderite in some grains (Fig. 23 C).

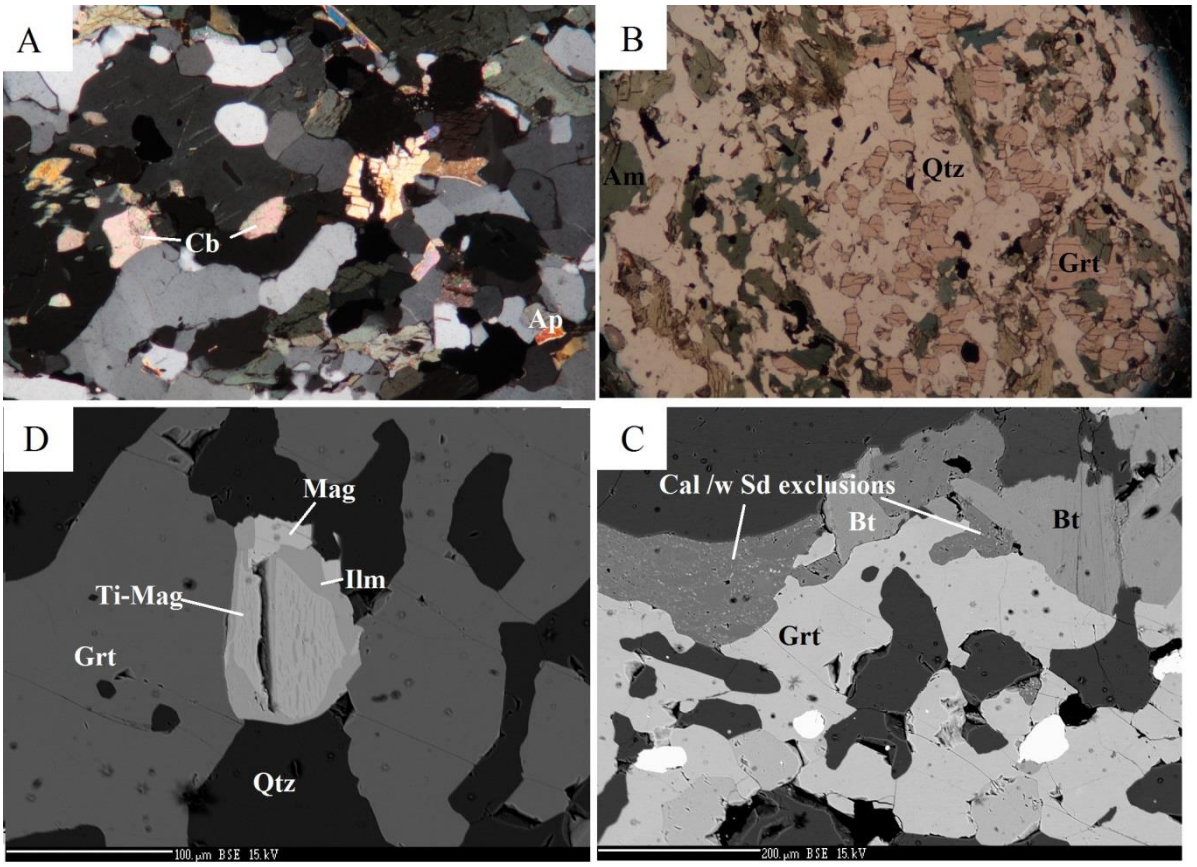

Figure 23 A) Quartz, amphibole, carbonate, apatite and clinopyroxeneClinopyroxene, XPL, FOV = 1.8 mm. B) Garnet, quartz and amphibole bands, PPL, FOV = 3.6 mm. C) Ti-Mag exclusions in Ilmenite, BSE. D) Calcite with siderite exclusion, BSE.

SGP08

The hand specimen is banded and consists of about 50% white fine grained minerals, 40% 1-2 mm large magnetite and 10% fine grained green minerals.

The thin section contains about 40% magnetite (grain size >0.5 mm), (Fig. 24 A, C), Ti-Magnetite has not been observed, 40% quartz 10% amphibole, 5% epidote and allanite, less than 1% carbonates and clinopyroxene, which is mainly present as inclusions in magnetite. Magnetite and quartz bands dominate the section (figure 24 E). Much less than 1% is made up of biotite that is being replaced by chlorite. This occurs in association with magnetite and amphibole (figure 24 C).

EMP-Analysis of 2 amphiboles shows 2 edenite.

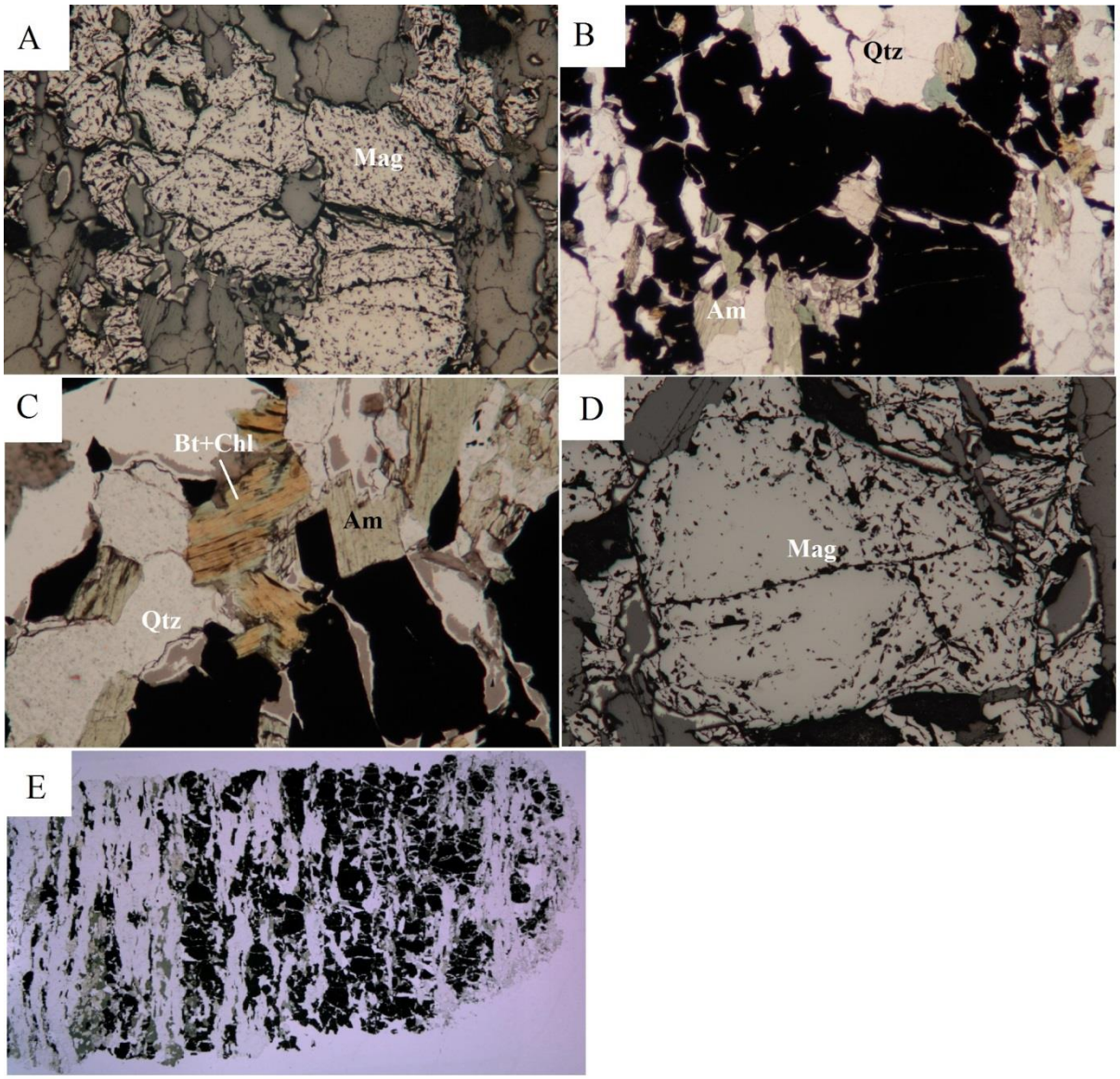

Figure 24 A, B) Magnetite, quartz, amphibole, FOV = 3.6mm. C) Biotite partly replaced by chlorite, FOV = 0.9mm. D) Magnetite, FOV = 1.8mm. E) Picture of the thin section.

SGP09

The hand specimen consists of about 45% green minerals, 45% quartz and 10% magnetite. The quartz and green minerals form bands.

The thin section consists of 15% magnetite (and Ti-Magnetite), 5% carbonates, <<1% hematite, <1% ilmenite, 35% quartz, 15% amphibole and about 30 % of epidote and clinozoisite. The rock is banded; the most obvious bands consist of elongated quartz or magnetite (figure 25 A, B, C). The opaque minerals consist of a mix of approximately 50/50

magnetite to Ti- magnetite. Epidote, amphibolite and magnetite (figure 25 E) aggregates comprise about 20 % of the thin section. Amphibole sometimes shows zonation (figure 25 F).

EMP-Analysis of 2 amphiboles shows magnesio-hornblende.

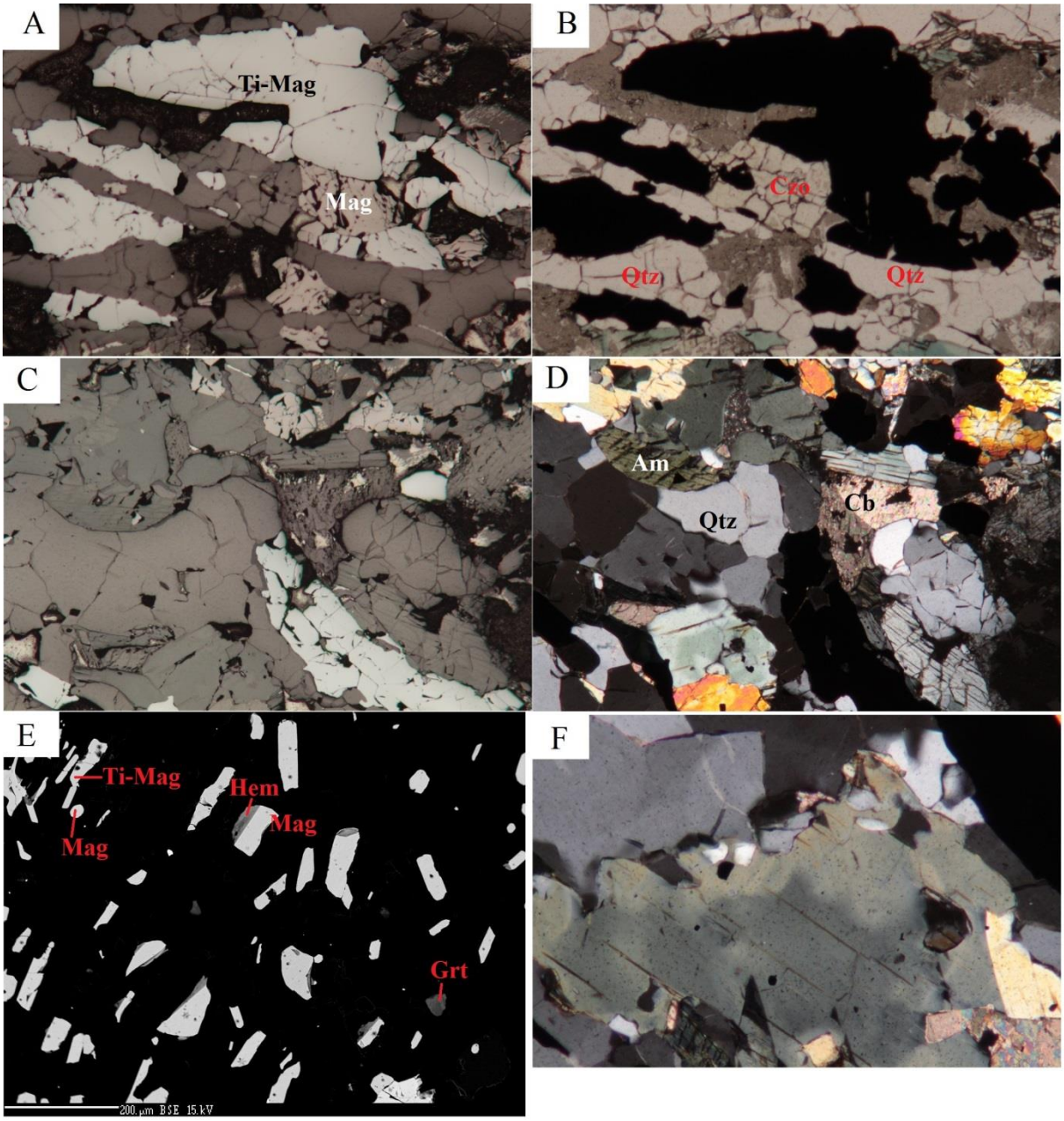

Figure 25 A, B) bands of elongated Ti- magnetite and magnetite and quartz with clinozoisite, FOV = 1.8mm. C, D) Ti- magnetite, magnetite, amphibole, carbonate and quartz, FOV = 1.8mm. E) Iron oxides in aggregate, BSE. F) Zoned amphibole, XPL, FOV= 0.9mm.

SGP10

The thin section contains 30% magnetite, 25% quartz, 20% amphibole, 5-10% clinopyroxene, 5-10% epidote, <1% apatite and 5% Ti-magnetite. The thin section is banded

primarily quartz and magnetite bands (figure 26 A, B, C, D), aggregates amphibole + epidote + magnetite + Ti-magnetite + quartz (plagioclase) (figure 26 E, F).

A fibrous brown mineral is associated with Amphibole and mag. Some of the Amphiboles show anomalous purple-grey-green-interference colors. EMP-Analysis of one amphibole shows magnesio-hornblende.

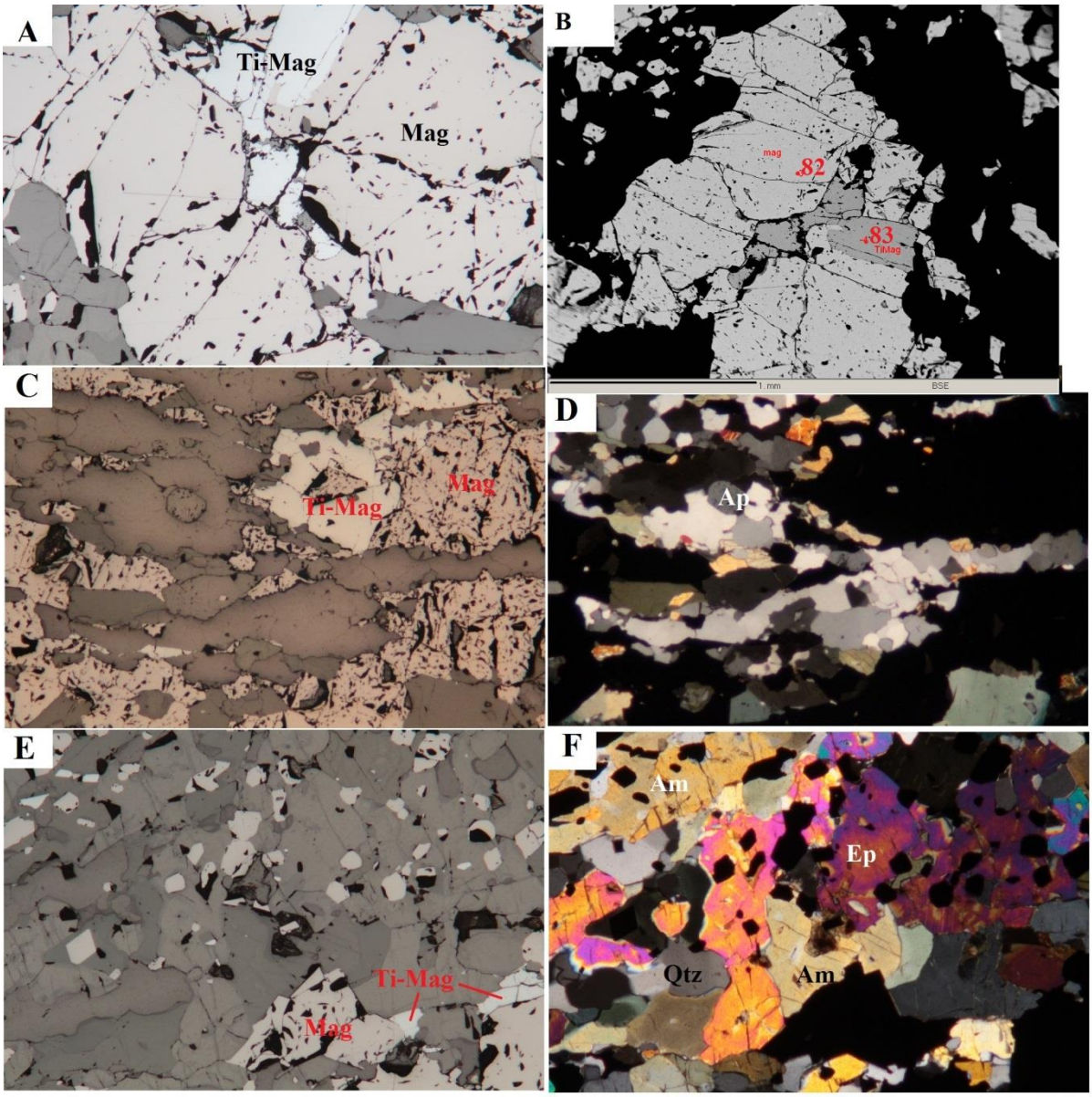

Figure 26 A, B) Ti-magnetite inter grown with magnetite, FOV; A = 1.8mm. C, D) magnetite/Ti-magnetite and quartz bands with some amphibole and apatite, FOV = 3.6mm. E, F) Epidote overgrowing smaller magnetite crystals, FOV = 1.8mm.

SGP11

The hand specimen is banded gneiss, consisting of 40% pyroxene, 20% garnet 2-5 mm, 20% black minerals and 15% white minerals. The sample is magnetic.

The thin section consist of 20% quartz (0.25-0.5 mm), 20% amphibole (0.25-0.5 mm), 20% garnet (1.5 -2 mm and 0.1-0.2 mm), 15% biotite (0.05-0.25x0.25-0.75 mm), 5% carbonate (0.2-0.5 mm), 5% magnetite (0.1-1 mm), 3% epidote (0.2-0.5 mm), <1% each of apatite, clinozoisite, allanite, Ti-Magnetite and Ilmenite.

Aggregates of amphibole, quartz and magnetite occur in some bands (Fig. 27 B). Amphibole and biotite riming garnet occurs commonly where the garnet isn't in contact with quartz (Fig. 27 A). The analyzed garnet doesn't show significant variation from core to rim. Inclusions in garnet are commonly Ti-magnetite, plagioclase, quartz, magnetite, biotite + plagioclase, carbonate and amphibole. Larger epidote and clinozoisit crystal have cores of allanite (Fig. 27 C, D). A spot check with EMPA showed that the carbonate to be calcite.

The sample displays banding. Quartz, biotite and carbonate form monomineralic bands with the aggregates forming fourth set of band.

Two recalculated EMP-Analyses of amphibole are potassian-hastingsite.

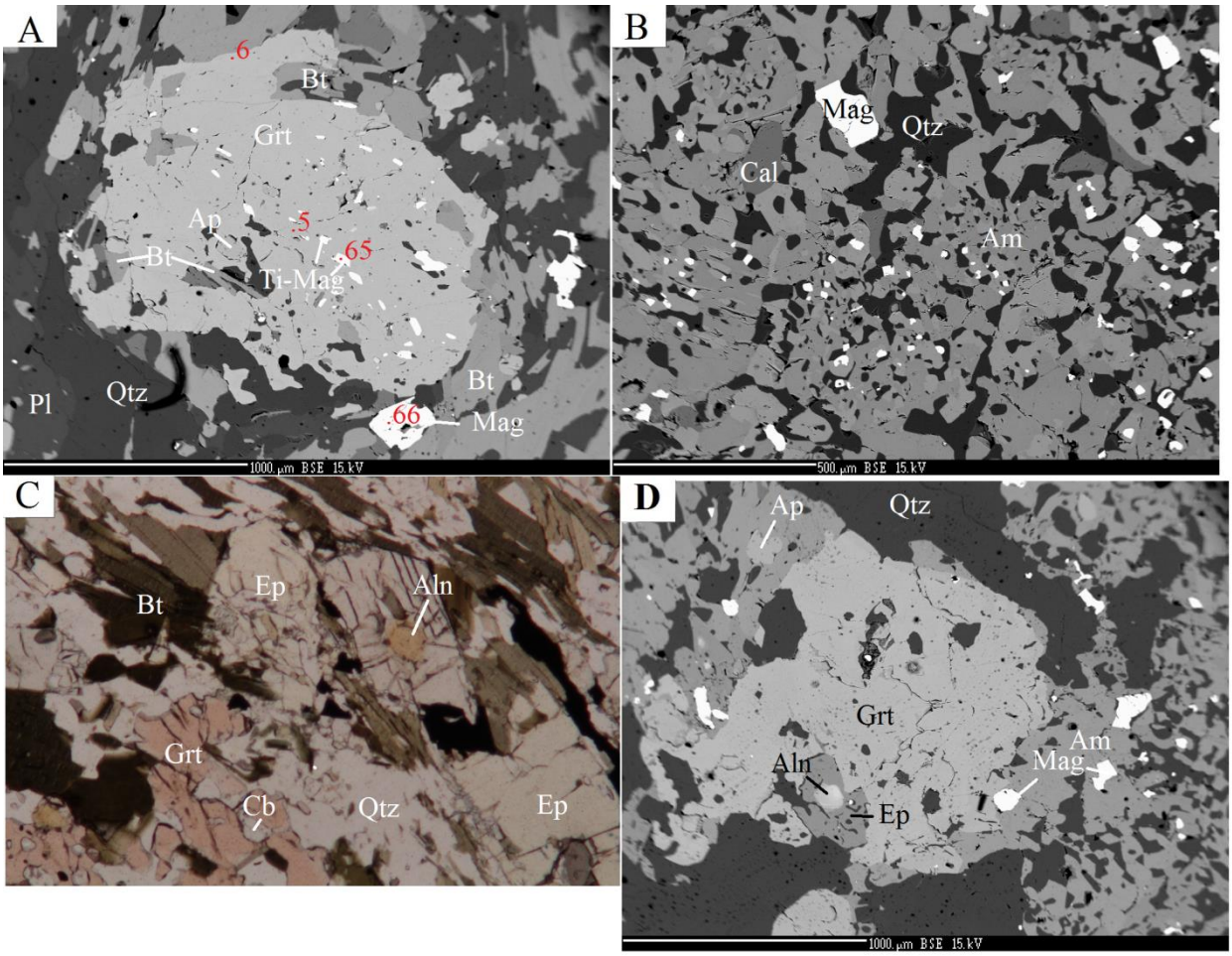

Figure 27 A) Garnet with inclusions and biotite rim. B) Amphibole, quartz, calcite and magnetite aggregate. C) Epidote with allanite core, FOV = 1.8 mm. D) typical garnet, quartz amphibole association.

SGP89

The hand sample shows a weak banding and consists of about 10% magnetite with grain sizes of less than 1 mm, 20% 1-2mm large garnets, fine grained white minerals and 60% fine grained green minerals. The weathered side shows rust like colors of brown-red iron hydroxides.

The thin section consists of about 60 % amphibole, 10% carbonate (mostly calcite, determined by EMPA), 10% clinopyroxene and 5% each of garnet and opaque minerals, the opaque minerals are mostly magnetite or Ti-magnetite and hematite. Two other non-identified opaque minerals also occurs (figure 28 B). Diopside shows exsolution lamellas of magnetite and carbonate + augite (figure 28 A). Garnet is anhedral to subhedral and commonly associated with quartz and amphibole (figure 28 C, D)

Three EMPA analyzes of amphibole classify as magnesio-hornblende.

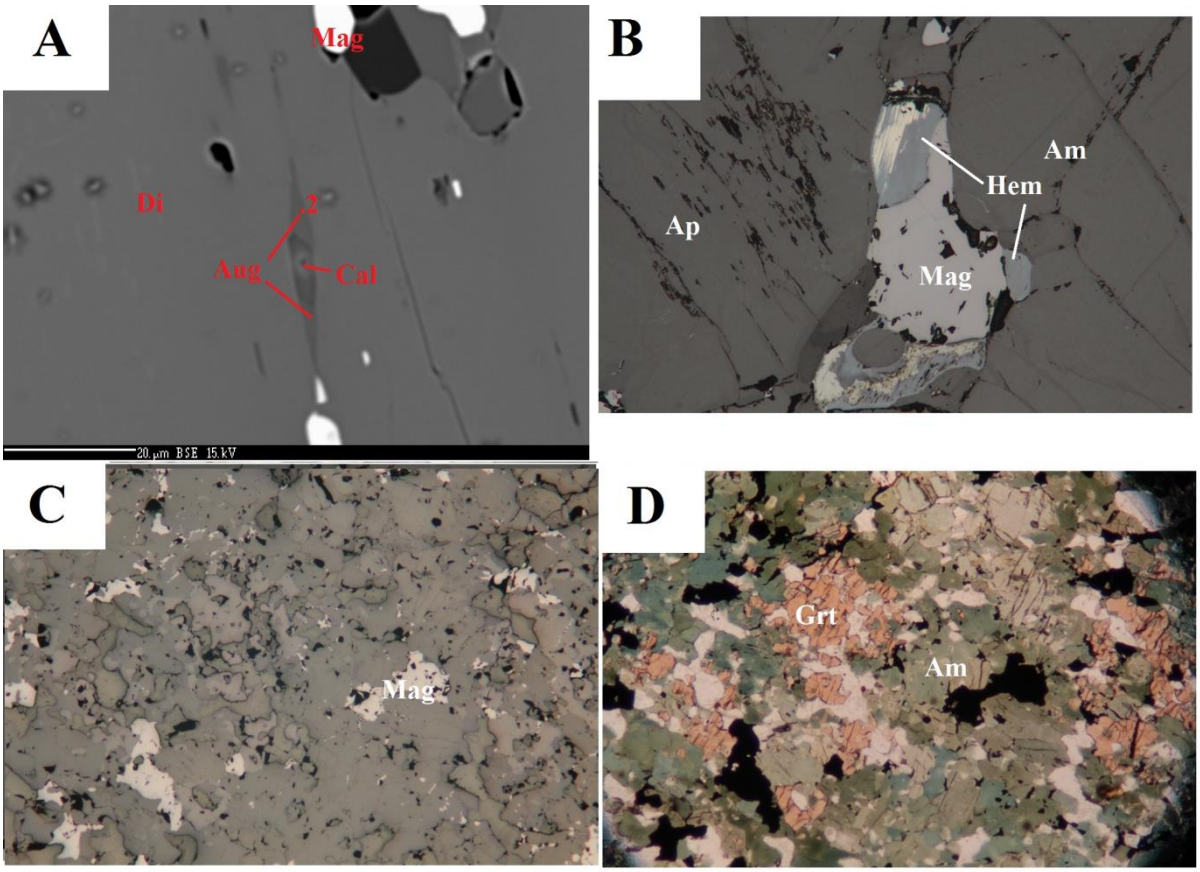

Figure 28 A) Lamellas in clinopyroxene, BSE. B) Magnetite with rand of hematite which is intergrown with two or three unknown minerals, FOV = 0.45mm. C, D) Magnetite overgrown with amphibole and garnet-quartz intergrowths, FOV = 3.6mm.

6.2 Description of minerals

Calculated mineral formulas can be found in Appendix B.

Clinopyroxene

Green to colorless, two cleavages at around 90°, extinction not parallel to cleavage and high relief. Clinopyroxene occurs as both primary rock forming minerals and as inclusions in garnet (Fig. 19 D) and magnetite (Fig. 22 G). The inclusions both in garnet and magnetite contain anhedral omphacite and these inclusions also commonly contain the products of the breakdown of omphacite, plagioclase and amphibole.

As a main constituent of some thin sections, clinopyroxene primarily occurs as euhedral to subhedral grains with sizes ranging between 0.5 mm to 1.5 mm, occasionally zoned, in some places with magnetite exsolution lamella.

Results from calculation of structural formulae of clinopyroxene are shown in figure 30**.** Figure 30 A) shows clinopyroxene compositions in the enstatite-ferrosilite-wollastonite ternary diagram, while Fig. 30 B) shows the (enstatite-ferrosilite-wollastonite) - jadeite–aegirine diagram. Clinopyroxene compositions predominantly show solid-solution between aegerin-augite and diopside.

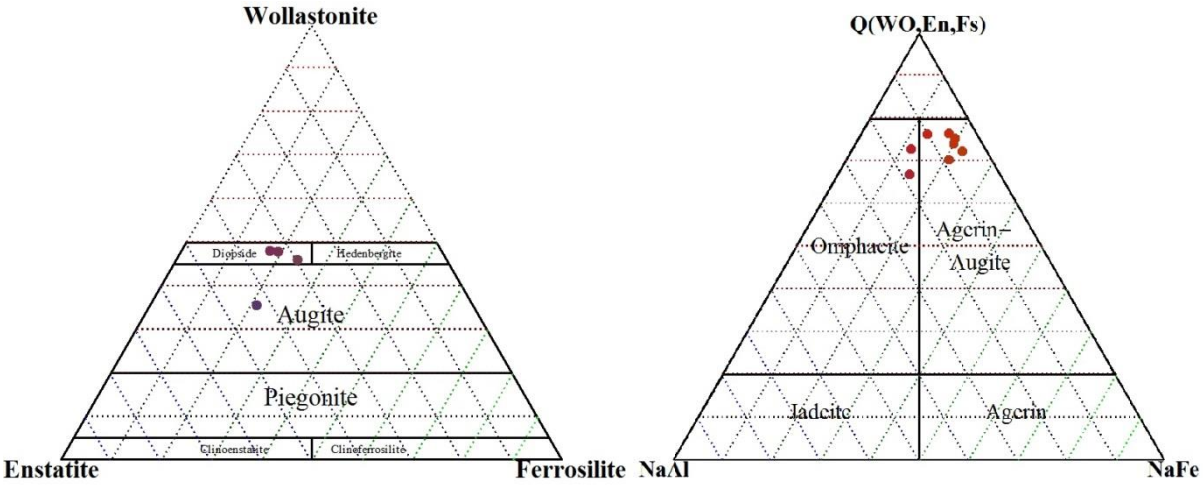

Figure 30 Diagrams showing pyroxene compositions after Morimoto (1989). A) Ca-Mg-Fe pyroxenes. B) Ca-Mg-Fe and Na pyroxenes.

Amphiboles

A range of calcium amphiboles are found in the thin sections (Fig. 31). Amphibole displays two good cleavages at 60^{o}-120^{o}, pleochroic green-green, green-blue green, colorless at times. Most of the thin sections contain amphibole, usually as medium sized crystals, occasionally zoned or with lamellas of various minerals usually monomineralic such as magnetite and quartz.

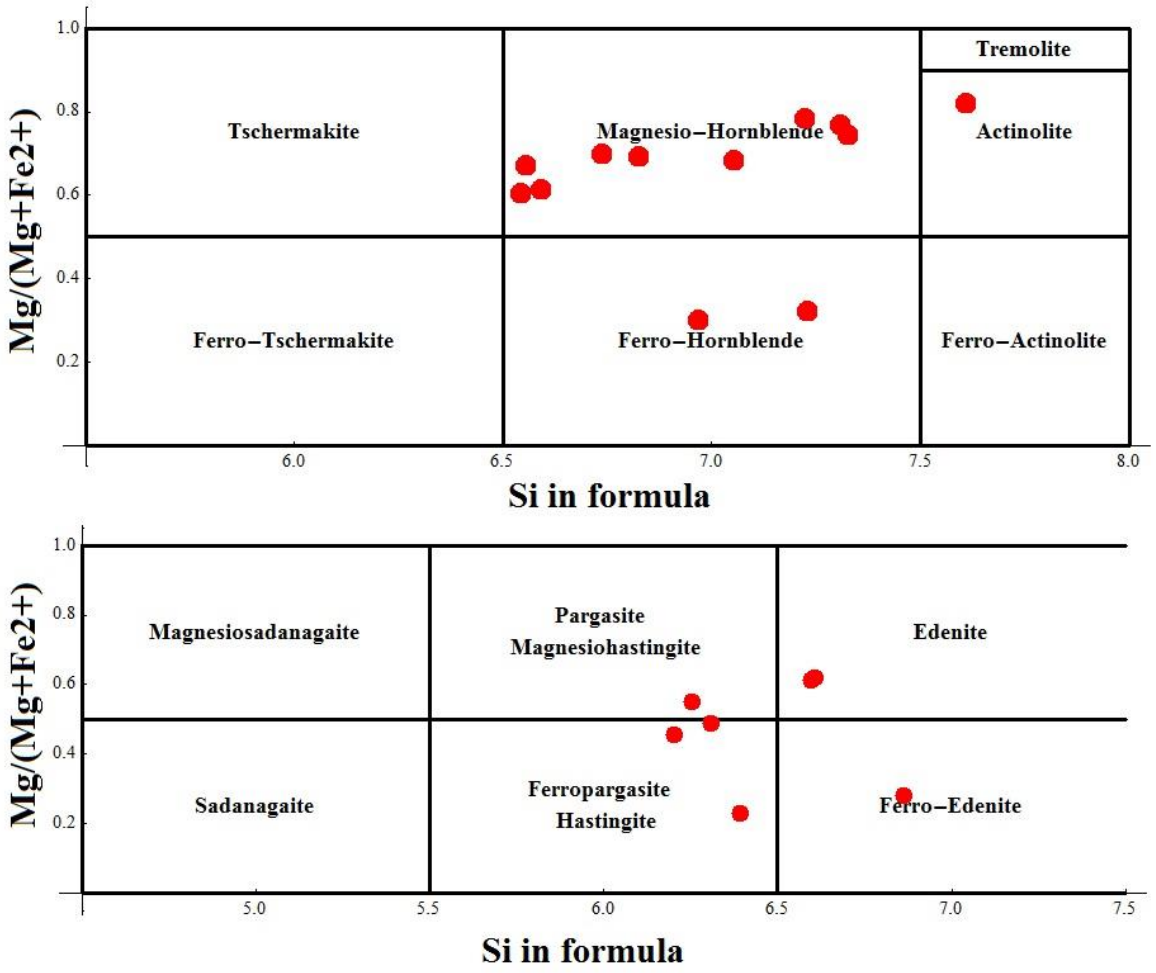

Figure 31 Recalculated amphibole analyses shown in diagrams after LEAKE et al. (1997); top $Ca_B \geq 1.50; (Na+K)_A < 0.50; Ca_A < 0.50$. *Bottom* $Ca_B \geq 1.50; (Na+K)_A \geq 0.50;$ $Ti < 0.50$.

Quartz

Colorless, low relief, low birefringence, no twinning and no cleavage. Commonly found in monomineralic ribbons/bands (Fig. 22 D, 26 D), it is also found in polymineralic aggregates with epidote or amphibole (Fig.22 B, 27 B).

Plagioclase

Colorless, low relief, low birefringence, twinning and cleavage. Plagioclase occurs as small grains in aggregates of epidote+quartz+plagioclase+/-amphibole+/-Ilmenite+/-Magnetite+/-Ti-Magnetite and as inclusions intergrown with amphibole and pyroxene

(determined with EMPA) makes distinction from quartz nearly impossible with optical means.

Garnet

Garnet is isotropic, colorless to pink and has high relief. Garnet is common in the thin sections and occurs as euhedral to anhedral crystals. Figure 32 shows the result from the calculations of structural formulae from EMP-analyzes of garnet. Growth zonation is common in garnet (Fig. 19 E). Inclusions of quartz, plagioclase or carbonate are common, epidote, magnetite, Ti-magnetite and ilmenite inclusions are rarer. Polymineralic inclusions of amphibole+/-plagioclase+/-quartz+/-clinopyroxene+/-magnetite+/-Ti-magnetite occur but aren't as common as the monomineralic inclusions.

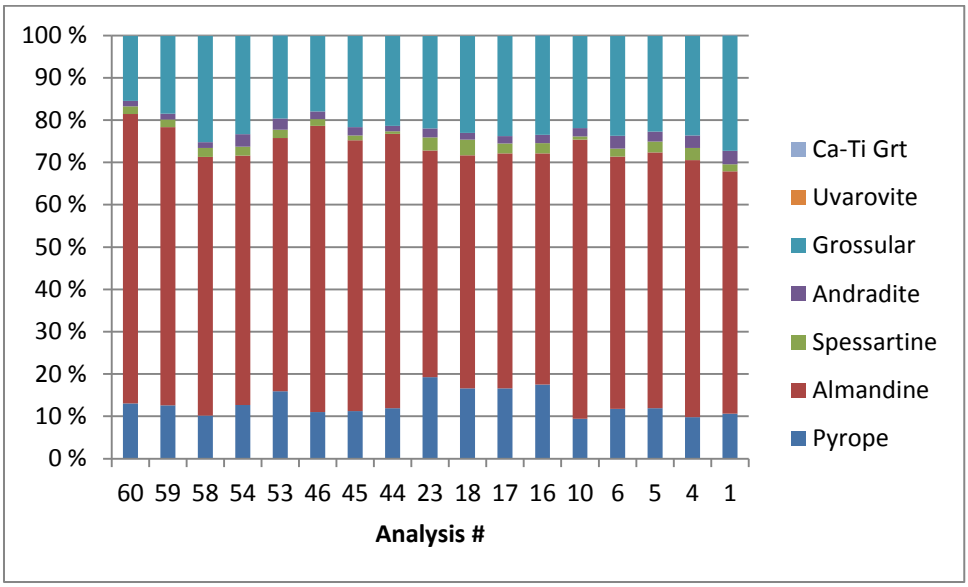

Figure 32 Calculated garnet compositions from EMPA.

Epidote, clinozoisite and allanite

Epidote is pale yellowish green weakly pleochroic, high relief, high 2nd and 3rd orders interference colors, grains display multiple interference colors, one perfect cleavage.

Clinozoisite is colorless, shows high relief, 1st order to anomalous interference colors and have one perfect cleavage.

Allanite is brown to yellow (Fig. 19 C, Fig. 27 C), shows high relief, one perfect cleavage. It is usually found as cores in epidote and clinozoisite, as small anhedral aggregates or intergrown with epidote.

Sheet silicates

Biotite is brown, pleochroic, one prefect cleavage, characteristic cleavage polishing pits, "birds eye", texture. It's found primarily associated with garnet and epidote (Fig. 27 C).

Chlorite is green, shows one perfect cleavage and has anomalous blue-violet interference colors. The blue-violet interference colors indicate high iron content of the chlorite. Chlorite is only found replacing biotite (Fig. 24 C).

Carbonates – Calcite, Dolomite and Siderite

Calcite appears to be the dominating carbonate in most thin sections with occasional occurrence of siderite and dolomite. Siderite occurs as exolution lamellas in calcite (Fig. 23 C). Species determined by EMPA.

These rhombohedral carbonates have extreme birefringence, are colorless and polysynthetic twinning is very common.

Magnetite and Ti-Magnetite

Magnetite is gray with a brownish tint and is isotropic with medium (R% 20) reflectivity; it is non-pleochroic, shows no internal reflections and no visible twining.

Ti-magnetite is gray and isotropic with low reflectivity, it is non-pleochroic, shows no internal reflections and no visible twining.

Magnetite is found in all of the studied thin sections and displays a large range of grain sizes from less than 10 µm to about 1 mm, the grain size is thus very variable and making reporting grain sizes more difficult. Magnetite and Ti-magnetite form exsolution lamella in clinopyroxene and amphibole varying in size from around 10 µm to 50µm wide and 50 µm to 200 µm long. Usually magnetite dominate the opaque minerals in the thin sections, a few however show about equal amount of Ti-magnetite and magnetite. Results of calculations of structural formulae of magnetite/Ti-magnetite is shown in the bar diagram in Figure 33, Fe-Ti-oxides are shown in a ternary diagram in Figure 34.

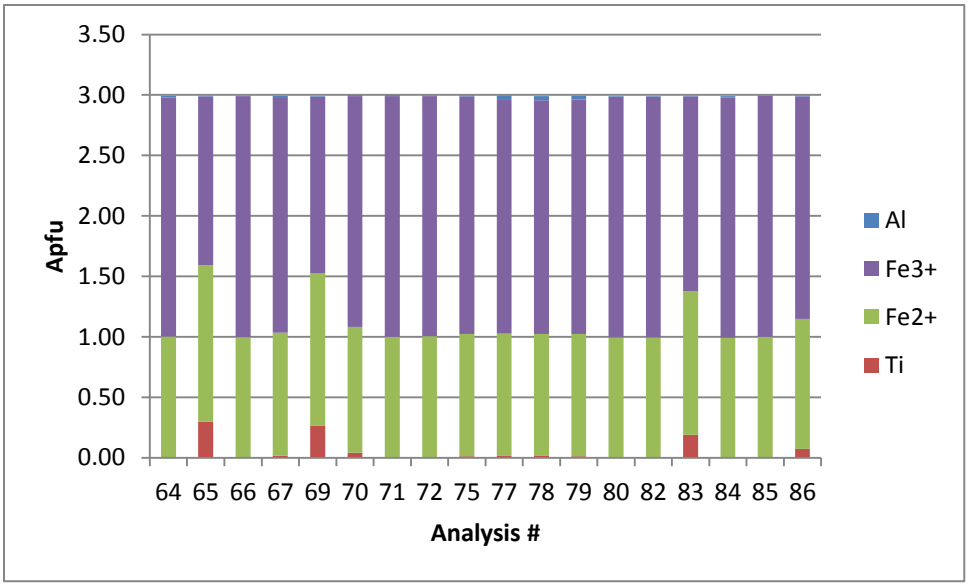

Figure 33 recalculated EMP analyses of magnetite.

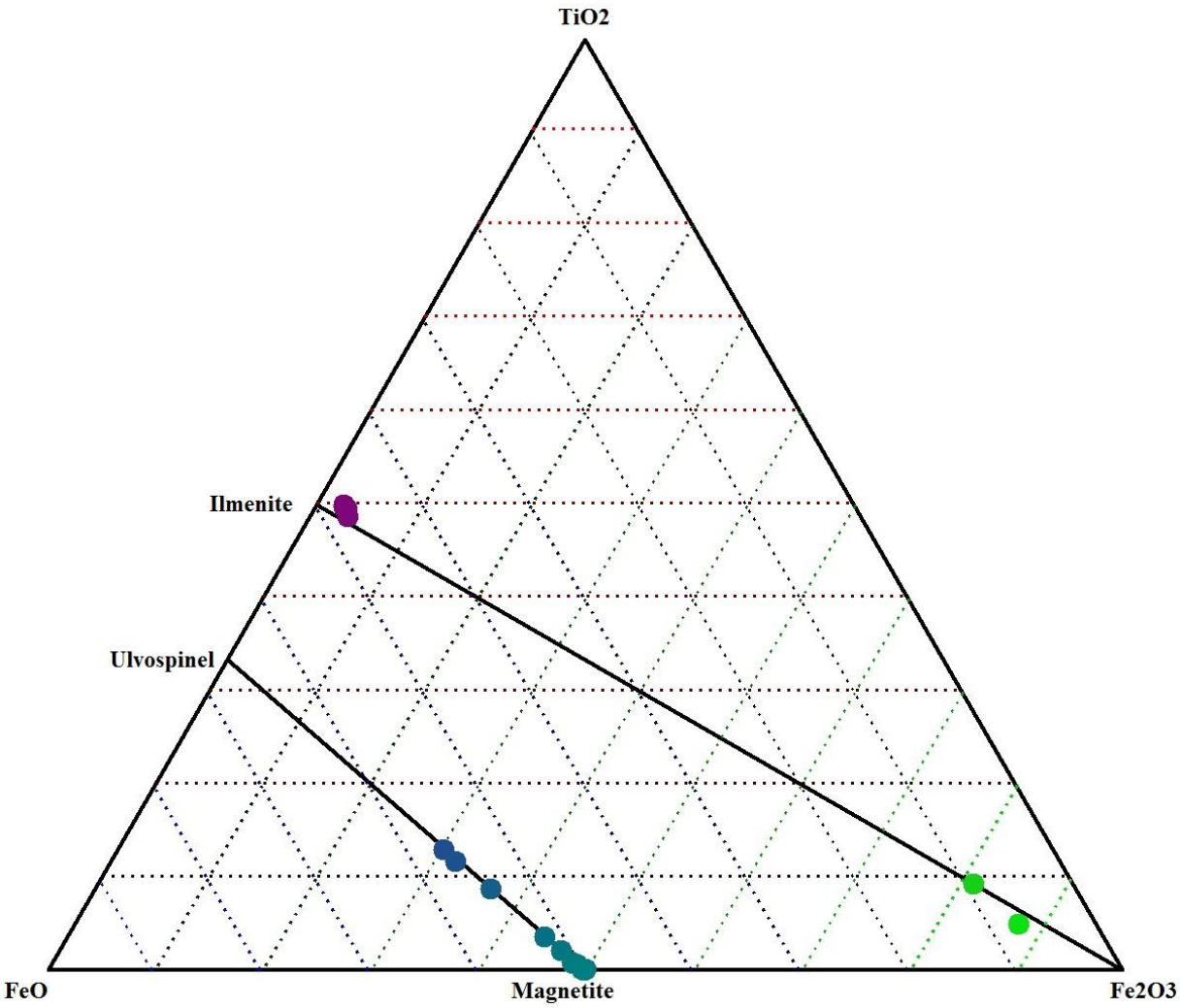

Figure 34 Iron-titanium oxides ternary plot. Solid lines in the diagram are; Ti-magnetite solid solution series between ulvospindel and magnetite, hemoilmenite solid solution series between ilmenite and Fe2O3 (hematite).

Ilmenite

Ilmenite is gray white with lower reflectivity than for magnetite, it shows weak pleochroism and it is anisotropic. Ilmenite occurs with Ti-magnetite exolutions (Fig. 19 A, B) and occasionally as small blocky grains in aggregates (Fig. 20).

Hematite

Hematite is gray with a bluish tint, it shows medium reflectivity that is slightly brighter than for magnetite, it shows weak pleochroism, it is anisotropic and deep red internal reflections are characteristic, twinning is common.

Hematite occurs as an accessory mineral in some thin sections, commonly in association with magnetite (Fig. 28 B). In one place hematite overgrows a euhedral magnetite crystal.

7. Whole rock geochemistry

Whole rock analyzes of all samples and correlation coefficients for the strongly magnetic, all magnetic and all samples can be found in Appendix A. The samples were divided into "strongly" mineralized, "weakly" magnetic and unmineralized/non-magnetic. Non-mineralized samples of basic composition (45-55wt % SiO_2), and with loss of ignition under 10wt % were selected for immobile element discriminant diagrams.

As mentioned in chapter 5 the mineralized samples can be differentiated into 2 types by magnetic susceptibility, the first type being strongly magnetic while second type is weakly magnetic. Applying this field classification with Fe_2O_3t concentrations measured by XRF one can see that the weakly magnetized group contains all but one samples between 10.0 and 21.0 wt % Fe with the strongly magnetic rocks having higher iron concentrations and the non-magnetic rocks having lower Fe concentrations except for one that has 10.2 wt % Fe.

Binary diagrams for some of the elements can be seen in figure 36 while figures 38 and 39 show some ternary diagrams. The intermediate to acidic rocks plot just under the thoeliitic trend in figure 38 A.

7.1 Mineralized samples

Strongly magnetic

The Iron content in these samples varies between 22.0 and 44.1 wt% Fe (total) (Fe_2O_3 = 34.57 - 61.70 wt %, average 48.78 wt %), TiO_2 between 0.12 - 0.49 wt % average 0.25 wt %, V = 86.10 - 686.40 PPM average 215.86 PPM, SiO2 = 21.51 - 51.51 wt % average 35.22 wt %, Al2O3 = 1.16 - 6.18 wt % average 2.95 wt %, MnO = 0.01 - 0.18 wt % average 0.07 wt %, MgO = 0.31 - 5.05 wt % average 2.40 wt %, CaO 4.02 - 19.01 wt % average 8.21 wt %, Na2O = 0.05 - 1.01 wt % average 0.40 wt %, K2O = 0.01 - 0.25wt % average 0.08 wt % one sample below detection limit, P2O5 = 0.70 - 3.65 wt % average 1.64 wt % and net loss of ignition -4.04 to 9.09 wt % average 0.20 wt %, SiO_4 + Fe_2O_3t = 71.0 - 92.3 wt % average 84.0 wt %. Figure 35 shows iron, vanadium, phosphorus and titanium contents of the samples.

A summary of correlation coefficients is given in Table 4. Strong positive correlations (>0.8) are found for Al with Ti and Ni, Ca with Mg and LOI. Fe displays

moderate positive correlation (0.6 to 0.79) with V, weak (0.4 to 0.59) positive correlation with P, moderate negative with Si and weak negative with Mn, Mg, Ca, Nb and LOI. Rb and K don't show good positive correlation due to both approaching detection limit (and resolution limit).

	Si	Ti	Al	Fe	Mn	Mg	Ca	Na	K	P	LOI
0.8 to 1	-	Al	Ti, Ni	-	-	Ca	Mg, LOI	-	-	-	Ca
0.6 to 0.79	-	Sc, Ni, Zr, Nb	Sc, Zr, Nb	V	Mg, Ca	Mn, LOI	Mn	-	-	-	Mg
0.4 to 0.59	-	Mg	K, Zn, La, Ce	P	LOI, Nb	Ni, Nb	Sr	Zr	Al, Zr, Nb, Sr	Fe	Mn
-1 to 0.8	-	-	-	-	-	-	-	-	-	-	-
-0.79 to 0.6	Fe	-	-	Si	-	P, Cr	Cr	-	-	Mg	-
-0.59 to -0.4	V	-	-	Mn, Mg, Ca, LOI, Nb	P, Cr, Fe	Fe	P, Fe	-	-	Ca, Mn	Fe

Table 4. Summary of correlation coefficients of major oxides and LOI for the strongly magnetic samples.

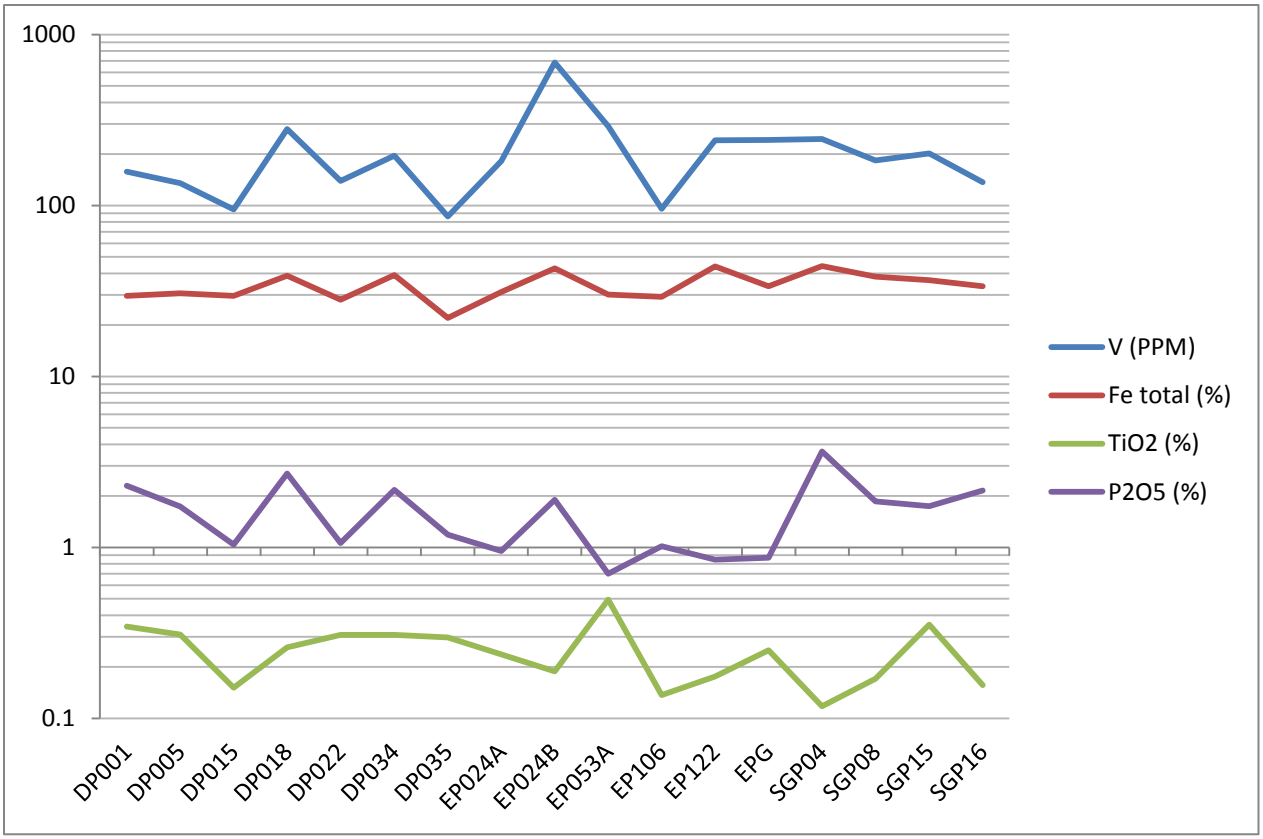

Figure 35 diagram of selected elements related to magnetite ores.

Weakly magnetic

The iron content in these low grade mineralization's are significantly lower than in the strongly magnetic type and varies between 10.0 and 21.0 wt % Fe (total) (Fe_2O_3 16.92 – 31.80 wt %, average 24.23 wt %), Fe, P, V, Cr, Cu, Zn, Ga and Pb are lower in the weakly magnetic samples while the remaining elements have higher concentrations; a full comparison is shown in Table 5.

	Strongly magnetic samples, n=17			*Weakly magnetic samples, n=13*		
	Min	*Max*	*Average*	*Min*	*Max*	*Average*
SiO_2 (wt %)	*21.51*	*51.51*	*35.22*	*31.49*	*54.23*	*44.68*
TiO_2 (wt %)	*0.12*	*0.49*	*0.25*	*0.20*	*0.62*	*0.42*
Al_2O_3 (wt %)	*1.16*	*6.18*	*2.95*	*3.15*	*10.14*	*6.71*
Fe_2O_3t (wt %)	*34.57*	*61.70*	*48.78*	*16.92*	*31.80*	*24.23*
Fe tot[3] (wt %)	*21.98*	*44.11*	*34.22*	*10.04*	*20.99*	*16.08*

MnO (wt %)	*0.01*	*0.18*	*0.07*	*0.06*	*0.39*	*0.17*
MgO (wt %)	*0.31*	*5.05*	*2.40*	*2.08*	*11.84*	*5.91*
CaO (wt %)	*4.02*	*19.01*	*8.21*	*4.47*	*31.09*	*16.11*
Na_2O (wt %)	*0.05*	*1.01*	*0.40*	*0.21*	*3.05*	*0.90*
K_2O (wt %)	*0.00*	*0.25*	*0.08*	*0.00*	*1.19*	*0.26*
P_2O_5 (wt %)	*0.70*	*3.65*	*1.64*	*0.24*	*1.47*	*0.60*
Net LOI[1] (wt %)	*-4.04*	*9.09*	*0.20*	*0.31*	*15.12*	*5.41*
Sc (PPM)	*7.20*	*34.50*	*18.06*	*9.70*	*19.10*	*14.48*
V (PPM)	*86.10*	*686.40*	*215.86*	*55.10*	*205.00*	*102.37*
Cr (PPM)	*132.60*	*669.90*	*393.23*	*74.00*	*375.00*	*192.92*
Co (PPM)[2]	*0.00*	*0.00*	*0.00*	*0.00*	*1.70*	*0.17*
Ni (PPM)	*1.30*	*35.10*	*9.63*	*1.30*	*48.50*	*17.01*
Cu (PPM)	*11.50*	*53.70*	*18.57*	*9.20*	*18.30*	*13.25*
Zn (PPM)	*21.00*	*110.80*	*46.56*	*28.60*	*80.10*	*52.15*
Ga (PPM)	*0.00*	*11.10*	*3.14*	*0.00*	*15.70*	*7.00*
Rb (PPM)	*1.80*	*17.00*	*7.88*	*0.90*	*71.20*	*12.52*
Sr (PPM)	*44.90*	*303.60*	*159.17*	*79.70*	*454.60*	*194.21*
Y (PPM)	*19.70*	*68.10*	*33.51*	*12.00*	*41.80*	*28.64*
Zr (PPM)	*21.50*	*88.30*	*47.18*	*34.80*	*180.60*	*105.69*
Nb (PPM)	*1.50*	*7.90*	*4.14*	*3.10*	*13.00*	*6.95*
Ba (PPM)	*0.00*	*62.40*	*11.69*	*0.00*	*243.80*	*35.12*
La (PPM)	*6.90*	*38.70*	*20.82*	*6.90*	*52.10*	*25.79*
Ce (PPM)	*0.00*	*86.40*	*41.22*	*9.50*	*97.60*	*52.62*
Pb (PPM)	*6.50*	*167.30*	*21.16*	*2.60*	*17.80*	*10.05*
Th (PPM)	*0.00*	*8.70*	*3.89*	*0.00*	*25.10*	*9.51*

Table 5: maximum, minimum and average compositions of the mineralized samples Major elements normalized volatile free. [1]Net loss on ignition, negative numbers indicate gain on ignition. [2]Most mineralized samples return 0 Co due to interference from Fe. [3]Fe total calculated from non-volatile free base.

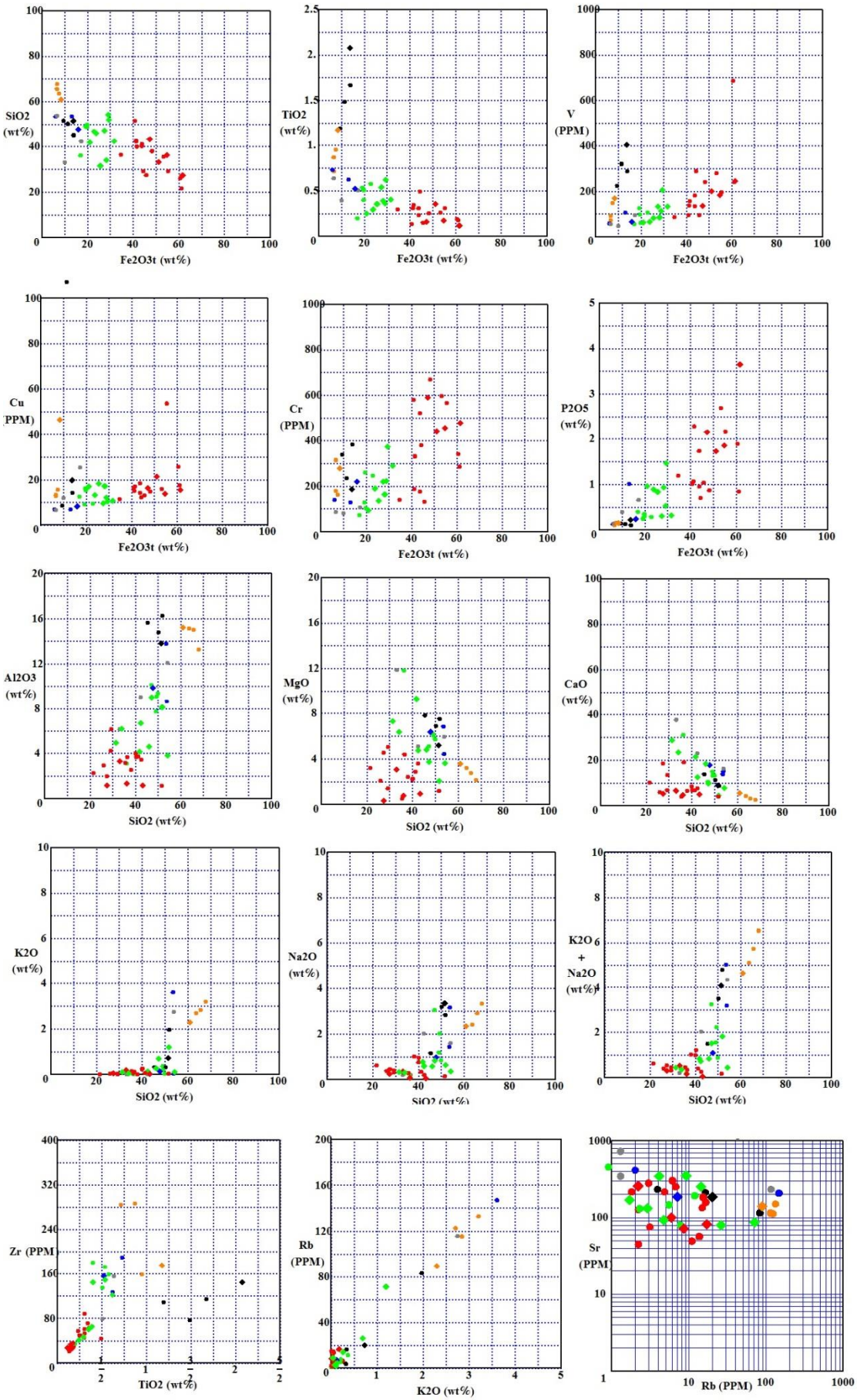
SiO2 (wt%)
Fe2O3t (wt%)
TiO2 (wt%)
Fe2O3t (wt%)
V (PPM)
Fe2O3t (wt%)
Cu (PPM)
Fe2O3t (wt%)
Cr (PPM)
Fe2O3t (wt%)
P2O5 (wt%)
Fe2O3t (wt%)
Al2O3 (wt%)
SiO2 (wt%)
MgO (wt%)
SiO2 (wt%)
CaO (wt%)
SiO2 (wt%)
K2O (wt%)
SiO2 (wt%)
Na2O (wt%)
SiO2 (wt%)
K2O + Na2O (wt%)
SiO2 (wt%)
Zr (PPM)
TiO2 (wt%)
Rb (PPM)
K2O (wt%)
Sr (PPM)
Rb (PPM)

Figure 36 Binary diagrams; oxides normalized to volatile free basis. Red – Strongly magnetic samples, Green – weakly magnetic samples, Black – low LOI mafic rocks, Blue- high LOI mafic rocks, Orange- intermediate to acidic rocs.

7.2 Samples with basic composition

These samples ranges of major elements and V in these samples (Appendix A) are; SiO_2 =45.35 - 53.71 wt % average 51.03 wt %, TiO_2 = 0.62 - 2.08 wt % average 1.3 wt %, Al_2O_3 = 8.66 - 16.27 wt % average 13.83 wt %, Fe_2O_3 = 5.98 - 13.84 wt % average 11.25 wt %, MnO = 0.13 - 0.22 wt % average 0.17 wt %, MgO = 4.43 - 7.84 wt % average 6.46 wt %, CaO = 8.75 - 15.16 wt % average 11.99 wt %, Na_2O = 1.17 - 3.36 wt % average 2.53 wt %, K_2O = 0.03 - 3.6 wt % average 1.16 wt %, P_2O_5 = 0.11 - 1.01 wt % average 0.29 wt % and V (PPM) = 58 - 406.2 PPM average 234.28 PPM. All these samples are

These samples were plotted in immobile element discriminant diagrams for basic rocks (Figure 37 and 38 B). Those diagrams show two groups, one having net loss on ignition under 3 wt % (colored black in the diagrams) and a high net LOI group 3-10 wt %. As there is evidence for metasomatism and partial melting in this unit caution has to be applied to the discriminant diagrams as these are based for the most part on relatively fresh rocks.

In the diagrams from Pearce and Cann (1973) (Fig. 37 A), the high LOI samples plot in the calc-alkaline field while the main samples plot in the combined calc-alkaline, low-K-tholeiites and ocean floor basalts for the Zr-Ti-Y diagram. In the Ti-Zr diagram (Fig. 37 B), the low LOI data plots in the field of ocean floor, the high LOI samples plot in the calc-alkali basalt field. In the Pearce et al. (1984) Cr-Y diagram (Fig. 37 C) all the samples plot in the MORB-field.

In the diagram after Cabains and Lecolle (1989) (Fig. 37 E) the low LOI plots inconclusive, while the high LOI samples plot in the orogenic domain. The diagram after Meschede (1986) (Fig. 37 D) the low LOI samples plot in the N-MORB field while the high LOI samples plot in the within plate tholeiites and volcanic arc basalt.

When looking at the diagram from Mullen (1983) (Fig. 37 F) the low LOI samples clusters in the N-Morb field, with the high LOI samples showing an affinity for arc settings. In the diagram after Shervai (1982) (Fig. 38 B), the low LOI samples cluster along the border between the field for the MORB and the field for ocean island and alkali basalts, the high LOI samples plot in the OIB/alkali basalt field.

Since the low LOI samples plot in the MORB field of most of the discriminant diagrams and the high LOI samples show affinity for arc these may represent two phases of magmatic activity.

The spider diagram (Fig. 40) shows some affinity for Ocean Island Basalt and E-MORB from Sun and McDonough (1989). Thorium and lead are high for basalts.

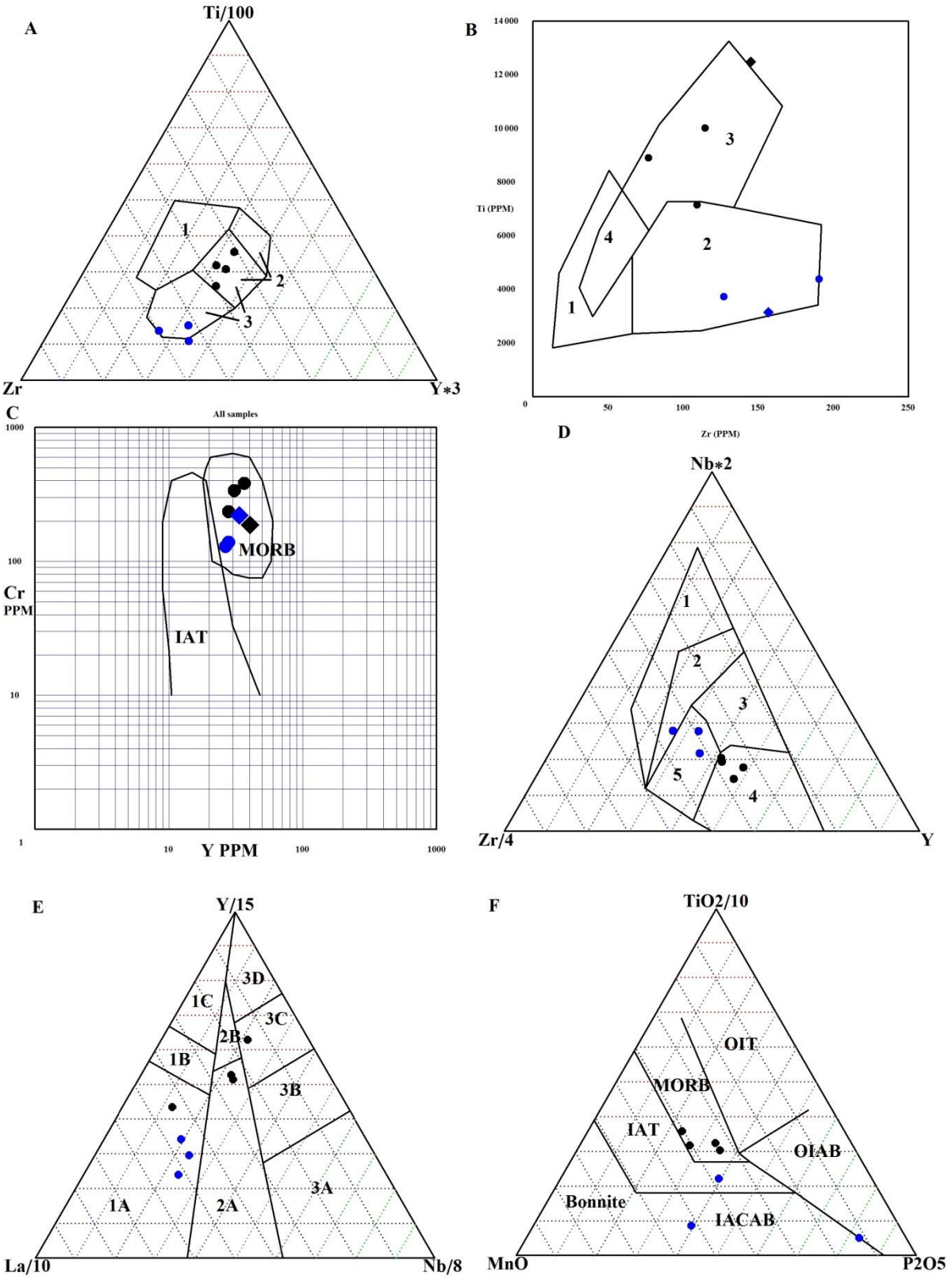

Figure 37 Basic rocks plotted in tectonic setting discriminant diagrams A) Zr-Ti-Y diagram after (Pearce and Cann, 1973) 1- Within-plate basalts, 2- Low-K arc tholeiites, 3- calc-alkaline basalts, 4- Ocean floor basalts. B) Zr-Ti diagram after Pearce and Cann

(1973); 1 - Low-K tholeiites 2 - Calc-alkali basalts 3 - Ocean floor basalts, 4 - Groups 1, 2 and 3. C)Cr-Ydiagram after (Pearce et al., 1984). D) Nb-Y-Zr diagram after (Meschede, 1986); 1 - Within plate alkali basalts, 2 within plate tholeiites, 3- P-MORB, 4 - N-MORB, 5 Volcanic arc basalts. E) Y-La-Nb diagram after Cabanis and Lecolle (1989) 1- Orogenic (compresive) domains (Island arc, active margin), 2- Late to post orogenic (compressive to distensive) intra-continental domains, 3 Anorogen (distensive) domains. F) MnO/TiO2/P2O5 (Mullen, 1983); OIT-Ocean Island Thoeliite, OIAB- Ocean island alkaline basalt, IAT- Island Arc Thoeliite, IACAB - Island Arc Calc-Alkaline Basalt.

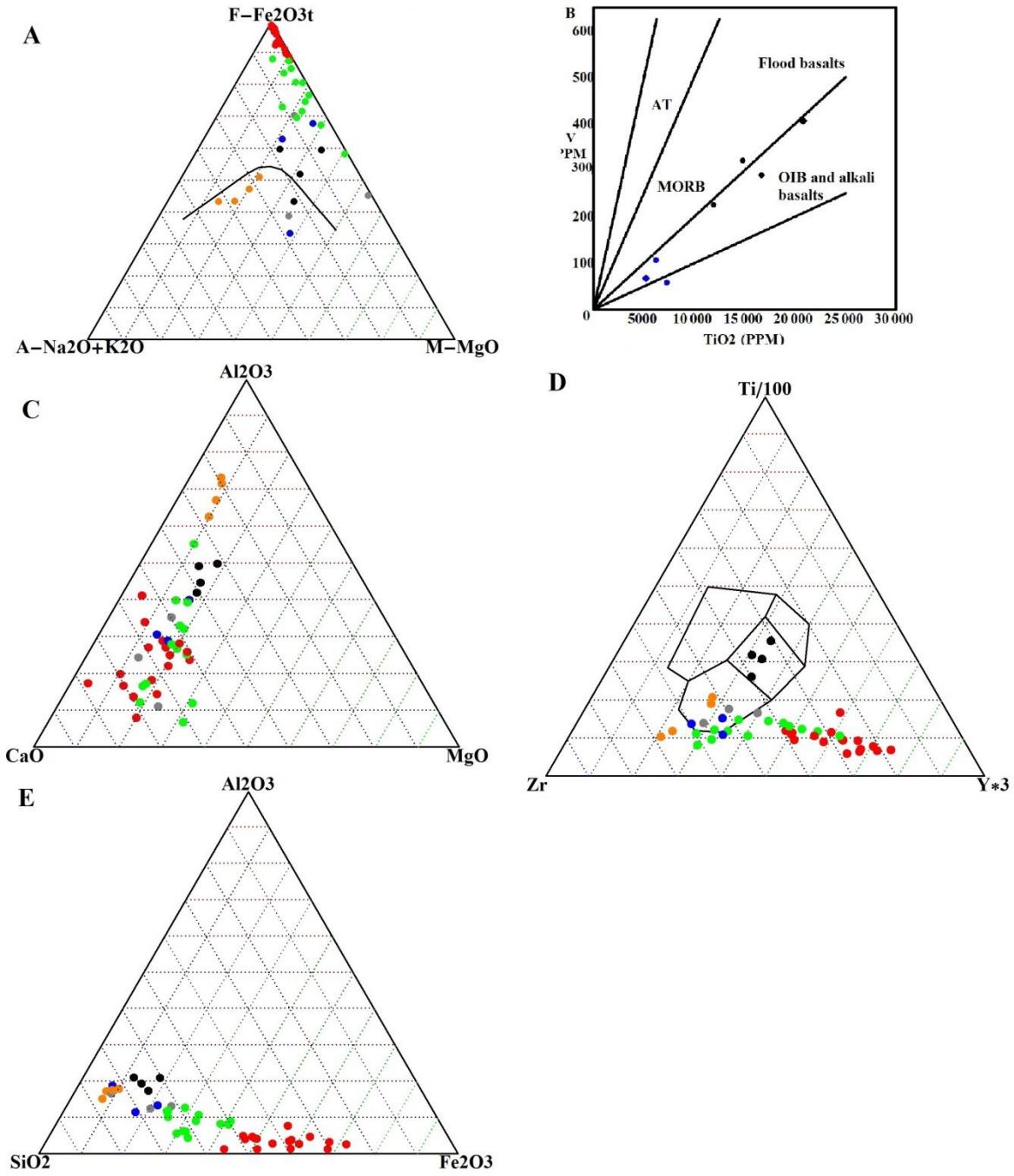

Figure 38 select ternary diagrams, Red – Strongly magnetic samples, Green – weakly magnetic, Orange- intermediate to acidic samples, Black – basic samples with lower LOI than 3wt % and blue basic samples with LOI of 3 to 10 wt %; AFM diagram showing all samples calc-alkaline trend shown for black and blue samples in particular. B) Ti-V diagram after (Shervai, 1982); AT - Arc tholeiites, OIB - Ocean Island basalt, Alkali basalt, low and high LOI basic rocks only. C) CaO -Al_2O_3- MgO. D) Zr-Ti-Y – diagram all samples. E) SiO_2-Al_2O_3-Fe_2O_3

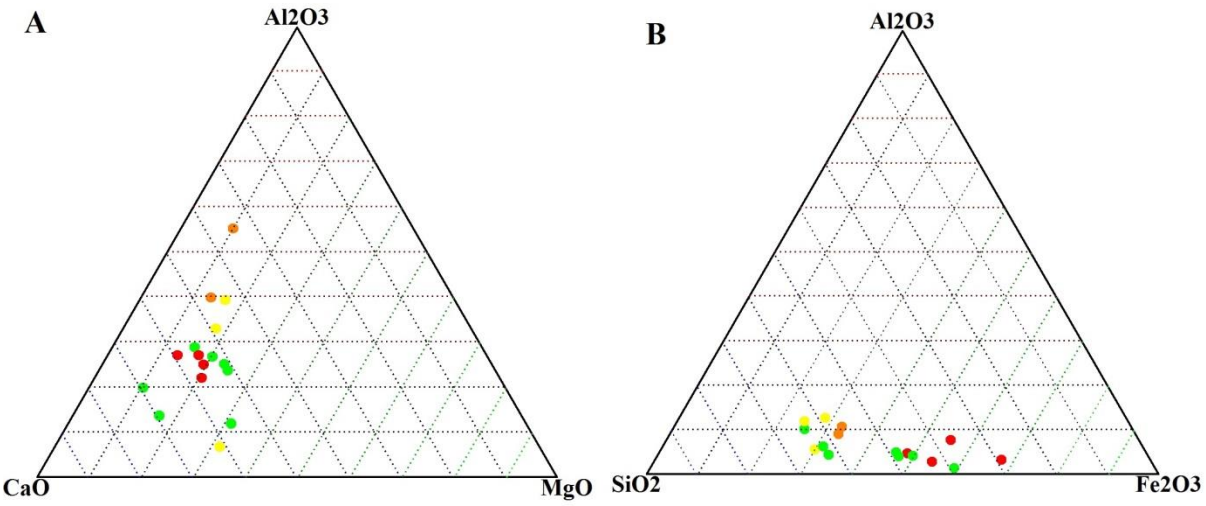

Figure 39 Red- more than 10% pyroxene, Orange – more than 10% garnet + biotite, Yellow – more than 10% garnet, Green – Amphibole and epidote dominated less than 10% garnet or clinopyroxene A) CaO -Al_2O_3- MgO. SiO_2-Al_2O_3-Fe_2O_3

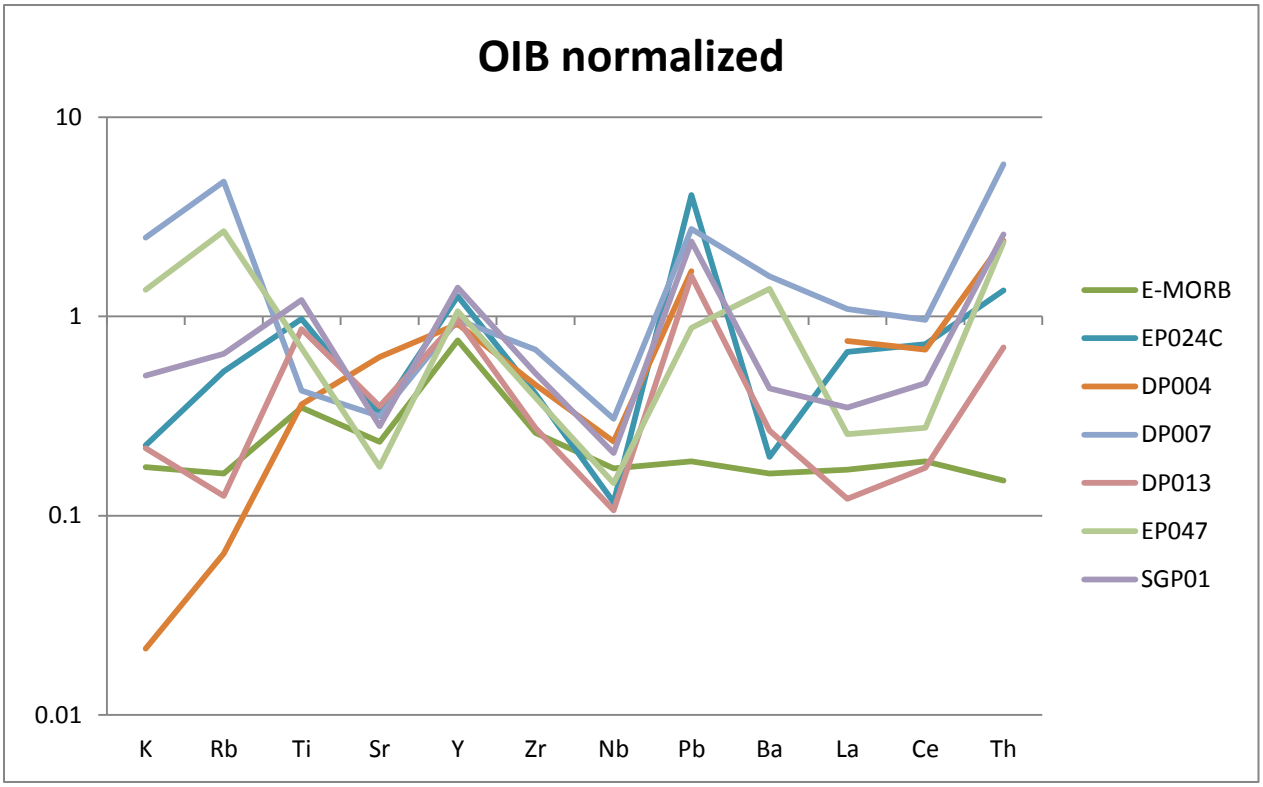

Figure 40 OIB normalized spider diagram for the basic samples; OIB and E-MORB from Sun and McDonough (1989).

8. Discussion

8.1 Categorization of rocks

Since the literature doesn't contain any specific names for these kind of high iron, high pressure high temperature rocks, structural root names will be used after Schmid et al. (2007) and Rosen et al. (2007).

The rocks are banded at different scales from microscopic sub millimeter bands to larger bands of several decimeters. The schistosity varies greatly form poor sub-centimeter to good decimeter scale which makes the differentiation of schist and gneiss gliding and a little problematic, most of the mineralized rocks are however gneisses. Table 6 summarizes the mineral contents of the thin sections. Table 7 summaries the systematic names of the samples.

Samples/mineral	SGP-03	SGP-08	SGP-09	SGP-10	SGP-11	SGP-89	EPG	EP024B	EP053A	DP-005	DP-008	DP-022	DP-030	DP-031	DP-035
Quartz	45 %	40 %	35 %	25 %	20 %		40 %	35 %		15 %	15-20%	32 %	15 %	15 %	10 %
Plagioclase					+			+						+	
Magneitte	*	40 %	15 %	30 %	5 %	5%(opaque)	30 %	32 %	15 %	25 %	5-10%	25 %	18 %	*	18 %
Titano-Magnetite	*		+	5 %	+	*	+	3 %				5 %	12 %	*	2 %
Ilmenite	*			+	*	*				*	+			*	
Hematite	*		+			*		*							
Epidote	*	5 %	30 %	5-10%	3 %			5 %				8 %	5 %		15 %
Clinozoisite					*							5 %		*	
Allanite		*			*									*	
unspecified Ep G		*		*										*	*
Carbonate		*	5 %		5 %	10 %			5 %		5 %	5 %		10 %	20 %
Amphibole	20 %	10 %	15 %	20 %	20 %	60 %		10 %	5-10%	60 %	55 %	20 %	30 %	30 %	20 %
Paragasite														+	
Hornblende			+			+		+	+	+			+	+	
Actenolite													+		
Hastingite					+					+					
Edenite		+						+		+					
Clinopyroxene		*		5-10%		10 %	30 %	<5%	35 %				5-10%	*	
Omphacite														+	
Augite						+									
Augite-Agerine							+	+						+	
Diopside						+			+						
Biotite	2 %				15 %						*				*
Apatite				*	*			2-3%		*		*	3 %	1-2%	1-2%
Garnet	30 %			30 %	20 %	5 %			30 %		10 %			40 %	

*Table 6 Summary of mineral compositions; *= Less than 1 %, **= Much less than 1%, + = From EMPA,*

Rosen et al. (2007) defines carbonate-silicate and calc-silicate rocks as follows:

"Carbonate-silicate rock: Metamorphic rock mainly composed of silicate minerals (including calc-silicate minerals) and containing between 5 and 50% vol. of carbonate minerals (calcite and/or aragonite and/or dolomite).

Calc-silicate rock: Metamorphic rock mainly composed of calc-silicate minerals and containing less than 5% vol. of carbonate minerals (calcite and/or aragonite and/or dolomite). "

SGP-03	*amphibole garnet quartz gneiss*	
SGP-09	*amphibole magnetite epidote quartz gneiss*	*carbonate-silicate*
SGP-08	*epidote amphibole quartz magnetite gneiss*	*calc-silicate*
SGP-10	*amphibole quartz garnet magnetite gneiss*	
SGP-11	*magnetite carbonate biotite garnet amphibole quartz schist*	*carbonate-silicate*
SGP-89	*ironoxide garnet clinopyroxene carbonate amphibole gneiss*	*carbonate-silicate*
EPG	*clinopyroxene magnetite quartz gneiss*	
EP024B	*epidote amphibole magnetite quartz gneiss*	
EP053A	*carbonate magnetite garnet clinopyroxene gneiss*	*carbonate-silicate*
DP-005	*quartz magnetite amphibole gneiss*	
DP-008	*carbonate magnetite garnet quartz amphibole gneiss*	*carbonate-Silicate*
DP-022	*carbonate clinozoisite epidote amphibole magnetite quartz gneiss*	*carbonate-Silicate*
DP-030	*epidote clinopyroxene quartz magnetite amphibole gneiss*	
DP-031	*carbonate quartz amphibole garnet gneiss*	*carbonate-silicate*
DP-035	*quartz epidote carbonate amphibole magnetite gneiss*	*carbonate-silicate*

Table 7 Systematic names after Schmid et al. (2007) and Rosen et al. (2007).

The mineralized rocks can be subdivided by mineralogy into three groups;

Type 1 – Magnetite + quartz + amphibole (+/-garnet+/-epidote+/-apatite+/-carbonate)

Type 2 – Magnetite + quartz + clinopyroxene (+/-garnet+/-epidote+/-apatite+/-carbonate)

Type 3 – Magnetite + quartz + clinopyroxene + amphibole (+/-epidote+/-apatite+/-carbonate)

The strength of the foliation, grain size and relative amount of gangue minerals could be used to subdivide the samples further; this is however not done here.

8.2 Geothermometry

Two geothermometers, Ilmenite-Magnetite and Garnet-Clinopyroxene, were used to gain some insight into peak temperature and how this compared to temperatures and P-T paths in chapter 2.2

The excel spreadsheet ILMAT (Lepage, 2003) was used to recalculated the Ilmenite – magnetite geothermometer (Table 8) from EMPA analyses #68 and #69 (figure 19 A).

The garnet-clinopyroxene Fe^{2+} - Mg geothermometer, calibration after RAVNA (2000), Eq. 1, was also used to estimate peak temperatures. Oxidation states of iron were calculated by stoichiometry and Fe^{3+} = Na-Al-Cr giving a low and high estimate of the temperature respectively (Fig. 41).

Eq. 1 from RAVNA (2000):

$$T(\ ^{o}C) = \left\lfloor \left(1939.9 + 3270\, X_{Ca}^{Grt} - 1396(X_{Ca}^{Grt})^2 + 3319 X_{Mn}^{Grt} - 3535(X_{Mn}^{Grt})^2 + 1105 X_{Mg\#}^{Grt} - 3561\left(X_{Mg\#}^{Grt}\right)^2 + 2324\left(X_{Mg\#}^{Grt}\right)^3 + 169.4\, P(GPa)\right) / (\ln K_D + 1.223) \right\rfloor - 273,$$

where K_D=$(Fe^{2+}/Mg)^{Grt}/(Fe^{2+}/Mg)^{Cpx}$, X_{Ca}^{Grt}=Ca/(Ca+Mn+Fe^{2+}+Mg) in garnet, X_{Mn}^{Grt}= Mn/(Ca+Mn+Fe^{2+}+Mg) in garnet, and $X_{Mg\#}^{Grt}$=Mg/(Mg+Fe^{2+}) in garnet.

Geothermobarometer by:			Andersen and Lindsley (1985)
X'Usp & X'Ilm from:		Temp (°C)	log10 fO_2
Carmichael (1967)		*738*	*0.00*
Anderson (1968)		*737*	*-15.76*
Lindsley and Spencer (1982)		*736*	*-15.81*
Stormer Jr (1983)		*737*	*-15.79*

Table 8 results from ILMAT using analyses #68 magnetite and #69 ilmenite from the thin section DP031.

The magnetite-ilmenite thermometer show similar temperature as stages II and III described in RAVNA and ROUX (2006), but measures a down going temperature. In between the garnet-pyroxene geothermometers lines lies the 3.36 GPa, 735 ^{o}C Stage II eclogite stage The geothermometers only indicates what was already discussed in chapter 2, that these deposits are located in an high to ultra-high-pressure terrain.

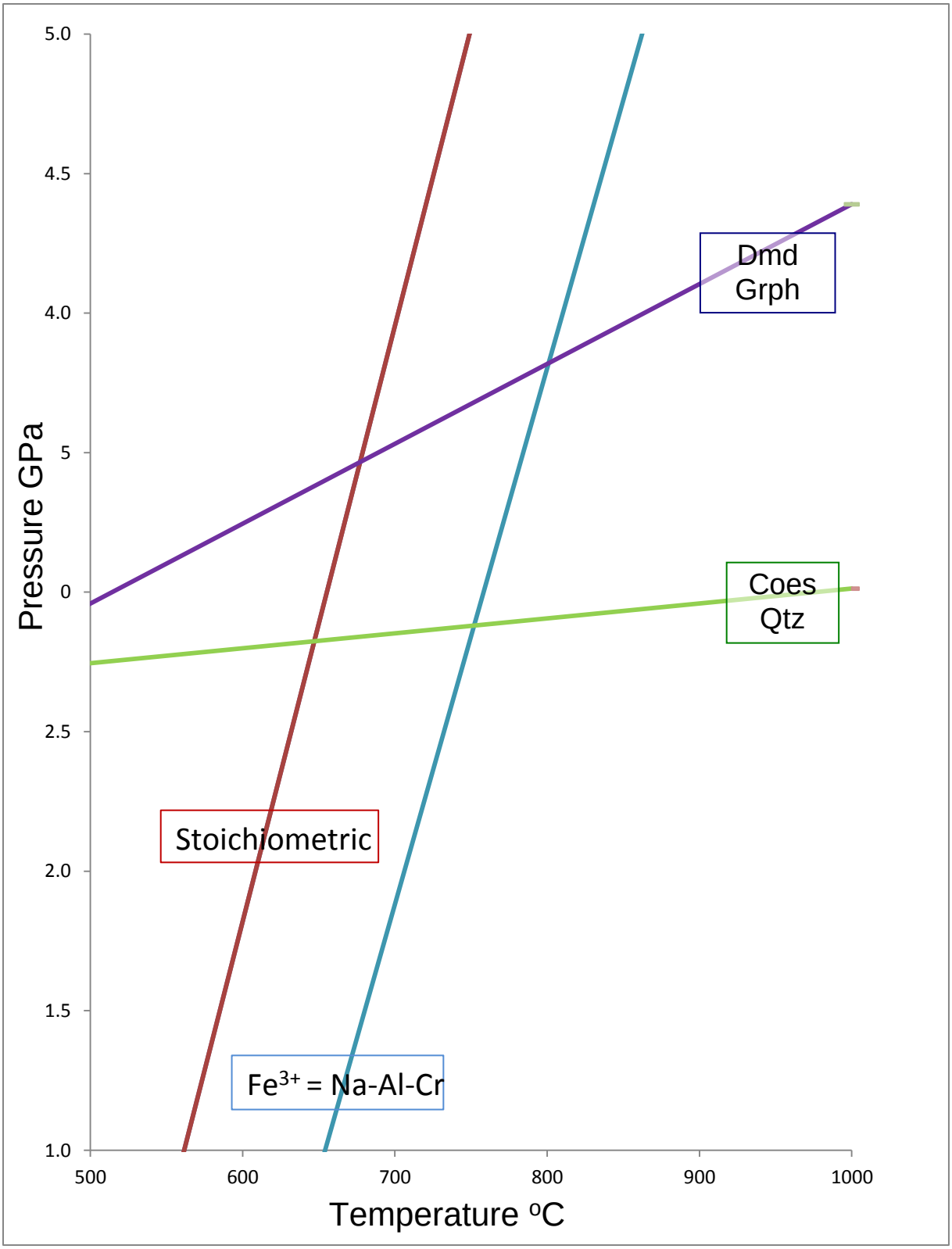

Figure 41 Garnet – Pyroxene thermometer

8.3 Magnetite mineralizations

The estimated amount of magnetite (magnetite + Ti-magnetite) from the thin sections appears to show a linear relationship with the Fe_2O_3 total (normalized) of the whole rock

geochemistry (Fig. 42). The estimated median grain size of magnetite seams to follow the same pattern, increasing with modal magnetite content. The prospective grades of the ore seems to be more in line with the 1910s (Hasselbom et al., 1909) sampling than with the numbers given by Eriksen and Bugge (1943), with total iron contents in the strongly magnetic samples of 21.98-44.11 wt % Fe averaging 34.22 wt %, however proper channel sampling, magnetic susceptibility readings or target drilling would be required to get a better understanding of the actual grades.

The numbers given by both groups of prospectors in the first half of the 20th century must be seen in the light of what there aims might have been and the political situation for the 1940s reports.

Metallogenesis

It is clear that these rocks have undergone high-grade metamorphism, metasomatism and partial melting in places. As the primary textures are over printed, there are several types of protolith to consider; banded iron formation, iron skarn and Kiruna type magmatic rocks. Garnets in iron skarns are typically andradite and grossularite dominated (MEINERT et al., 2005) while almandine is common in medium to high metamorphic grade iron formations (KLEIN, 2005), the garnets here are almandine rich, with notable grossularite and pyrope components.

Iron formations are defined in Gross (2007) and sources there in as ”*all stratigraphic units of layered, bedded, or laminated rocks that contain 15 per cent or more iron, in which the iron minerals are commonly interbanded with quartz, chert, or carbonate, and where the banded structure of the ferruginous rocks conforms in pattern and attitude with the banded structure of the adjacent sedimentary, volcanic, or metasedimentary rocks”*. He also states that iron formations tend to retain banding during metamorphism.

Since the rocks are have micro to meso scale bands of quartz, magnetite and silicates and these bands are apparently conformal to the surrounding marble as seen in chapter 5 and 6 the petrography points toward iron formation type protolith.

As the terrain is HP-metamorphosed one can’t expect to find/recognize textural evidence for mixtites and glaciogenic rocks, which are commonly associated with rapitan type iron formation (Gross, 2009).

A geochemical comparison with banded iron formations is difficult as “*They (BIFs) commonly form distinct stratiform units and may be interlayered or mixed with clastic sediment, volcanogenic rocks, limestone and dolomite sedimentary rocks and with stratiform*

or massive sulphide beds, layers and lenses. Stratigraphic units commonly classified as mixed lithofacies may consist of interlayered beds deposited as clastic sediment and as chemical and biochemically mediated precipitates as well as strata developed by diagenetic alteration of detrital sediment, lutite and argillaceous muds" (Gross, 2009). In addition to the mix of protoliths there is recrystallization and metamorphic overprinting, these complex interactions makes geochemical comparisons difficult.

The phosphorus content is quite high for a banded iron formation (Fig. 43). MnO, K_2O, Ni and Ba appear to be relatively depleted compared to the averages of the iron formations. K_2O depletion can easily be accounted for by metasomatism which we have seen some evidence for in chapter 5. As I do not have similar data for rapitan type iron formations which should have more similar phosphor content (KLEIN, 2005), no comparison has been made.

An iron skarn consisting of iron oxides, quartz, carbonates and silicate rock of a similar composition to an iron formation should look much the same if it was metamorphosed into gneiss. Both such a meta-iron skarn and banded iron formation where the hydrolytic sediments are interlaid with bands of other types of sediments should display similar mineralogies and structural relations. This makes being certain of the protolith of the mineralized rocks difficult at the least. As the contact between the marble and the nearby rocks appear to be sharp and similar in dip/dip direction to the banding of the iron rich rocks this might imply a sedimentary relationship.

But as this iron ore field is part of a string of similar occurrences (Sandstad, 2012) which makes the likelihood of the deposit being part of a banded iron formation higher.

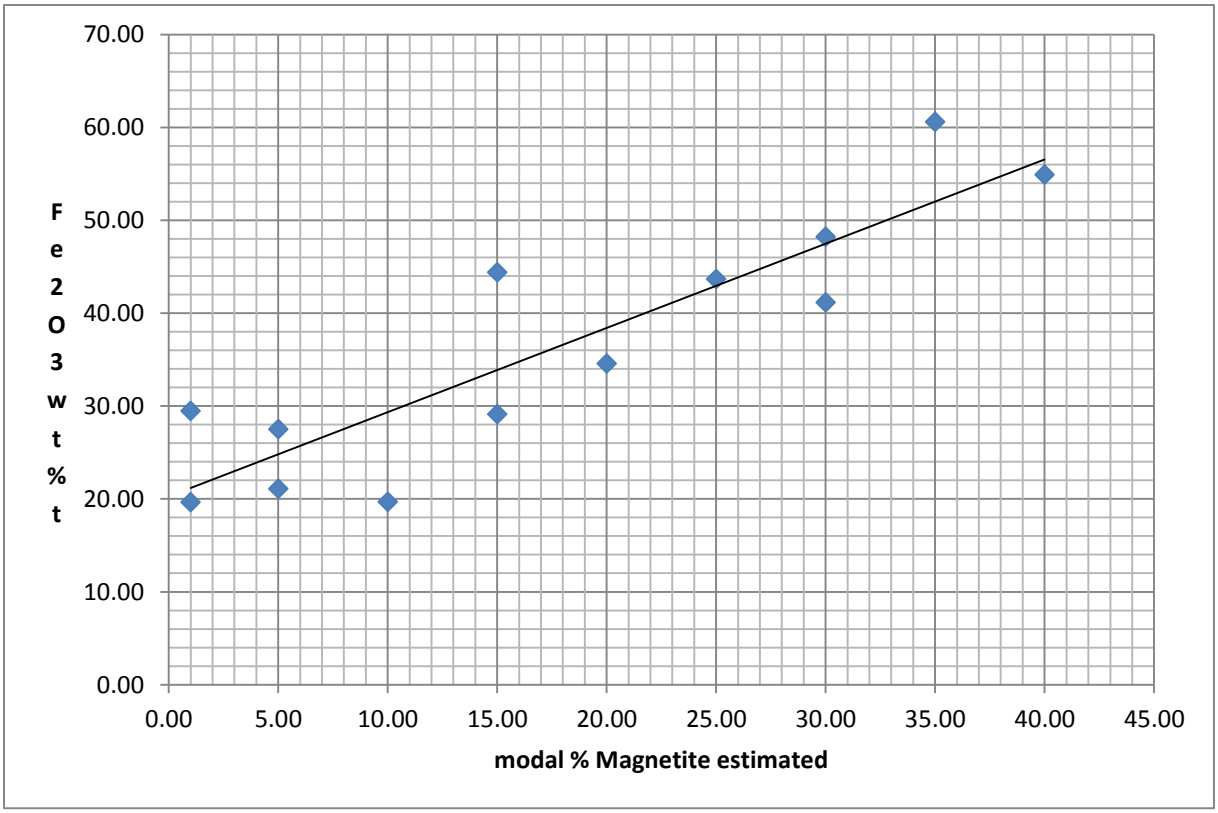

Figure 42 estimated amount of magnetite in thin sections vs. Fe_2O_3 total from whole rock geochemistry.

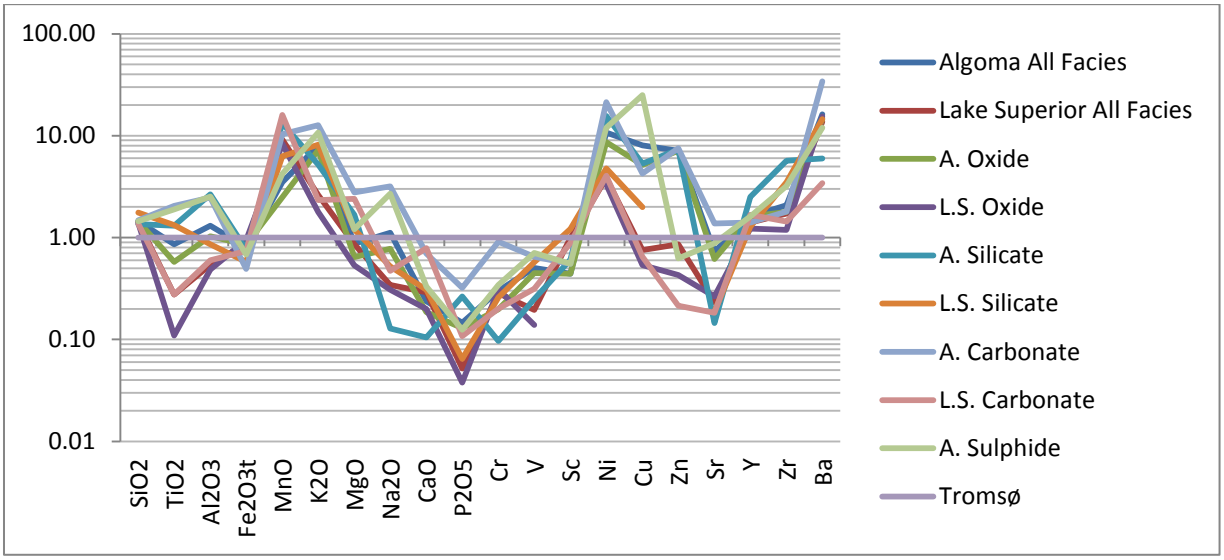

Figure 43 Comparison of the strongly mineralized rocks with averages of iron formation facies from (GROSS and McLEOD, 1980) (oxides normalized by same procedure as in chapter 7)

9. Conclusion

Magnetite is the only iron oxide of import in the studied thin sections. The magnetite mineralizations in Sollidalen, Sollidalsaksla (møllendalsaksla) and Kalvebekli (Djupdalen) appear to be of sufficiently high grade that they may be considered iron ore at the present. The amount of these mineralizations, the tonnage, can't be estimated in any meaningful way with the current data. The magnetite does not contain sufficient quantities of vanadium or titanium to be considered as ores for these metals and there does not appear to be any other metals of interest in sufficient quantity in these rocks to be considered potential ore.

The strongly magnetic, potential ore, rocks are contained in bands (decimeter to decameter thick) in a lower grade iron formation.

The associated rock of basic composition appears to be of both MORB and IAT types, alto these result must be interpreted with caution as there is evidence of partial melting and metasomatism. The deposit most likely has a sedimentary protolith, alto the primary/ early secondary structures appear to have been over printed by metamorphic proses.

References

ANDERSEN, D. J. & LINDSLEY, D. H. 1985. New (and final!) models for the Ti-magnetite/ilmenite geothermometer and oxygen barometer. Abstract AGU 1985 Spring Meeting Eos Transactions. American Geophysical Union 66 (18), 416.

ANDERSON 1968. Oxidation of the La Blanche Lake titaniferous magnetite deposit, Qu!ebec. . Journal of Geology, 76**,** 528-547.

ANDRESEN, A. 1988. Caledonian terranes of northern norway and their characteristics. Trabajos de geologia, 17**,** 103-117.

ANDRESEN, A. & STELTENPOHL, M. G. 1994. Evidence for ophiolite abduction, terrane accretion and polyorogenic evolution of the north Scandinavian Caledonides. Tectonophysics, 231**,** 59-70.

BINNS, R. E. 1978. Caledonian nappe correlation and orogenic history in Scandinavia north of lat 67°N. Geological Society of America Bulletin, 89**,** 1475-1490.

BROKS, T. M. 1985. Berggrunnsgeologiske undersøkelser innen Tromsø dekkekompleks i området Tromsdalen-Ramfjord-Breivikeidet, Troms. Unpubl. Cand. Scient. Thesis, University of Tromsø.

CABANIS, B. & LECOLLE, M. 1989. Le diagramme La/10-Y/15-Nb/8; un outil pour la discrimination des series volcaniques et la mise en evidence des processus de melange et/ou de contamination crustale.: . Comptes Rendus de l'Academie des Sciences, Serie 2, Mecanique, Physique, Chimie, Sciences de l'Univers, Sciences de la Terre, 309**,** 2023-2029.

CARMICHAEL, I. S. E. 1967. The iron-titanium oxides of salic volcanic rocks and their associated ferromagnesian silicates. Contributions to Mineralogy and Petrology 14**,** 36-64.

CORFU, F., RAVNA, E. J. K. & KULLERUD, K. 2003. A Late Ordovician U–Pb age for the Tromsø Nappe eclogites, Uppermost Allochthon of the Scandinavian Caledonides. Contrib Mineral Petrol, 145**,** 502–513.

DAMBERG, A. J. 2012. Post-eklogitt deformasjon, mineralreaksjoner og metamorfose innen Tromsødekket. Master, Universitet i Tromsø.

ELORANTA, J. W. 1983. DETERMINATION OF MAGNETITE CONTENT THROUGH THE USE OF MAGNETIC SUSCEPTIBILITY IN LARGE DIAMETER BLAST HOLES. DEGREE OF MASTER OF SCIENCE, Major in Mining Engineering, UNIVERSITY OF WISCONSIN - MADISON.

ERIKSEN, A. 1943. Bericht uber die untersuchungen in Tromsøysund Jernfelter. Bergarkivet.

ERIKSEN, A. & BUGGE, J. 1943. BA795. Bericht über die untersuchungen in "Tromsösund Jernfelter" in 1942 & 1943.

GEE, D. G., FOSSEN, H., HENRIKSEN, N. & HIGGINS, A. K. 2008. From the Early Paleozoic Platforms of Baltica and Laurentia to the Caledonide Orogen of Scandinavia and Greenland. Episodes, 31**,** 44-51.

GEE, D. G. & STURT, B. A. 1985. The Caledonide Orogen - Scandinavia and Related Areas. Chichester: John Wiley and Sons.

GROSS, G. A. 2009. Iron Formation in Canada, Genesis and Geochemistry. [Online].

GROSS, G. A. & MCLEOD, C. R. 1980. A PRELIMINARY ASSESSMENT OF THE CHEMICAL COMPOSITION OF IRON FORMATIONS IN CANADA. Canadian Mineralogist, 18**,** 223-229.

HASSELBOM, A., MELVÆR, T., STOEREN, R. & SMITH, H. H. 1909. BA4177. In: BOHOLM, H. D. H. (ed.) Aktieneinladung mit rentabilitatsberecnungen fur A/S Nordenfjeldske Jern og Staalverker.

HÅBREKKE, H., BRANDHAUG, K., BLOKKUM, O. & AALSTAD, I. 1967. NGU rapport 797. Magnetisk flymåling TROMSØSUND JERNMALMFELT Tromsø.

JANAK, M., RAVNA, E. J. K. & KULLERUD, K. 2012. Constraining peak P–T conditions in UHP eclogites: calculated phase equilibria in kyanite- and phengite-bearing eclogite of the Tromsø Nappe, Norway. Journal of Metamorphic Geology, 12**,** 377–396.

JANÁK, M., RAVNA, E. J. K., KULLERUD, K., YOSHIDA, K., 4, R. M. & HIRAJIMA, T. 2013. Discovery of diamond in the Tromsø Nappe, Scandinavian Caledonides (N. Norway). Journal of Metamorphic Geology.

KLEIN, C. 2005. PRESIDENTIAL ADDRESS TO THE MINERALOGICAL SOCIETY OF AMRICA, BOSTON, NOVEMBER 6, 2001 Some Precambrian banded iron-formations (BIFs) from around the world: Their age, geologic setting, mineralogy, metamorphism, geochemistry, and origin. American Mineralogist, 90, 1473–1499.

KROGH, E. J., ANDRESEN, A., BRYHNI, BROKS, T. M. & KRISTENSEN, S. E. 1990. Eclogites and polyphase P–T cycling in the Caledonian Uppermost Allochthon in Troms, northern Norway. Journal of Metamorphic Geology, 8, 289-309.

LEAKE, B. E., WOOLLEY, A. R., ARPS, C. E. S., BIRCH, W. D., GILBERT, M. C., GRICE, J. D., HAWTHORNE, F. C., KATO, A., KISCH, H. J., KRIVOVICHEV, V. G., LINTHOUT, K., LAIRD, J., MANDARINO, J. A., MARESCH, W. V., NICKEL, E. H., ROCK, N. M. S., SCHUMACHER, J. C., SMITH, D. C., STEPHENSON, N. C. N., WHITTAKER, E. J. W. & YOUZHI, G. 1997. NOMENCLATURE OF AMPHIBOLES: REPORT OF THE SUBCOMMITTEE ON AMPHIBOLES OF THE INTERNATIONAL MINERALOGICAL ASSOCIATION, COMMISSION ON NEW MINERALS AND MINERAL NAMES. The Canadian Mineralogist, 35, 219-246.

LEPAGE, L. D. 2003. ILMAT: an Excel worksheet for ilmenite–magnetite geothermometry and geobarometry. Computers & Geosciences, 29, 673-678.

LIAN, C. & SMITH, H. H. Mars 1944. BA3519 Correspondens between C. Lian and H.H. Smith.

LINDSLEY, D. H. & SPENCER, K. J. 1982. Fe–Ti oxide geothermometry: Reducing analyses of coexisting Ti-magnetite (Mt) and ilmenite (Ilm) abstract AGU 1982 Spring Meeting Eos Transactions. American Geophysical Union 63 18.

MATHIEU 1911. BA1660. Tromsøsundets Jernleier/Mines de fer de Tromsoe.

MEINERT, L. D., DIPPLE, G. M. & NICOLESCU, S. 2005. World Skarn Deposits. Economic Geology 100th Anniversary Volume, 299–336.

MELEZHIK, V. A., ZWAAN, B. K., MOTUZA, G., ROBERTS, D., ARNE SOLLI, ANTHONY E. FALLICK, GOROKHOV, I. M. & KUSNETZOV, A. B. 2003. New insights into the geology of high-grade Caledonian marbles based on isotope chemostratigraphy. NORWEGIAN JOURNAL OF GEOLOGY, 83.

MESCHEDE, M. 1986. A method of discriminating between different types of mid-ocean ridge basalts and continental tholeiites with the Nb-Zr-Y diagram. Chemical Geology, 56, 207-218.

MORIMOTO, N. 1989. OMENCLATURE OF PYROXENES. Canadian Mineralogist, 27, 143-156.

MULLEN, E. D. 1983. MnO/TiO2/P2O5: a minor element discriminant for basaltic rocks of oceanic environments and its implications for petrogenesis. Earth and Planetary Science Letters, 62, 53-62.

NAGATA, T. 1961. Rock Magnetism, Maruzen Comp. Limited.

NESSE, W. D. 1999. Introduction to Mineralogy.

OHLE, E. L. 1972. Evaluation of Iron Ore Deposits. Economic Geology, 67, 953-964.

PEARCE, J. A. & CANN, J. R. 1973. Tectonic setting of basic volcanic rocks determined using trace element analyses. Earth and Planetary Science Letters, 19, 290–300.

PEARCE, J. A., LIPPARD, S. J. & ROBERTS, S. 1984. Characteristics and tectonic significance of supra-subduction zone ophiolites. Geological Society, London, Special Publications, 16, 77-94.

POHL, W. L. 2011. Economic Geology Principles and Practice:, Wiley-Blackwell.

RAVNA, E. J. K., KULLERUD, K. & ELLINGSEN, E. 2006. Prograde garnet-bearing ultramafic rocks from the Tromsø Nappe, northern Scandinavian Caledonides. Lithos, 92, 336–356.

RAVNA, E. J. K. & ROUX, M. R. M. 2006. Metamorphic Evolution of the Tønsvika Eclogite, Tromsø Nappe—Evidence for a New UHPM Province in the Scandinavian Caledonides. International Geology Review, 38.

RAVNA, E. K. 2000. The garnet–clinopyroxene Fe2+–Mg geothermometer: an updated calibration. J. metamorphic Geol, 18, 211-219.

RICKWOOD, P. C. 1968. On Recasting Analyses of Garnet into End-Member Molecules. Contr. Mineral. and Petrol., 18, 175-198.

RIIBER, C. & SMITH, H. H. 1948. BA1540 Correspodanse between C. Riiber and H.H. Smith.

ROBERTS, D. 2003. The Scandinavian Caledonides: event chronology, palaeogeographic settings and likely modern analogues. Tectonophysics, 365, 283– 299.

ROBERTS, D., MELEZHIK, V. M. & HELDAL, T. 2002. Carbonate formations and early NW-directed thrusting in the highest allochthons of the Norwegian Caledonides: evidence of a Laurentian ancestry. Journal of the Geological Society, London, 159, 117-120.

ROSEN, O., DESMONS, J. & FETTES, D. 2007. 7. Metacarbonate and related rocks: Provisional recommendations by the IUGS Subcommission on the systematics of metamorphicrocks. Web version of 01.02.07 Available: http://www.bgs.ac.uk/scmr/docs/papers/paper_7.pdf.

SANDSTAD, J. S. 2012. N034 troMs fe. In: EILU, P. (ed.) Special Paper 53. GEOLOGICAL SURVEY OF FINLAND.

SCHMID, R., FETTES, D., HARTE, B., DAVIS, E. & DESMONS, J. 2007. 1. HOW TO NAME A METAMORPHIC ROCK: Recommendations by the IUGS Subcommission on the Systematics of Metamorphic Rocks: Web version 01/02/07 Available: http://www.bgs.ac.uk/scmr/docs/papers/paper_1.pdf.

SHERVAI, J. W. 1982. Ti-V plots and the petrogenesis of modern and ophiolitic lavas Earth and Planetary Science Letters, 59, 101 - 118.

SMITH, H. H. 1909. BA2912. Rapport övfer Tromsösundets jernfelter tromsö/Repport on the Tromsösundet ironore field/Bericth uber das Tromsösundet esenertzfeld.

SMITH, H. H. 1910. BA2255. Rapport öfver Tromsösundets Jernfelter Tromsö/Rapport über die Eisenerzfelder von Tromsösundet, Tromsö.

SPRY, P. G. & GEDILINSKE, B. L. 1987. Tables for the Determination of Common Opaque Minerals.

STORMER JR, J. C. 1983. The effects of recalculation on estimates of temperature and oxygen fugacity from analyses of multicomponent iron-titanium oxides. . American Mineralogist 68, 586-594.

SUN, S.-S. & MCDONOUGH, W. F. 1989. Chemical and isotopic systematics of ocean basalts: implications for mantle composition and processes. In: SAUNDERS, A. D. & NORRY, M. J. (eds.) Magmatism in the Ocean Basins Spec. Publ. Vol. Geol. Soc. Lond. , No. 42.

ØIESVOLD, M. B. G. 2007. OVERGANGEN FRA EKLOGITT TIL AMFIBOLITT – ET DETALJSTUDIUM. Master, Universitetet i Tromsø.

APPENDIX A Whole rock geochemistry

Sample	DP001	DP005	DP015	DP018	DP022	DP034	DP035	EP024A	EP024B	EP053A	EP106	EP122	EPG	SGP04	SGP08	SGP15	SGP16
SiO2 (%)	40.62	40.38	25.38	36.89	41.5	29.5	33.12	41.77	26.24	28.43	52.65	22.07	37.92	28.07	36.18	33.85	44.29
TiO2 (%)	0.35	0.31	0.14	0.27	0.3	0.31	0.27	0.24	0.19	0.48	0.14	0.18	0.25	0.12	0.17	0.36	0.16
Al2O3 (%)	4.07	3.7	1.85	3.32	3.4	4.27	3.36	3.82	2.99	6	1.19	2.31	2.55	1.2	1.32	3.41	1.2
Fe2O3 (%)	42.26	43.87	42.25	55.51	40.18	55.91	31.43	44.47	61.28	43.1	41.67	62.78	48.11	63.07	54.81	52.21	48.22
MnO (%)	0.117	0.102	0.164	0.031	0.076	0.032	0.074	0.096	0.059	0.09	0.039	0.044	0.079	0.015	0.05	0.116	0.059
MgO (%)	2.25	2.27	4.21	0.53	3.51	1.41	4	2.92	2.09	4.9	1.21	3.28	2.41	0.32	0.75	3.11	0.95
CaO (%)	8.66	6.86	17.21	4.2	7.39	6.89	17.28	6.82	5.96	13.09	4.11	10.45	6.6	5.39	4.56	6.63	5.04
Na2O (%)	0.77	0.98	0.43	0.31	0.2	0.42	0.18	0.35	0.38	0.31	0.14	0.64	1.01	0.26	0.08	0.35	0.05
K2O (%)	0.25	0.25	0.06	0.17	0.04	0.04	0.12	0.06	0.03	0.01	0.03	0	0.01	0.05	0.07	0.18	0.01
P2O5 (%)	2.329	1.741	0.96	2.805	1.036	2.191	1.08	0.967	1.918	0.681	1.038	0.87	0.867	3.727	1.852	1.773	2.201
H2O (%)	0	0	7.33	0	2.36	0	9.09	0	0	2.9	0	0	0.2	0	0.16	0	0
	101.676	100.463	99.984	104.036	99.992	100.973	100.004	101.513	101.137	99.991	102.217	102.624	100.006	102.222	100.002	101.989	102.18
Net Loi	-1.676	-0.463	7.346	-4.036	2.368	-0.973	9.086	-1.513	-1.137	2.909	-2.217	-2.624	0.194	-2.222	0.158	-1.989	-2.18
Fe tot %	29.6	30.7	29.6	38.8	28.1	39.1	22.0	31.1	42.9	30.1	29.1	43.9	33.6	44.1	38.3	36.5	33.7
Normalized																	
SiO2 (%)	39.95	40.19	27.39	35.46	42.51	29.22	36.43	41.15	25.95	29.28	51.51	21.51	37.99	27.46	36.24	33.19	43.35
TiO2 (%)	0.34	0.31	0.15	0.26	0.31	0.31	0.30	0.24	0.19	0.49	0.14	0.18	0.25	0.12	0.17	0.35	0.16
Al2O3 (%)	4.00	3.68	2.00	3.19	3.48	4.23	3.70	3.76	2.96	6.18	1.16	2.25	2.55	1.17	1.32	3.34	1.17
Fe2O3 (%)	41.56	43.67	45.60	53.36	41.15	55.37	34.57	43.81	60.59	44.39	40.77	61.17	48.20	61.70	54.90	51.19	47.19
MnO (%)	0.12	0.10	0.18	0.03	0.08	0.03	0.08	0.09	0.06	0.09	0.04	0.04	0.08	0.01	0.05	0.11	0.06
MgO (%)	2.21	2.26	4.54	0.51	3.60	1.40	4.40	2.88	2.07	5.05	1.18	3.20	2.41	0.31	0.75	3.05	0.93
CaO (%)	8.52	6.83	18.57	4.04	7.57	6.82	19.01	6.72	5.89	13.48	4.02	10.18	6.61	5.27	4.57	6.50	4.93
Na2O (%)	0.76	0.98	0.46	0.30	0.20	0.42	0.20	0.34	0.38	0.32	0.14	0.62	1.01	0.25	0.08	0.34	0.05
K2O (%)	0.25	0.25	0.06	0.16	0.04	0.04	0.13	0.06	0.03	0.01	0.03	0.00	0.01	0.05	0.07	0.18	0.01
P2O5 (%)	2.29	1.73	1.04	2.70	1.06	2.17	1.19	0.95	1.90	0.70	1.02	0.85	0.87	3.65	1.85	1.74	2.15
Sc (PPM)	19.9	23.1	16.5	10.3	21.5	34.5	13.8	19.6	12.2	27	12.8	16	16.1	7.7	15.3	22.7	7.2
V (PPM)	157.3	135.2	94.6	280.1	138.8	195.7	86.1	182	686.4	290.3	95.7	240.3	241.7	244.7	183.2	201.7	136.9
Cr (PPM)	332.8	177	132.6	597	187.4	567.1	140.8	521	341.7	380.7	580.5	286.7	669.9	478.8	454.8	442.8	589.8
Co (PPM)	0	0	0	0	0	0	0	0	0	0	0	0	0	0	0	0	0
Ni (PPM)	9.8	10.4	6.9	10	10.1	10.5	7	14.6	7.6	35.1	7	1.3	9.4	1.8	3.1	9.4	6.6
Cu (PPM)	17	14.4	13.2	16	15	53.7	11.5	18.6	25.7	12.3	16.4	17.7	14.7	15.5	13.9	21.5	16.4
Zn (PPM)	53	27.3	22.6	39.2	33	86.1	27.5	59.9	110.8	39.9	24.8	45.2	53.9	22.3	21	78.4	31.6
Ga (PPM)	3	2.7	0.9	5.2	1.5	3.3	1.7	6.1	11.1	0	3.1	0	4.5	0	3.7	3.5	0
Rb (PPM)	6.1	6.7	3	16.5	2.2	14.9	4.8	13.6	2.2	1.8	10.9	15.2	3.1	2.2	5.9	17	8.6
Sr (PPM)	303.6	252.3	281.2	158.6	127.6	134.5	217.8	57.3	44.9	217.2	49.4	184.7	75.9	258.6	101	82.1	72.7
Y (PPM)	31.3	25.2	33.1	27.5	39.8	68.1	30.7	25.9	34	34.8	19.7	33.8	22.1	25.2	37.5	47.4	20.6
Zr (PPM)	71.9	61	29.1	49.3	52.7	88.3	45.2	57.8	30.9	43.6	21.5	36.6	50	28	26.8	62.2	33.8
Nb (PPM)	4.4	7.2	3.6	1.9	4.6	4.4	5.3	5.3	2.2	6.4	1.5	3	2.9	2.3	3.3	7.9	3.2
Ba (PPM)	10.9	13	0	9.4	0.3	62.4	5.5	10.5	1.1	0	1.5	0	0	3.6	30.2	38.6	0.1
La (PPM)	23.9	10.1	19.5	25.9	27.4	38.7	18.1	14.1	6.9	18.8	18.4	16.7	12.6	24.9	21.9	35.2	20.1
Ce (PPM)	44.6	15.5	33.6	53.7	48.1	86.4	35.9	35.7	0	38.2	41.7	39.9	27.9	33.9	50.1	74.3	43.1
Pb (PPM)	6.8	7.5	19.6	9.6	14	167.3	10	12	10.5	8	11.9	10.7	6.5	9.7	8.8	25.7	22.9
Th (PPM)	3.8	3.7	2.1	6	0.7	0.7	7.4	2.1	0.9	8.7	0.6	2.4	5.7	7.2	5.1	5.1	0

Sample	DP008	DP-031_I	EP046A	EP-050_I	EP056B	SGP03	SGP09	SGP11	SGP14	SGP74	SGP82	SGP89	SGP91	DP004	DP007	DP013	EP047	EP024C	SGP01	SGP05
SiO2 (%)	46.81	46.31	46.47	30.65	46.99	51.74	52.58	46.46	40.18	27.71	43.8	40.61	31.69	51.86	49.04	49.47	50.33	44.53	50.84	43.7
TiO2 (%)	0.38	0.47	0.57	0.17	0.51	0.62	0.35	0.53	0.38	0.31	0.28	0.24	0.36	0.6	0.67	1.46	1.16	1.64	2.05	0.48
Al2O3 (%)	7.4	8.73	10.02	2.67	8.7	8.09	3.71	8.85	6.33	4.38	4.39	4.05	5.76	8.36	12.66	14.56	15.82	15.38	13.61	9.04
Fe2O3 (%)	18.82	18.24	22.54	14.36	18.3	29.37	28.23	26.97	30.01	22.58	22.67	20.49	26.29	12.62	5.48	11.14	9.19	13.59	13.63	14.58
MnO (%)	0.139	0.358	0.255	0.072	0.251	0.061	0.084	0.151	0.205	0.232	0.129	0.127	0.067	0.137	0.115	0.186	0.129	0.185	0.214	0.289
MgO (%)	5.9	5.32	5.04	10.05	5.79	2.07	3.51	3.68	4.5	6.42	4.53	9.04	5.9	4.28	6.29	6.81	7.3	7.7	5.1	5.85
CaO (%)	14.29	12.36	10.42	26.39	12.6	4.46	7.55	9.67	11.79	25.24	17.42	20.78	21.68	14.64	12.66	11.2	8.51	13.59	8.87	16.32
Na2O (%)	1.14	0.78	3.01	0.18	1.93	0.63	0.34	0.81	0.56	0.29	0.54	0.75	0.29	3.05	1.32	3.15	2.76	1.15	3.31	0.89
K2O (%)	0.35	0.03	0.2	0	0.19	1.19	0.1	0.68	0.13	0.09	0.25	0.07	0.04	0.03	3.3	0.31	1.91	0.32	0.72	0.11
P2O5 (%)	0.333	0.274	0.285	0.34	0.232	1.461	0.506	0.303	0.295	0.74	0.846	0.931	0.867	0.978	0.119	0.126	0.136	0.107	0.212	0.22
H2O (%)	4.45	7.13	1.18	15.11	4.5	0.3	3.04	1.92	5.61	12.01	5.16	2.9	7.05	3.45	8.34	1.59	2.75	1.81	1.44	8.52
	100.012	100.002	99.99	99.992	99.993	99.992	100	100.024	99.99	100.002	100.015	99.988	99.994	100.005	99.994	100.002	99.995	100.002	99.996	99.999
Net Loi	4.438	7.128	1.19	15.118	4.507	0.308	3.04	1.896	5.62	12.008	5.145	2.912	7.056	3.445	8.346	1.588	2.755	1.808	1.444	8.521
Fe tot %	13.2	12.8	15.8	10.0	12.8	20.5	19.7	18.9	21.0	15.8	15.9	14.3	18.4	8.8	3.8	7.8	6.4	9.5	9.5	10.2
Normalized																				
SiO2 (%)	48.98	49.86	47.03	36.11	49.21	51.90	54.23	47.36	42.57	31.49	46.18	41.83	34.10	53.71	53.51	50.27	51.76	45.35	51.58	47.77
TiO2 (%)	0.40	0.51	0.58	0.20	0.53	0.62	0.36	0.54	0.40	0.35	0.30	0.25	0.39	0.62	0.73	1.48	1.19	1.67	2.08	0.52
Al2O3 (%)	7.74	9.40	10.14	3.15	9.11	8.11	3.83	9.02	6.71	4.98	4.63	4.17	6.20	8.66	13.81	14.79	16.27	15.66	13.81	9.88
Fe2O3 (%)	19.69	19.64	22.81	16.92	19.16	29.46	29.12	27.49	31.80	25.66	23.90	21.10	28.29	13.07	5.98	11.32	9.45	13.84	13.83	15.94
MnO (%)	0.15	0.39	0.26	0.08	0.26	0.06	0.09	0.15	0.22	0.26	0.14	0.13	0.07	0.14	0.13	0.19	0.13	0.19	0.22	0.32
MgO (%)	6.17	5.73	5.10	11.84	6.06	2.08	3.62	3.75	4.77	7.30	4.78	9.31	6.35	4.43	6.86	6.92	7.51	7.84	5.17	6.39
CaO (%)	14.95	13.31	10.55	31.09	13.19	4.47	7.79	9.86	12.49	28.68	18.36	21.40	23.33	15.16	13.81	11.38	8.75	13.84	9.00	17.84
Na2O (%)	1.19	0.84	3.05	0.21	2.02	0.63	0.35	0.83	0.59	0.33	0.57	0.77	0.31	3.16	1.44	3.20	2.84	1.17	3.36	0.97
K2O (%)	0.37	0.03	0.20	0.00	0.20	1.19	0.10	0.69	0.14	0.10	0.26	0.07	0.04	0.03	3.60	0.32	1.96	0.33	0.73	0.12
P2O5 (%)	0.35	0.30	0.29	0.40	0.24	1.47	0.52	0.31	0.31	0.84	0.89	0.96	0.93	1.01	0.13	0.13	0.14	0.11	0.22	0.24
Sc (PPM)	13.5	10.3	19.1	13.6	17.5	16.9	17	18.2	13.5	15.4	9.7	10.5	13.1	12.6	8	46.9	27.7	48.4	58.1	9.9
V (PPM)	61.5	97.9	107.5	55.1	125.9	205	113.6	133.5	132.4	82.1	66.3	64.3	85.7	106.1	58	320.9	225.1	289.4	406.2	67.1
Cr (PPM)	104.7	260.6	248.6	74	128.6	375	222.4	219.3	290	136.2	190.8	93.5	164.3	129.5	139.1	235.4	339	384.3	186.8	221
Co (PPM)	0	0	0	0	0	0	0	0	0	0	0.5	0	1.7	2.3	5.4	25.8	30.7	35.6	30	0
Ni (PPM)	12	20.1	19.8	1.3	41.7	48.5	18.4	18.9	14.6	6.8	6.3	4.6	8.1	30	22.4	51	105.5	82.3	9.3	14.7
Cu (PPM)	15.4	16.2	9.5	12.7	9.2	10.5	12.1	9.7	10.8	18.3	13.4	17.1	17.3	6.9	7.1	107.3	8.6	14.4	19.9	8.4
Zn (PPM)	55.1	53.7	80.1	34.6	76.6	71.1	28.6	57.7	50.9	43.1	55.5	35.6	35.4	34.7	76.4	90.7	59.2	72.1	98.1	51.3
Ga (PPM)	7.8	7.8	13.9	0	15.7	9.7	0	9	8.1	6.3	4.8	3	4.9	11.7	14.4	16.4	16	14.1	20	7
Rb (PPM)	11.9	2.3	7.8	0.9	5.5	71.2	1.7	26.2	4.7	4.1	14.3	2.9	9.2	2	147.2	3.9	83	16.4	20.1	7.1
Sr (PPM)	193	130.8	80.4	454.6	147.2	86.8	171.4	79.7	93.8	344.9	255	133.5	353.6	413.4	208.3	233.5	116.2	213.4	185.5	186
Y (PPM)	29.9	30.5	30.9	12	27.4	30.6	30.5	41.8	27.8	26.3	34.7	23.7	26.2	26.6	27.9	27.9	30.8	36.7	40.5	33.7
Zr (PPM)	180.6	135.3	158.8	34.8	172.4	122.2	62.2	149.3	145.3	61	46.6	40.7	64.8	127.1	190.5	77.1	109.4	114.7	145.2	156.9
Nb (PPM)	7	3.1	4.7	4.2	12.3	9	4.9	13	9.3	6	5.7	5.5	5.6	11.3	14.7	5.1	7	5.6	9.9	10.1
Ba (PPM)	11	0	73.7	0	6.1	243.8	2.5	67	0	1.6	48.7	0	2.2	0	555.7	93.4	481.2	69.1	152.4	0
La (PPM)	39.4	34.1	26.3	6.9	52.1	32.4	28.4	30	11.7	17.3	18.7	13.9	24.1	27.8	40.3	4.5	9.5	24.6	12.9	30.3
Ce (PPM)	73.9	69.3	54.6	9.5	97.6	61.5	69.1	59.9	29.9	36.8	33.6	27.3	61.1	54.4	77	13.9	22.1	58.1	37	63.5
Pb (PPM)	12	8.4	7.8	4.8	11.6	5.4	12	2.6	11.5	15.6	13.1	8.1	17.8	5.4	8.8	5.1	2.8	13	7.6	10.8
Th (PPM)	21.1	13.9	13.8	0.5	25.1	7.2	7.5	15.8	12	1.4	0	3.9	1.4	9.6	23.2	2.8	9.4	5.4	11.8	21.5

Sample	DP002	DP012	DP016	DPO-23_I	DP-024_I	DP028	SGP93
SiO2 (%)	62.48	65.08	47.61	62.14	33.68	27.74	60.33
TiO2 (%)	0.66	0.86	0.56	0.93	0.4	0.33	1.16
Al2O3 (%)	12.23	14.89	10.66	14.8	7.18	5.17	15.08
Fe2O3 (%)	6.14	6.5	5.77	7.31	13.64	8.41	8.49
MnO (%)	0.055	0.077	0.162	0.09	0.039	0.078	0.103
MgO (%)	1.98	2.74	5.24	3.13	4.05	9.96	3.51
CaO (%)	2.45	3.11	14.26	4.09	18.27	31.61	5.45
Na2O (%)	3.07	2.88	1.41	2.35	1.61	0.17	2.32
K2O (%)	2.95	2.81	2.42	2.64	0.01	0.01	2.27
P2O5 (%)	0.125	0.105	0.128	0.158	0.525	0.331	0.15
H2O (%)	7.86	0.96	11.79	2.36	20.6	16.2	1.14
	100	100.012	100.01	99.998	100.004	100.009	100.003
Net Loi	7.86	0.948	11.78	2.362	20.596	16.191	1.137
Fe tot %	4.3	4.5	4.0	5.1	9.5	5.9	5.9
Normalized							
SiO2 (%)	67.81	65.70	53.97	63.64	42.42	33.10	61.02
TiO2 (%)	0.72	0.87	0.63	0.95	0.50	0.39	1.17
Al2O3 (%)	13.27	15.03	12.08	15.16	9.04	6.17	15.25
Fe2O3 (%)	6.66	6.56	6.54	7.49	17.18	10.03	8.59
MnO (%)	0.06	0.08	0.18	0.09	0.05	0.09	0.10
MgO (%)	2.15	2.77	5.94	3.21	5.10	11.88	3.55
CaO (%)	2.66	3.14	16.16	4.19	23.01	37.72	5.51
Na2O (%)	3.33	2.91	1.60	2.41	2.03	0.20	2.35
K2O (%)	3.20	2.84	2.74	2.70	0.01	0.01	2.30
P2O5 (%)	0.14	0.11	0.15	0.16	0.66	0.39	0.15
Sc (PPM)	10.5	11.3	6.3	13.4	10.6	14.3	15.7
V (PPM)	72.6	93.5	56.4	149.2	96.1	46.4	170.7
Cr (PPM)	315.9	180.4	86.6	163.3	108	82.6	278.5
Co (PPM)	4.7	11.9	4.9	7.4	0	0	14.7
Ni (PPM)	17.4	26.7	18.4	31.8	5.8	4.2	37.5
Cu (PPM)	13	13.4	6.7	15.6	25.4	12	46.3
Zn (PPM)	31.8	80.2	54.7	60.3	43.9	32.5	88
Ga (PPM)	12.1	18.2	13.2	17.3	5.9	4.5	19
Rb (PPM)	133	115.5	115.9	122.7	1.3	1.3	89.7
Sr (PPM)	150.7	114.4	234	112.5	346.7	730	141.3
Y (PPM)	29.2	33.6	26.4	28.2	24.2	14.6	31.3
Zr (PPM)	285.4	286.9	155.9	158.7	79	65.9	175.5
Nb (PPM)	16.1	14.5	12.5	14.3	7.3	5.2	18.5
Ba (PPM)	861.7	514.1	312	559.5	0	0	347.6
La (PPM)	13	32.3	31.5	6	20.2	17.4	44.8
Ce (PPM)	23.5	97.1	68.9	42.1	42.3	28.1	99.5
Pb (PPM)	1.5	8.7	5.7	1.3	11.2	7.5	12.1
Th (PPM)	21.5	23.2	17.4	13.2	4.9	3.6	14.1

Color code for sample names

Strongly Magnetic samples

Weakly Magnetic Samples

Basic Samples

Color codes for normalized SiO2 content

Ultra Basic composition

<45% SiO2

Basic Composition

45-52% SIO2

Intermediate Composition

52-63% SiO2

Acidic Composition

>63% SiO2

H2O% is a placeholder for the difference between the total of measured oxides and 100%

Where this total or CaO % (Normalized) exceeds 10% or 15 % respectively this is noted with yellow color

	Range of calibration (Major Mafic)		
	Min	Max	Std. Deviation
Na2O (%)	1.63	4.26	0.0382
MgO (%)	1.53	13.15	0.0333
Al2O3 (%)	10.07	29.8	0.118
SiO2 (%)	38.2	58.84	0.291
Fe2O3 (%)	3.36	13.15	0.0991
P2O5 (%)	0.01	1.05	0.0176
K2O (%)	0.03	2.92	0.00952
CaO (%)	4.94	15.9	0.0727
TiO2 (%)	0.2	2.61	0.0146
MnO (%)	0.04	0.22	0.0037

A2 Correlation coefficients

Only Strongly magnetic samples

All Magnetic Samples

	SiO2 (%)	TiO2 (%)	Al2O3 (%)	Fe2O3 (%)	MnO (%)	MgO (%)	CaO (%)	Na2O (%)	K2O (%)	P2O5 (%)	H2O (%)	Sc (PPM)	V (PPM)	Cr (PPM)	Ni (PPM)	Cu (PPM)	Zn (PPM)	Ga (PPM)	Rb (PPM)	Sr (PPM)	Y (PPM)	Zr (PPM)	Nb (PPM)	Ba (PPM)	La (PPM)	Ce (PPM)	Pb (PPM)	Th (PPM)
SiO2 (%)	X	-0.027	-0.027	-0.693	-0.012	-0.236	-0.322	-0.285	0.265	-0.074	-0.106	-0.110	-0.505	0.143	0.021	-0.222	-0.353	-0.015	0.096	-0.257	-0.361	0.021	0.052	-0.071	0.009	0.085	-0.167	-0.299
TiO2 (%)	0.493	X	0.926	-0.365	0.320	0.525	0.252	0.275	0.331	-0.270	0.112	0.699	-0.011	-0.143	0.790	0.069	0.230	-0.057	-0.025	0.206	0.401	0.639	0.717	0.339	0.180	0.204	0.075	0.258
Al2O3 (%)	0.493	0.933	X	-0.317	0.296	0.569	0.329	0.278	0.251	-0.298	0.163	0.728	0.134	-0.212	0.810	0.192	0.356	0.089	-0.017	0.228	0.459	0.657	0.637	0.185	0.089	0.111	0.198	0.328
Fe2O3 (%)	-0.683	-0.575	-0.685	X	-0.482	-0.459	-0.423	0.113	-0.344	0.432	-0.527	-0.171	0.609	0.372	-0.346	0.344	0.386	0.235	0.153	-0.189	0.159	-0.158	-0.418	0.191	0.055	0.000	0.186	0.007
MnO (%)	0.350	0.555	0.688	-0.634	X	0.695	0.600	0.356	0.331	-0.460	0.487	0.272	-0.260	-0.511	0.269	-0.303	-0.038	-0.068	-0.252	0.334	0.009	0.158	0.529	-0.140	-0.157	-0.160	-0.228	0.024
MgO (%)	0.110	0.244	0.387	-0.758	0.488	X	0.828	0.191	-0.055	-0.751	0.682	0.398	-0.122	-0.624	0.498	-0.259	0.002	-0.222	-0.286	0.276	0.187	0.095	0.538	-0.262	-0.178	-0.150	-0.167	0.198
CaO (%)	-0.110	0.062	0.196	-0.619	0.384	0.894	X	0.084	0.005	-0.472	0.916	0.165	-0.251	-0.672	0.225	-0.243	-0.213	-0.362	-0.343	0.544	0.123	-0.040	0.299	-0.238	-0.126	-0.139	-0.075	0.290
Na2O (%)	0.308	0.575	0.668	-0.390	0.553	0.215	0.007	X	0.307	-0.153	-0.164	0.278	0.053	-0.077	0.040	0.000	0.176	0.114	-0.088	0.287	-0.032	0.400	0.187	-0.062	-0.329	-0.293	-0.055	0.115
K2O (%)	0.460	0.599	0.496	-0.300	0.036	-0.100	-0.170	0.206	X	0.306	0.007	0.141	-0.230	-0.305	-0.043	-0.130	-0.051	0.098	0.176	0.460	0.004	0.465	0.468	0.235	0.124	0.063	-0.143	0.249
P2O5 (%)	-0.419	-0.495	-0.596	0.715	-0.604	-0.676	-0.487	-0.401	-0.067	X	-0.369	-0.317	0.179	0.284	-0.369	0.223	0.035	0.054	0.062	0.210	0.028	0.072	-0.267	0.263	0.353	0.149	0.167	0.140
H2O (%)	0.006	0.088	0.203	-0.627	0.443	0.803	0.911	-0.085	-0.146	-0.496	X	0.234	0.026	0.088	-0.036	0.180	0.149	0.161	-0.128	-0.096	-0.037	0.143	0.047	0.151	-0.171	-0.140	0.087	-0.261
Sc (PPM)	-0.164	0.309	0.152	0.180	-0.074	-0.108	-0.177	0.128	0.061	-0.060	0.177	X	-0.126	-0.148	0.527	0.552	0.348	-0.042	0.168	0.118	0.753	0.750	0.647	0.615	0.391	0.453	0.609	-0.035
V (PPM)	-0.487	-0.174	-0.222	0.655	-0.355	-0.454	-0.466	-0.144	-0.073	0.420	0.040	0.065	X	0.126	0.102	0.215	0.694	0.683	-0.151	-0.299	0.090	-0.144	-0.260	-0.096	-0.326	-0.419	-0.058	-0.004
Cr (PPM)	-0.226	-0.334	-0.437	0.705	-0.449	-0.735	-0.698	-0.242	-0.218	0.547	0.016	0.083	0.408	X	0.021	0.296	0.206	0.222	0.390	-0.583	-0.101	0.037	-0.390	0.235	0.198	0.321	0.237	-0.031
Ni (PPM)	0.456	0.807	0.686	-0.340	0.308	0.016	-0.179	0.395	0.597	-0.315	0.077	0.298	0.041	-0.119	X	-0.037	0.116	-0.048	-0.154	0.071	0.152	0.269	0.480	-0.048	-0.031	0.018	0.013	0.336
Cu (PPM)	-0.391	-0.249	-0.236	0.412	-0.280	-0.244	-0.162	-0.239	-0.259	0.379	0.166	0.475	0.283	0.374	-0.255	X	0.661	0.271	0.409	-0.233	0.807	0.578	0.003	0.763	0.500	0.513	0.940	-0.411
Zn (PPM)	-0.004	0.425	0.456	0.000	0.214	-0.038	-0.190	0.431	0.262	-0.094	0.090	0.309	0.501	0.082	0.369	0.389	X	0.697	0.256	-0.418	0.562	0.442	0.103	0.399	0.077	0.071	0.416	-0.266
Ga (PPM)	0.379	0.626	0.736	-0.385	0.547	0.097	-0.059	0.686	0.416	-0.344	0.119	-0.024	0.147	-0.166	0.533	-0.130	0.694	X	0.093	-0.525	0.030	0.099	-0.176	0.137	-0.306	-0.291	0.004	-0.215
Rb (PPM)	0.284	0.416	0.289	-0.059	-0.187	-0.253	-0.287	0.015	0.881	0.072	0.011	0.099	0.033	0.060	0.520	-0.023	0.292	0.277	X	-0.305	0.307	0.367	0.085	0.510	0.427	0.608	0.363	-0.214
Sr (PPM)	-0.276	-0.128	-0.093	-0.268	0.029	0.514	0.726	-0.172	-0.164	-0.001	-0.192	-0.064	-0.354	-0.514	-0.267	-0.094	-0.405	-0.377	-0.267	X	0.029	0.136	0.214	-0.134	0.067	-0.084	-0.096	0.416
Y (PPM)	-0.184	0.240	0.167	0.253	-0.047	-0.272	-0.254	0.001	0.126	0.123	-0.049	0.682	0.189	0.110	0.122	0.668	0.491	0.058	0.200	-0.234	X	0.651	0.358	0.741	0.684	0.639	0.819	-0.163
Zr (PPM)	0.546	0.805	0.895	-0.570	0.622	0.216	0.007	0.687	0.495	-0.492	0.077	0.144	-0.249	-0.313	0.589	-0.156	0.463	0.747	0.281	-0.217	0.199	X	0.554	0.626	0.468	0.498	0.583	-0.034
Nb (PPM)	0.387	0.693	0.656	-0.497	0.365	0.279	0.147	0.333	0.591	-0.445	0.077	0.276	-0.259	-0.444	0.594	-0.275	0.275	0.481	0.363	-0.061	0.203	0.669	X	0.339	0.180	0.204	0.075	0.258
Ba (PPM)	0.317	0.360	0.388	-0.138	-0.071	-0.188	-0.246	0.190	0.871	0.045	0.039	0.205	0.015	-0.018	0.571	-0.004	0.372	0.358	0.918	-0.247	0.267	0.343	0.360	X	0.690	0.740	0.783	-0.070
La (PPM)	0.385	0.412	0.501	-0.230	0.265	-0.102	-0.208	0.339	0.332	-0.058	0.012	0.248	-0.215	-0.051	0.514	0.127	0.291	0.384	0.288	-0.180	0.462	0.621	0.412	0.306	X	0.935	0.613	0.015
Ce (PPM)	0.396	0.385	0.480	-0.230	0.241	-0.101	-0.198	0.283	0.263	-0.140	0.005	0.305	-0.298	0.027	0.474	0.178	0.236	0.319	0.286	-0.215	0.475	0.588	0.385	0.280	0.952	X	0.641	-0.030
Pb (PPM)	-0.234	-0.080	-0.081	0.253	-0.189	-0.197	-0.118	-0.112	-0.149	0.244	0.064	0.577	0.034	0.289	-0.081	0.909	0.308	-0.100	0.044	-0.069	0.735	0.023	-0.080	0.117	0.307	0.374	X	-0.330
Th (PPM)	0.443	0.595	0.737	-0.444	0.544	0.175	-0.036	0.637	0.329	-0.416	0.046	-0.010	-0.160	-0.266	0.572	-0.375	0.242	0.618	0.063	-0.207	0.008	0.842	0.595	0.101	0.620	0.542	-0.209	X

Red- Some linear correlation 0.4 to 0.6 & -0.4 to -0.6

Yellow - Good linear correlation 0.6 to 0.8 & -0.6 to -0.8

Green- Very good linear correlation 0.8 to 1 & -0.8 to -1

ALL SAMPLES	SiO2 (%)	TiO2 (%)	Al2O3 (%	Fe2O3 (%	MnO (%)	MgO (%)	CaO (%)	Na2O (%)	K2O (%)	P2O5 (%)	H2O (%)	Sc (PPM)	V (PPM)	Cr (PPM)	Ni (PPM)	Cu (PPM)	Zn (PPM)	Ga (PPM)	Rb (PPM)	Sr (PPM)	Y (PPM)	Zr (PPM)	Nb (PPM)	Ba (PPM)	La (PPM)	Ce (PPM)	Pb (PPM)	Th (PPM)
SiO2 (%)	X																											
TiO2 (%)	0.538	X																										
Al2O3 (%)	0.538	0.852	X																									
Fe2O3 (%)	-0.758	-0.626	-0.828	X																								
MnO (%)	0.214	0.324	0.381	-0.440	X																							
MgO (%)	0.016	0.260	0.322	-0.617	0.449	X																						
CaO (%)	-0.295	-0.110	-0.056	-0.341	0.291	0.837	X																					
Na2O (%)	0.685	0.723	0.808	-0.666	0.273	0.117	-0.185	X																				
K2O (%)	0.696	0.434	0.701	-0.582	-0.050	-0.011	-0.268	0.547	X																			
P2O5 (%)	-0.575	-0.535	-0.699	0.801	-0.512	-0.606	-0.297	-0.531	-0.416	X																		
H2O (%)	-0.008	-0.063	0.127	-0.482	0.215	0.645	0.811	0.000	0.062	-0.389	X																	
Sc (PPM)	-0.017	0.705	0.328	-0.065	0.165	0.128	-0.118	0.304	-0.130	-0.169	0.070	X																
V (PPM)	-0.300	0.264	-0.016	0.413	-0.177	-0.307	-0.410	0.035	-0.160	0.289	0.070	0.469	X															
Cr (PPM)	-0.221	-0.187	-0.348	0.628	-0.383	-0.659	-0.627	-0.292	-0.201	0.543	0.122	0.096	0.407	X														
Ni (PPM)	0.415	0.645	0.683	-0.439	0.215	0.208	-0.183	0.472	0.348	-0.394	0.024	0.430	0.184	0.024	X													
Cu (PPM)	-0.020	0.310	0.171	0.002	-0.044	-0.022	-0.107	0.218	-0.078	0.013	-0.135	0.467	0.324	0.123	0.125	X												
Zn (PPM)	0.226	0.563	0.532	-0.221	0.256	0.029	-0.252	0.446	0.285	-0.266	0.106	0.450	0.521	0.028	0.358	0.406	X											
Ga (PPM)	0.687	0.798	0.890	-0.682	0.364	0.148	-0.203	0.822	0.642	-0.567	0.064	0.309	0.185	-0.235	0.578	0.188	0.700	X										
Rb (PPM)	0.661	0.378	0.653	-0.522	-0.110	-0.061	-0.299	0.486	0.989	-0.366	-0.017	-0.165	-0.158	-0.129	0.342	-0.102	0.269	0.596	X									
Sr (PPM)	-0.233	-0.029	-0.033	-0.282	0.005	0.594	0.797	-0.055	-0.161	-0.064	-0.222	-0.045	-0.320	-0.518	-0.165	-0.029	-0.336	-0.186	-0.195	X								
Y (PPM)	-0.115	0.166	0.072	0.264	0.015	-0.343	-0.374	0.010	-0.002	0.141	0.064	0.433	0.280	0.214	0.088	0.224	0.425	0.077	0.019	-0.385	X							
Zr (PPM)	0.770	0.501	0.780	-0.686	0.334	0.073	-0.192	0.701	0.730	-0.581	0.078	-0.020	-0.241	-0.301	0.329	-0.098	0.404	0.739	0.692	-0.159	0.118	X						
Nb (PPM)	0.714	0.478	0.722	-0.674	0.176	0.094	-0.110	0.607	0.777	-0.545	0.096	-0.061	-0.257	-0.401	0.293	-0.077	0.327	0.678	0.741	-0.058	0.076	0.823	X					
Ba (PPM)	0.689	0.710	0.690	-0.547	-0.102	-0.051	-0.321	0.603	0.951	-0.390	-0.013	-0.054	-0.107	-0.111	0.392	-0.036	0.249	0.617	0.948	-0.185	0.036	0.720	0.710	X				
La (PPM)	0.201	0.346	0.143	-0.108	0.195	-0.102	-0.109	0.001	0.157	-0.019	0.106	-0.169	-0.290	-0.045	0.066	-0.127	0.212	0.153	0.161	-0.116	0.345	0.391	0.346	0.022	X			
Ce (PPM)	0.355	0.452	0.297	-0.215	0.179	-0.131	-0.193	0.124	0.286	-0.159	0.095	-0.088	-0.307	-0.031	0.137	-0.072	0.279	0.288	0.298	-0.200	0.391	0.500	0.452	0.157	0.924	X		
Pb (PPM)	-0.282	-0.158	-0.184	0.306	-0.172	-0.198	-0.084	-0.199	-0.164	0.295	0.054	0.218	0.037	0.302	-0.122	0.329	0.202	-0.185	-0.118	-0.083	0.673	-0.096	-0.158	-0.122	0.272	0.292	X	
Th (PPM)	0.645	0.742	0.633	-0.559	0.343	0.064	-0.180	0.561	0.656	-0.499	0.053	-0.162	-0.246	-0.306	0.272	-0.245	0.278	0.616	0.607	-0.193	0.014	0.877	0.742	0.583	0.509	0.543	-0.230	X

APPENDIX B Electron Micro Probe Analyzes

Magnetite and Ti-Magnetite

No	64	65	66	67	69	70	71	72	75
Sample name	SGP-11	SGP-11	SGP-11	DP-031	DP-031	DP-030	DP-030	DP-008	DP-008
Ana No	an4	an7	an8	an13	an15	an1	an2	an4	an7
mineral	Mag	Ti-Mag	Mag	Mag	Ti-Mag	Mag	Mag	Mag	Mag
SiO2	0.0479	0.0161	0.0044	0.0061	0.0183	0.0078	0.0111	0.0189	0.0236
Al2O3	0.2828	0.0906	0.0883	0.2651	0.1439	0.1518	0.1459	0.1164	0.1666
MgO	0.0235	0	0.0148	0	0.002	0	0	0.014	0
CaO	0.0276	0.045	0.0239	0.025	0	0.0096	0	0.0256	0.0404
TiO2	0.0726	9.8651	0.0034	0.5806	8.7227	1.3792	0.0014	0.1433	0.3988
FeO	91.4664	80.4423	91.8806	91.8707	81.2795	88.1592	92.3297	91.7138	91.08
MnO	0.0537	0	0.0509	0.0009	0.0297	0	0.0407	0	0
Cr2O3	0.026	0.047	0	0.053	0.0345	0.0044	0.0121	0.0135	0.0738
NiO	0	0	0	0	0	0	0	0	0
ZnO	0.0219	0.0352	0.0296	0	0	0.0042	0	0.0415	0.0086
V2O3	0.0148	0.0816	0.0451	0.0904	0.1964	0.0595	0.0139	0.001	0
Total	92.0372	90.6229	92.141	92.8918	90.427	89.7757	92.5548	92.088	91.7918
Normalized to 3 cations									
Al (apfu)	0.01	0.00	0.00	0.01	0.01	0.01	0.01	0.01	0.01
Ti	0.00	0.30	0.00	0.02	0.26	0.04	0.00	0.00	0.01
Fe2+	1.00	1.29	1.00	1.02	1.26	1.04	1.00	1.00	1.01
Fe3+	1.98	1.40	1.99	1.95	1.46	1.91	1.99	1.98	1.96
V	0.00	0.00	0.00	0.00	0.01	0.00	0.00	0.00	0.00
Σ	3	3	3	3	3	3	3	3	3

No	77	78	79	80	82	83	84	85	86
Sample name	EPG	EPG	EPG	SGP10	SGP10	SGP10	SGP10	SGP10	SGP09
Ana No	ana 3	ana 4	ana 5	an 1	an 3	an 4	an 5	an 6	an 3
mineral	Mag	Mag	Mag	Mag	Mag	Ti-Mag	Mag	Mag	Mag
SiO2	0	0.0317	0.0427	0.0012	0.013	0	0.0033	0.0253	0.0275
Al2O3	0.8125	0.7877	0.6612	0.1172	0.1308	0.1317	0.2332	0.0855	0.1536
MgO	0.018	0.0719	0.0774	0.0457	0.0527	0.0178	0.0615	0	0
CaO	0.0334	0.0124	0	0	0.0008	0.0051	0.0092	0.0001	0.003
TiO2	0.5229	0.4937	0.452	0.0226	0.0284	6.2836	0.0281	0.0225	2.4467
FeO	91.1347	91.0517	90.7312	91.7633	91.9617	83.2875	91.552	92.0107	87.417
MnO	0.0378	0.0535	0.0324	0.1233	0.1328	0.0659	0.1042	0.0286	0
Cr2O3	0.0042	0.0328	0.0059	0.0322	0.0221	0	0.0196	0.0136	0.0419
NiO	0	0	0	0.0372	0	0	0	0	0.0135
ZnO	0	0	0	0	0	0.0359	0.0752	0.0319	0
V2O3	0.0156	0.0048	0.0223	0.0335	0	0.0363	0.0042	0.0082	0.0512
Total	92.5791	92.5402	92.0251	92.1762	92.3423	89.8638	92.0905	92.2264	90.1544
Al (apfu)	0.04	0.04	0.03	0.01	0.01	0.01	0.01	0.00	0.01
Ti	0.02	0.01	0.01	0.00	0.00	0.19	0.00	0.00	0.07
Fe2+	1.01	1.01	1.01	0.99	0.99	1.19	0.99	1.00	1.07
Fe3+	1.93	1.93	1.94	1.99	1.99	1.61	1.99	1.99	1.84
V	0.00	0.00	0.00	0.00	0.00	0.00	0.00	0.00	0.00
Σ	3	3	3	3	3	3	3	3	3

Hematite and ilmenite

No	87	68	73	74	76	81
Sample name	SGP07	DP-031	DP-008	DP-008	DP-008	SGP10
Ana No	an 4	an14	an5	an6	an6	an 2
mineral	hem	ilm	ilm	ilm	ilm	ilm
SiO2	3.503	0.0012	0.0108	0.0001	0.0267	0.027
Al2O3	0.8123	0.0028	0.0459	0.0426	0.0409	0.1021
MgO	1.568	0.2583	0.0501	0.0956	0	0
CaO	0.3543	0	0.2364	0.5305	0.2507	0
TiO2	2.4187	47.9855	48.6837	49.0401	48.9961	5.0558
FeO	80.8767	48.7366	47.2496	46.5109	46.8113	84.9808
MnO	0.009	0.625	1.6351	1.5392	1.7416	0.0848
Cr2O3	0.0238	0	0	0	0.015	0
NiO	0	0.002	0	0	0.057	0
ZnO	0	0.0349	0.0083	0.0074	0.0223	0.0129
V2O3	0.043	0.2156	0.117	0.1713	0.1139	0.0415
Total	89.6088	97.8619	98.0369	97.9377	98.0755	90.3049
	Normalized to 2 cations					
Si (apfu)	0.09	0.00	0.00	0.00	0.00	0.00
Al	0.02	0.00	0.00	0.00	0.00	0.00
Mg	0.06	0.01	0.00	0.00	0.00	0.00
Ca	0.01	0.00	0.01	0.01	0.01	0.00
Ti	0.05	0.93	0.94	0.95	0.95	0.10
Fe2+	0.07	0.90	0.89	0.89	0.90	0.10
Fe3+	1.70	0.14	0.12	0.10	0.10	1.79
Mn	0.00	0.01	0.04	0.03	0.04	0.00
	2	2	2	2	2	2

Clibnopyroxene

No	9	49	50	34	35	36
Sample name	EP-053A	SGP89	SGP89	EP-024B	EP-024B	EP-024B
Ana No	an1	ana 1	ana 2	an4	an5	an6
mineral	cpx	cpx	cpx	cpx	Cpx	Cpx
Na2O	0.6016	0.8893	0.4888	3.0717	3.3952	3.2865
SiO2	52.1725	51.9714	51.4982	51.0636	51.623	51.4963
Al2O3	0.7174	0.6881	1.6149	4.9966	3.918	4.0941
MgO	11.419	10.6222	14.0448	9.1716	9.101	9.1217
Cl	0.0055	0.0052	0.0158	0	0.001	0
K2O	0.0061	0.0047	0.0053	0.137	0.01	0.0095
CaO	22.3758	21.6545	16.0553	18.0066	17.5534	18.2001
TiO2	0.03	0	0.0313	0.0069	0	0.0006
FeO	13.1539	13.6761	12.3308	12.2808	13.2265	12.7284
MnO	0.0227	0.0385	0.1232	0.1122	0.0941	0.0954
Cr2O3	0	0.0357	0.0312	0	0	0
NiO	0	0	0.0096	0.0108	0	0
Total	100.5045	99.5857	96.2492	98.8578	98.9222	99.0326
-O=Cl	0.0012	0.0012	0.0036	0	0.0002	0
Total(F,Cl)	100.5033	99.5845	96.2456	98.8578	98.922	99.0326
	Normalized to 4 cations					
Na (apfu)	0.04	0.07	0.04	0.22	0.25	0.24
Si	1.96	1.98	2.00	1.92	1.94	1.93
Al	0.03	0.03	0.07	0.22	0.17	0.18
Mg	0.64	0.60	0.81	0.51	0.51	0.51
Ca	0.90	0.88	0.67	0.73	0.71	0.73
Fe2+	0.33	0.36	0.40	0.22	0.22	0.21
Fe3+	0.08	0.08	0.00	0.17	0.19	0.19
Σ	4.00	4.00	3.99	4.00	4.00	4.00

No	47	48	15	13	14	11
Sample name	EPG	EPG	DP-031	DP-031	DP-031	EP-053A
Ana No	ana 1	ana 2	an3	an1	an2	an3
mineral	Cpx	Cpx	cpx?	CPx	Cpx	Cpx
Na2O	3.8144	3.5654	4.4819	3.6579	3.2614	0.7477
SiO2	51.8476	51.2885	53.1072	53.2413	53.1593	51.2089
Al2O3	3.2712	3.3276	7.063	5.1013	4.5458	0.8533
MgO	7.463	7.8465	9.023	10.2775	10.9669	9.622
Cl	0.0054	0.0002	0.001	0.0055	0	0.0074
K2O	0	0	0.0008	0.0005	0.0054	0.0284
CaO	16.3265	16.9398	16.3511	17.7679	18.9684	20.7188
TiO2	0.0332	0.0517	0.1415	0.1639	0.1379	0.0407
FeO	16.3196	15.8968	10.2795	9.3895	8.9895	15.7725
MnO	0.0728	0.0393	0.1104	0.0986	0.072	0.0269
Cr2O3	0.0118	0.0023	0	0.0356	0.0296	0.0196
NiO	0	0.0147	0.025	0.0162	0.0011	0
Total	99.1655	98.9728	100.5844	99.7557	100.1373	99.0462
-O=Cl	0.0012	0	0.0002	0.0012	0	0.0017
Total(F,Cl)	99.1643	98.9728	100.5842	99.7545	100.1373	99.0445
Na (apfu)	0.28	0.26	0.32	0.26	0.23	0.06
Si	1.97	1.95	1.93	1.96	1.95	1.98
Al	0.15	0.15	0.30	0.22	0.20	0.04
Mg	0.42	0.44	0.49	0.56	0.60	0.55
Ca	0.66	0.69	0.64	0.70	0.74	0.86
Fe2+	0.32	0.29	0.17	0.17	0.14	0.45
Fe3+	0.20	0.22	0.14	0.12	0.13	0.06
Σ	4.00	4.00	4.00	4.00	4.00	4.00

Garnet

No	60	59	58	54	53	46	45	44
Sample name	SGP03	SGP03	SGP03	SGP89	SGP89	DP-008	DP-008	DP-008
Ana No	an 3	an 2	an 1	ana 6	ana 5	an3	an2	an1
mineral	grt	grt	grt	grt	grt	grt	grt	grt
Na2O	0.0163	0.0072	0.0047	0.0069	0	0	0.0331	0
SiO2	36.9316	37.0435	37.3917	37.4938	37.2389	37.2123	37.4608	37.5544
Al2O3	20.5067	20.4908	20.5814	19.4443	19.939	19.96	19.9601	20.6308
MgO	3.2351	3.1338	2.5554	3.1922	3.9723	2.7528	2.8199	3.0009
Cl	0.0008	0.0036	0.0078	0.0026	0.0065	0.0101	0.0034	0
K2O	0.0062	0	0.0015	0	0	0.014	0	0
CaO	5.7766	6.8638	9.2695	9.1919	7.7501	6.8689	8.2299	7.9356
TiO2	0.0257	0.0569	0.0125	0.041	0.0429	0.0265	0.0575	0.0379
FeO	32.609	31.2584	28.8941	29.8468	30.4355	32.9166	31.0558	30.8675
MnO	0.7831	0.7989	0.9322	0.9389	0.876	0.6967	0.5106	0.2956
Cr2O3	0.0232	0.0089	0.0123	0.0283	0	0.0368	0.0191	0.0348
NiO	0	0.0167	0.0157	0	0	0	0.02	0
Total	99.9143	99.6825	99.6788	100.1867	100.2612	100.4947	100.1702	100.3575
-O=Cl	0.0002	0.0008	0.0018	0.0006	0.0015	0.0023	0.0008	0
Total(F,Cl)	99.9141	99.6817	99.677	100.1861	100.2597	100.4924	100.1694	100.3575
	Normalized to 8 cations							
Si apfu	2.95	2.96	2.98	2.97	2.94	2.97	2.98	2.98
Al	1.93	1.93	1.93	1.82	1.86	1.87	1.87	1.93
Mg	0.39	0.37	0.30	0.38	0.47	0.33	0.33	0.35
Ca	0.49	0.59	0.79	0.78	0.66	0.59	0.70	0.67
Ti	0.00	0.00	0.00	0.00	0.00	0.00	0.00	0.00
Fe2+	2.01	1.95	1.82	1.75	1.76	2.00	1.90	1.93
Fe3+	0.17	0.14	0.11	0.23	0.25	0.19	0.16	0.12
Mn	0.05	0.05	0.06	0.06	0.06	0.05	0.03	0.02
Σ	8	8	8	8	8	8	8	8
Pyrope	0.13	0.13	0.10	0.13	0.16	0.11	0.11	0.12
Almandine	0.68	0.66	0.61	0.59	0.60	0.68	0.64	0.65
Spessartine	0.02	0.02	0.02	0.02	0.02	0.02	0.01	0.01
Andradite	0.01	0.01	0.01	0.03	0.03	0.02	0.02	0.01
Grossular	0.15	0.18	0.25	0.23	0.20	0.18	0.22	0.21
Uvarovite	0.0001	0.0001	0.0001	0.0002	0.0000	0.0002	0.0001	0.0002
Ca-Ti Grt	0.0001	0.0003	0.0001	0.0003	0.0003	0.0002	0.0004	0.0002

No	23	18	17	16	10	6	5	4	1
Sample name	DP-031	DP-031	DP-031	DP-031	EP-053A	SGP-11	SGP-11	SGP-11	SGP-11
Ana No	an11	an6	an5	an4	an2	an10	an19	an6	an1
mineral	grt	grt	grt	grt	grt	grt	grt	grt	grt
Na2O	0.012	0.0057	0.0078	0	0.0204	0.0208	0.0123	0	0.0212
SiO2	37.6062	37.8799	38.0464	38.1297	37.1713	37.0916	36.9578	36.933	37.4673
Al2O3	20.3465	20.5023	20.347	20.8242	19.8285	19.8112	20.5047	19.5425	20.0084
MgO	4.8552	4.2257	4.2424	4.4742	2.3469	2.9138	2.9557	2.4202	2.6696
Cl	0	0	0	0.0075	0	0.0043	0	0.0035	0.0019
K2O	0	0.0025	0	0	0.0049	0	0	0.0002	0
CaO	8.4721	8.6888	9.0726	9.0522	8.2806	9.245	8.6581	9.1599	10.6234
TiO2	0.1387	0.0225	0.0525	0.0374	0.0944	0.0202	0.063	0.0098	0.0178
FeO	26.9105	26.8282	27.4146	27.3091	31.8759	30.0039	29.7782	30.2818	28.8545
MnO	1.3734	1.6811	1.0368	1.1026	0.3194	0.8078	1.1119	1.2679	0.7303
Cr2O3	0.0081	0.0104	0.0185	0	0.0161	0.0046	0.0183	0.0213	0
NiO	0.0032	0	0	0	0	0	0	0.0188	0
Total	99.7259	99.8471	100.2386	100.9369	99.9584	99.9232	100.06	99.6589	100.3944
-O=Cl	0	0	0	0.0017	0	0.001	0	0.0008	0.0004
Total(F,Cl)	99.7259	99.8471	100.2386	100.9352	99.9584	99.9222	100.06	99.6581	100.394
Si apfu	2.96	2.98	2.99	2.97	2.97	2.95	2.93	2.96	2.96
Al	1.89	1.90	1.88	1.91	1.87	1.86	1.92	1.85	1.86
Mg	0.57	0.50	0.50	0.52	0.28	0.35	0.35	0.29	0.31
Ca	0.71	0.73	0.76	0.75	0.71	0.79	0.74	0.79	0.90
Ti	0.01	0.00	0.00	0.00	0.01	0.00	0.00	0.00	0.00
Fe2+	1.59	1.64	1.66	1.62	1.96	1.76	1.77	1.80	1.69
Fe3+	0.18	0.13	0.14	0.15	0.17	0.24	0.20	0.23	0.21
Mn	0.09	0.11	0.07	0.07	0.02	0.05	0.07	0.09	0.05
Σ	8	8	8	8	8	8	8	8	8
Pyrope	0.19	0.17	0.17	0.17	0.09	0.12	0.12	0.10	0.11
Almandine	0.54	0.55	0.56	0.55	0.66	0.60	0.60	0.61	0.57
Spessartine	0.03	0.04	0.02	0.02	0.01	0.02	0.03	0.03	0.02
Andradite	0.02	0.02	0.02	0.02	0.02	0.03	0.02	0.03	0.03
Grossular	0.22	0.23	0.24	0.23	0.22	0.24	0.23	0.24	0.27
Uvarovite	0.0001	0.0001	0.0001	0.0000	0.0001	0.0000	0.0001	0.0002	0.0000
Ca-Ti Grt	0.0010	0.0002	0.0004	0.0003	0.0007	0.0002	0.0004	0.0001	0.0002

Amphibole recalculated after Appendix 2 of Leake et al (1997)

No	2	8	19	20	21	27	28	29	30
Sample name	SGP-11	SGP-11	DP-031	DP-031	DP-031	DP-030	DP-030	SGP-08	SGP-08
Ana No	an2	an12	an7	an8	an9	an5	an6	an1	an2
mineral	Am	Am	Am	Am	Am	Am	Am	Am	Am
comment	Hastingsite	Hastingsite	Magnesio-hornblende	Magnesio-hornblende	Pargasite	Magnesio-hornblende	Actinolite	Edenite	Edenite
Na2O	1.7618	1.4668	2.0967	2.054	2.4206	0.9367	0.4897	1.262	1.2666
SiO2	40.4703	41.2122	44.8479	44.4233	41.9626	50.3657	53.8424	43.95	44.214
Al2O3	12.7447	11.8513	11.2209	11.7221	14.7134	5.7083	2.9921	9.7555	10.1071
MgO	7.7634	8.4084	11.1976	10.8754	9.4149	16.4503	18.2523	11.3879	11.3302
Cl	0.0034	0.0631	0	0.0015	0	0.0479	0.0217	0.1884	0.1986
K2O	1.4895	1.4124	0.0669	0.0522	0.0536	0.466	0.158	1.1456	1.2907
CaO	11.2005	11.4291	10.9153	11.1481	11.1191	12.388	12.6639	11.8586	11.7651
TiO2	0.1782	0.2053	0.2172	0.1435	0.1781	0	0.0146	0.2144	0.196
FeO	21.2831	20.3986	16.5078	16.7342	16.7181	11.0173	8.8674	16.6117	16.8112
MnO	0.1098	0.1238	0.1917	0.1546	0.1595	0.0543	0.1038	0.0991	0.0961
Cr2O3	0.0288	0.0333	0.0301	0.0096	0.0012	0.0174	0	0	0.0323
NiO	0.0199	0	0.0022	0	0	0.0342	0.0077	0	0
Total	97.0534	96.6043	97.2943	97.3185	96.7411	97.4861	97.4136	96.4732	97.3079
-O=Cl	0.0008	0.0142	0	0.0003	0	0.0108	0.0049	0.0425	0.0448
Total(F,Cl)	97.0526	96.5901	97.2943	97.3182	96.7411	97.4753	97.4087	96.4307	97.2631
APFU									
Si	6.21	6.33	6.62	6.57	6.28	7.23	7.62	6.62	6.61
Al	1.79	1.67	1.38	1.43	1.72	0.77	0.38	1.38	1.39
Sum T	8	8	8	8	8	8	8	8	8
Al	0.52	0.47	0.57	0.61	0.87	0.19	0.12	0.35	0.39
Ti	0.02	0.02	0.02	0.02	0.02	0.00	0.00	0.02	0.02
Fe3+	0.57	0.57	0.43	0.44	0.33	0.34	0.18	0.48	0.46
Cr	0.00	0.00	0.00	0.00	0.00	0.00	0.00	0.00	0.00
Mg	1.78	1.92	2.46	2.40	2.10	3.52	3.85	2.56	2.52
Ni	0.00	0.00	0.00	0.00	0.00	0.00	0.00	0.00	0.00
Fe2+	2.10	2.00	1.49	1.53	1.67	0.94	0.84	1.58	1.59
Mn	0.01	0.01	0.01	0.01	0.01	0.00	0.01	0.01	0.01
Sum C	5	5	5	5	5	5	5	5	5
Fe2+	0.07	0.05	0.12	0.10	0.09	0.04	0.03	0.03	0.05
Mn	0.01	0.01	0.01	0.01	0.01	0.00	0.01	0.01	0.01
Ca	1.84	1.88	1.73	1.77	1.78	1.90	1.92	1.91	1.88
Na	0.08	0.06	0.15	0.12	0.12	0.05	0.04	0.05	0.06
Sum B	2	2	2	2	2	2	2	2	2
Na	0.44	0.37	0.46	0.46	0.59	0.21	0.09	0.32	0.31
K	0.29	0.28	0.01	0.01	0.01	0.09	0.03	0.22	0.25
Sum A	0.73	0.65	0.47	0.47	0.60	0.29	0.12	0.54	0.55

No	31	37	38	40	41	42	43	56	57
Sample name	EP-024B	EP-024B	EP-024B	DP-005	DP-005	DP-005	DP-005	SGP09	SGP09
Ana No	an1	an7	an8	an1	an2	an3	an4	an 1	an 2
mineral	Am	Am	Am	Am	Am	Am	Am	Am	Am
comment	Magnesio-hornblende	Edenite	Magnesio-hornblende	Ferro-edenite	Hastingsite	Ferro-edenite	Ferro-hornblende	Magnesio-hornblende	Magnesio-hornblende
Na2O	1.7588	1.9368	1.0811	1.943	2.4236	2.2598	1.8373	1.5407	1.1396
SiO2	45.6957	44.6669	51.3477	44.7942	40.6215	44.0673	46.9261	46.2789	50.8327
Al2O3	9.9492	10.8967	5.5099	6.7957	10.4667	7.4912	5.0842	8.3159	5.1537
MgO	13.1809	12.3631	16.2431	5.6862	4.0343	5.2903	6.3269	13.383	15.7442
Cl	0.0028	0	0.0039	0.01	0.0401	0.0045	0.0247	0.0763	0.0229
K2O	0.116	0.1681	0.0387	0.4211	0.8654	0.4112	0.2479	0.8546	0.4289
CaO	11.6598	11.7022	12.143	10.0318	10.048	9.5379	9.7015	11.3688	11.7936
TiO2	0.2098	0.2575	0.0813	0.2788	0.484	0.2504	0.1445	0.0507	0.0148
FeO	13.3961	15.1179	11.2079	26.8776	28.215	27.6573	26.6667	14.5399	11.6403
MnO	0.097	0.1107	0.1139	0.1986	0.1857	0.2026	0.2637	0.1867	0.2057
Cr2O3	0	0	0.0257	0	0.0226	0	0	0.0094	0.0238
NiO	0.0152	0	0.0153	0.02	0	0.0032	0.0284	0.0411	0.0095
Total	96.0813	97.2199	97.8115	97.057	97.4069	97.1757	97.2519	96.646	97.0097
-O=Cl	0.0006	0	0.0009	0.0023	0.009	0.001	0.0056	0.0172	0.0052
Total(F,Cl)	96.0807	97.2199	97.8106	97.0547	97.3979	97.1747	97.2463	96.6288	97.0045
APFU									
Si	6.75	6.57	7.32	7.00	6.42	6.90	7.28	6.85	7.36
Al	1.25	1.43	0.68	1.00	1.58	1.10	0.72	1.15	0.64
Sum T	8	8	8	8	8	8	8	8	8
Al	0.48	0.46	0.25	0.25	0.37	0.28	0.21	0.30	0.24
Ti	0.02	0.03	0.01	0.03	0.06	0.03	0.02	0.01	0.00
Fe3+	0.37	0.49	0.25	0.35	0.48	0.42	0.29	0.44	0.17
Cr	0.00	0.00	0.00	0.00	0.00	0.00	0.00	0.00	0.00
Mg	2.90	2.71	3.45	1.32	0.95	1.23	1.46	2.95	3.40
Ni	0.00	0.00	0.00	0.00	0.00	0.00	0.00	0.00	0.00
Fe2+	1.22	1.30	1.02	3.03	3.12	3.02	3.00	1.28	1.17
Mn	0.01	0.01	0.01	0.01	0.01	0.01	0.02	0.01	0.01
Sum C	5	5	5	5	5	5	5	5	5
Fe2+	0.07	0.07	0.06	0.14	0.13	0.18	0.17	0.08	0.07
Mn	0.01	0.01	0.01	0.01	0.01	0.01	0.02	0.01	0.01
Ca	1.84	1.84	1.86	1.68	1.70	1.60	1.61	1.80	1.83
Na	0.08	0.08	0.08	0.17	0.16	0.21	0.21	0.10	0.09
Sum B	2	2	2	2	2	2	2	2	2
Na	0.42	0.47	0.22	0.42	0.59	0.47	0.35	0.34	0.23
K	0.02	0.03	0.01	0.08	0.17	0.08	0.05	0.16	0.08
Sum A	0.44	0.50	0.23	0.50	0.76	0.56	0.40	0.50	0.31

No	55	51	52	12
Sample name	SGP89	SGP89	SGP89	EP-053A
Ana No	ana 7	ana 3	ana 4	an4
mineral	Am	Am	Am	Am
comment	Magnesio-hornblende	Magnesio-hornblende	Magnesio-hornblende	Magnesio-hornblende
Na2O	1.3087	1.2186	1.549	1.8308
SiO2	48.9121	47.4128	45.732	47.0144
Al2O3	7.3591	8.2586	9.2928	6.9597
MgO	13.7974	12.6863	11.5864	10.5667
Cl	0.0803	0.1054	0.1543	0
K2O	0.204	0.35	0.4637	0.021
CaO	11.7406	11.7937	11.568	10.5313
TiO2	0.2787	0.362	0.4356	0.4276
FeO	14.5449	15.1557	16.648	19.832
MnO	0.0878	0.0884	0.0819	0.0406
Cr2O3	0.0096	0.0095	0.019	0.0396
NiO	0.0032	0.0621	0.0075	0
Total	98.3264	97.5031	97.5382	97.2637
-O=Cl	0.0181	0.0238	0.0348	0
Total(F,Cl)	98.3083	97.4793	97.5034	97.2637
APFU				
Si	7.06	6.95	6.77	7.03
Al	0.94	1.05	1.23	0.97
Sum T	8	8	8	8
Al	0.32	0.38	0.39	0.25
Ti	0.03	0.04	0.05	0.05
Fe3+	0.35	0.33	0.38	0.41
Cr	0.00	0.00	0.00	0.00
Mg	2.97	2.77	2.56	2.35
Ni	0.00	0.01	0.00	0.00
Fe2+	1.33	1.46	1.61	1.92
Mn	0.01	0.01	0.01	0.00
Sum C	5	5	5	5
Fe2+	0.08	0.06	0.07	0.14
Mn	0.01	0.01	0.01	0.00
Ca	1.82	1.85	1.84	1.69
Na	0.10	0.08	0.09	0.17
Sum B	2	2	2	2
Na	0.27	0.27	0.36	0.36
K	0.04	0.07	0.09	0.00
Sum A	0.31	0.33	0.44	0.37

Biotite

No	32.00
Sample name	EP-024B
Ana No	an2
mineral	Bt
comment	
Na2O	1.3016
SiO2	49.3469
Al2O3	18.0182
MgO	9.2012
Cl	0.0092
K2O	6.5528
CaO	0.214
TiO2	0.0211
FeO	9.3075
MnO	0.3078
NiO	0.0087
Total	94.289
-O=Cl	0.0021
Total(F,Cl)	94.2869
Normalized to 8 cations	
Na	0.20
Si	3.81
Al	1.64
Mg	1.06
K	0.65
Ca	0.02
Fe2+	0.60
Fe3+	0.00
Mn	0.02
∑	8

Epidote

No	39	24	25	26	3
Sample name	EP-024B	DP-031	DP-030	DP-030	SGP-11
Ana No	an9	an12	an3	an4	an3
mineral	epi	ep	ep	ep	epi
Na2O	0	0.06	0	0.0167	0
SiO2	37.9477	31.6573	37.3033	37.6032	37.6626
Al2O3	23.2638	17.9608	22.72	24.0673	24.1045
MgO	0.0504	0.4905	0.0781	0.1427	0.0685
Cl	0	0.0256	0	0	0
K2O	0	0.0066	0	0.0031	0
CaO	23.4108	15.554	23.289	23.2388	23.1938
TiO2	0.0561	0.0136	0	0	0.0344
FeO	12.5059	15.6001	13.2163	11.4591	11.3583
MnO	0.0632	0	0.056	0.0703	0.0429
Cr2O3	0	0	0.0271	0.0198	0.0156
NiO	0	0.0508	0.0054	0.0502	0.0348
Total	97.2979	81.4193	96.6952	96.6712	96.5154
-O=Cl	0	0.0058	0	0	0
Total(F,Cl)	97.2979	81.4135	96.6952	96.6712	96.5154
	Normalized to 8 cations				
Si	3.00	3.03	2.98	2.98	2.99
Al	2.17	2.03	2.14	2.25	2.26
Mg	0.01	0.07	0.01	0.02	0.01
Ca	1.99	1.60	1.99	1.98	1.98
Fe2+	0.01	0.34	0.00	0.00	0.01
Fe3+	0.82	0.91	0.88	0.76	0.75
∑	8	8	8	8	8

No	23	18	17	16	10	6	5	4	1
Sample name	DP-031	DP-031	DP-031	DP-031	EP-053A	SGP-11	SGP-11	SGP-11	SGP-11
Ana No	an11	an6	an5	an4	an2	an10	an19	an6	an1
mineral	grt	grt	grt	grt	grt	grt	grt	grt	grt
Na2O	0.012	0.0057	0.0078	0	0.0204	0.0208	0.0123	0	0.0212
SiO2	37.6062	37.8799	38.0464	38.1297	37.1713	37.0916	36.9578	36.933	37.4673
Al2O3	20.3465	20.5023	20.347	20.8242	19.8285	19.8112	20.5047	19.5425	20.0084
MgO	4.8552	4.2257	4.2424	4.4742	2.3469	2.9138	2.9557	2.4202	2.6696
Cl	0	0	0	0.0075	0	0.0043	0	0.0035	0.0019
K2O	0	0.0025	0	0	0.0049	0	0	0.0002	0
CaO	8.4721	8.6888	9.0726	9.0522	8.2806	9.245	8.6581	9.1599	10.6234
TiO2	0.1387	0.0225	0.0525	0.0374	0.0944	0.0202	0.063	0.0098	0.0178
FeO	26.9105	26.8282	27.4146	27.3091	31.8759	30.0039	29.7782	30.2818	28.8545
MnO	1.3734	1.6811	1.0368	1.1026	0.3194	0.8078	1.1119	1.2679	0.7303
Cr2O3	0.0081	0.0104	0.0185	0	0.0161	0.0046	0.0183	0.0213	0
NiO	0.0032	0	0	0	0	0	0	0.0188	0
Total	99.7259	99.8471	100.2386	100.9369	99.9584	99.9232	100.06	99.6589	100.3944
-O=Cl	0	0	0	0.0017	0	0.001	0	0.0008	0.0004
Total(F,Cl)	99.7259	99.8471	100.2386	100.9352	99.9584	99.9222	100.06	99.6581	100.394
Si apfu	2.96	2.98	2.99	2.97	2.97	2.95	2.93	2.96	2.96
Al	1.89	1.90	1.88	1.91	1.87	1.86	1.92	1.85	1.86
Mg	0.57	0.50	0.50	0.52	0.28	0.35	0.35	0.29	0.31
Ca	0.71	0.73	0.76	0.75	0.71	0.79	0.74	0.79	0.90
Ti	0.01	0.00	0.00	0.00	0.01	0.00	0.00	0.00	0.00
Fe2+	1.59	1.64	1.66	1.62	1.96	1.76	1.77	1.80	1.69
Fe3+	0.18	0.13	0.14	0.15	0.17	0.24	0.20	0.23	0.21
Mn	0.09	0.11	0.07	0.07	0.02	0.05	0.07	0.09	0.05
Σ	8	8	8	8	8	8	8	8	8

APPENDIX C Sample locations map

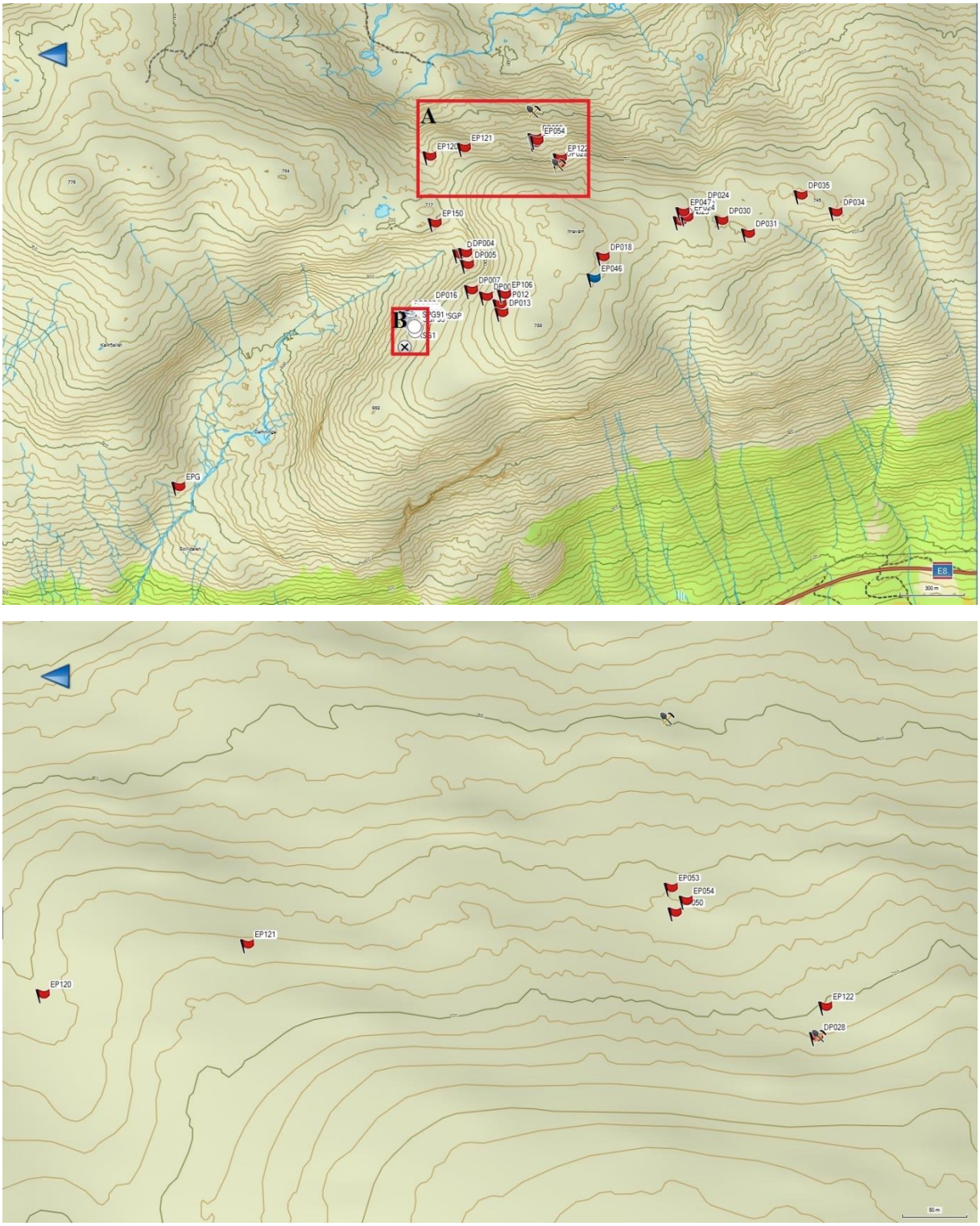

Uppermost: map with all the sample locations plotted in, Sollidalen and Sollidalsaksla. Above: Sample locations on the eastern side of Sollidalsaksla in the Kalvebekli and Solliskar deposit, A in overview map. Pickaxe and shovel symbols represent the entrances of the drifts.

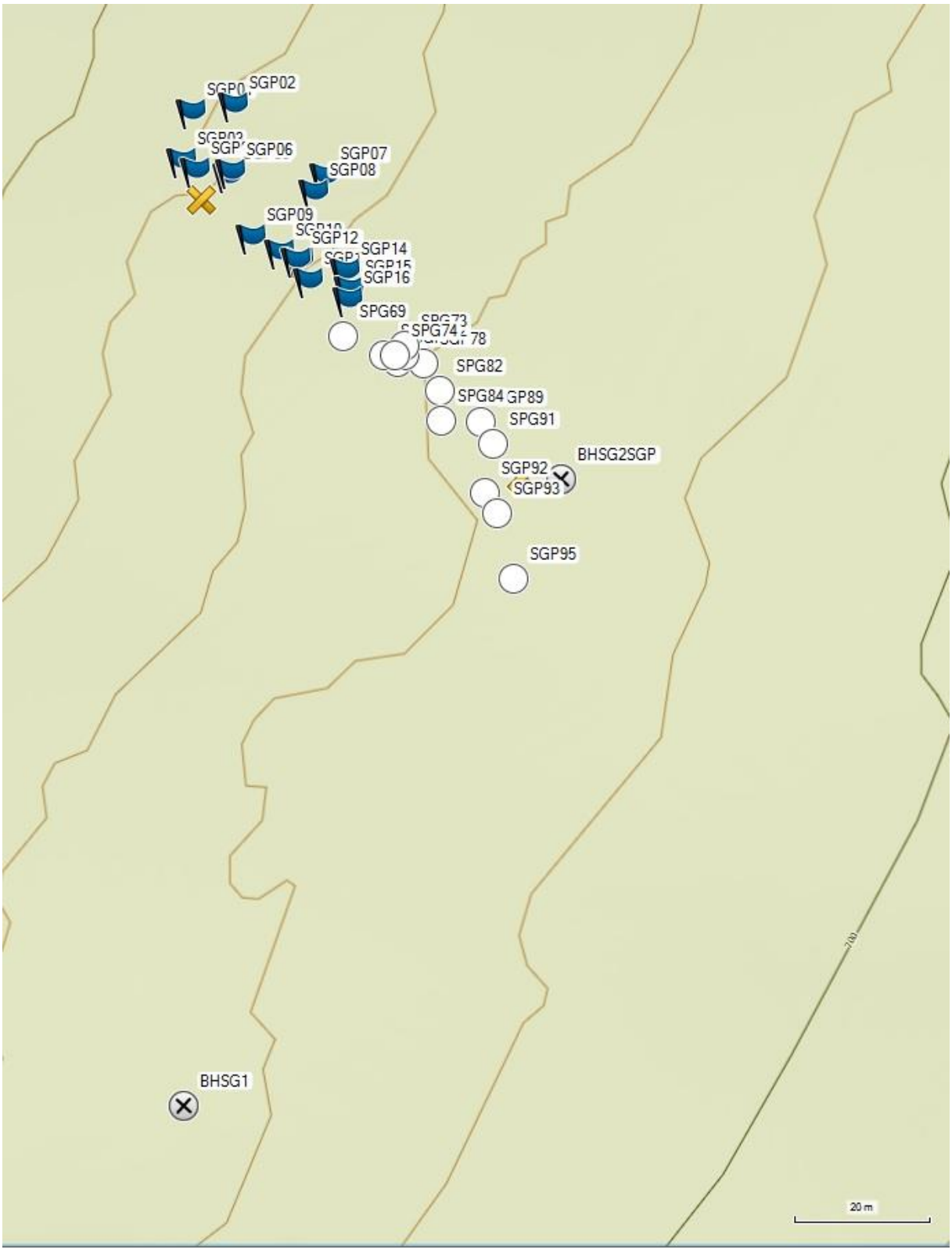

Sample location at the profile at Solligangen, boreholes indicated with circles with X in. yellow X`s show where the mapped profile starts and stops. North is to the left on the map, B in overview map

Appendix D R. Storens map from (Hasselbom et al., 1909)